EFFECTS OF THERMAL CONDITIONS ON THE MECHANICAL PROPERTIES OF SQUEEZE CAST ZA-27 ALLOY

by

Erol Morgül

B.S., Mechanical Engineering, İstanbul Technical University, 2003

Submitted to the Institute for Graduate Studies in
Science and Engineering in partial fulfillment of
the requirements for the degree of
Master of Science

Graduate Program in Mechanical Engineering
Boğaziçi University

2007

EFFECTS OF THERMAL CONDITIONS ON THE MECHANICAL PROPERTIES OF SQUEEZE CAST ZA-27 ALLOY

APPROVED BY:

Prof. Mahmut A. Savaş ……..
(Thesis Supervisor)

Prof. Sabri Altıntaş ……..

Prof. Gökhan Baykal ……..

DATE OF APPROVAL: 08. 06. 2007

ACKNOWLEDGEMENTS

It is a pleasure for me to thank many people who made this thesis possible.

Firstly, I would like to thank my supervisor, Prof. Mahmut A. Savaş, for many insightful conversations during the development of the ideas in this thesis, and for helpful comments on this research. I would not be able to finish this thesis, without his common-sense, knowledge and perceptiveness.

I also thank Uğur Osman Bozer, my patient and helpful friend, for the paper that inspired this thesis, as well as for the experiments carried out in materials laboratory lasting till late nights. Uğur also provided me a great courage for completing this research.

I am also grateful to the companies, Evren Dakro Kaplama, Ceylan Makina Montaj, Sentez Mühendislik and Yön Kimya; institutes, KOSGEB and TÜBİTAK for their support in supplying the experiment equipments and specimen analyses.

My sincere appreciation goes out to all of my committee members: Prof. Sabri Altıntaş and Prof. Gökhan Baykal.

I am also grateful to my wife Evren. Throughout my thesis-writing period, she provided encouragement, sound advice, and lots of good ideas. I also thank her for her incredible patience and continued moral support. So, I thank her for all she is and all she has done for me. To her I dedicate this thesis.

ABSTRACT

EFFECTS OF THERMAL CONDITIONS ON THE MECHANICAL PROPERTIES OF SQUEEZE CAST ZA-27 ALLOY

Squeeze casting is a generic term to specify a fabrication when solidification is promoted under high-pressure within a re-usable die. It is a metal-forming process, which combines permanent mould casting with die forging into a single operation where molten metal is solidified under applied hydrostatic pressure. Squeeze casting has a greater potential to produce less defective cast components contrary to the other conventional casting techniques.

In the present study, the aim was to search thermal solidification behavior and mechanical properties of a squeeze cast ZA-27 alloy in three different pressure ranges. For this purpose, totally 20 samples were cast under 0,1 MPa, 100 MPa and 150 MPa squeezing pressures. All of the samples were subjected to thermal analysis involving temperature measurement at three different points and die surface using K-type thermocouples, data logger and infrared camera. Heat transfer coefficient between the molten metal and die was calculated under some assumptions and cooling curves were obtained. Beside temperature analyses, some mechanical tests were carried out. During machining the samples by lathe, a lot of chips were collected and machinability characteristics were investigated depending on chip lengths; and the Brinell hardness tests, surface roughness measurements and tension tests were done. For microstructural analysis, the scanning electron microscope investigation and metallographic observation were carried out. 28 SEM photographs were taken and 3 metallographic observation done to observe the microstructure properties depending on squeezing pressures.

At result, it was found that, when the squeezing pressure was increased, the heat transfer coefficient between the molten metal and die and mechanic characteristics of cast samples were improved.

ÖZET

ISIL FAKTÖRLERİN BASINÇLI DÖKÜM ZA-27 ALAŞIMININ MEKANİK ÖZELLİKLERİ ÜZERİNDEKİ ETKİSİ

Sıkıştırılmış döküm, katılaşmanın yüksek basınç altında tekrar kullanılabilir kalıplarda gerçekleştiği imalat usülünü belirten genel bir terimdir. Eriyik metalin uygulanan hidrolik basınç altında katılaştığı bu yöntem, sürekli kalıp döküm tekniğini kalıpta dövme tekniğiyle birleştiren bir metal şekillendirme prosesidir. Sıkıştırılmış döküm, diğer geleneksel döküm tekniklerine kıyasla daha az kusurlu döküm parçası üretme gücüne sahiptir.

Bu tezde yapılan araştırmanın temel amacı, sıkıştırılmış dökümü yapılan alüminyum alaşımı ZA-27' nin termal soğuma davranışını ve mekanik özelliklerini 3 değişik sıkıştırma basınıcı altında incelemektir. Bu çerçevede, 0,1 MPa, 100 MPa ve 150 MPa sıkıştırma basınçları altında toplam 20 adet ZA-27 numunesinin dökümü yapılmıştır. K tipi termal eleman çifti, sıcaklık değeri kaydedici cihaz ve termal kamera yardımıyla numunelerin tümüne 3 değişik noktada ve kalıbın dış yüzeyinde sıcaklık ölçümünü içeren termal analiz uygulandı. Bazı kabüller altında eriyik metal ile kalıp arasındaki ısı taşınım katsayısı ve soğuma eğrileri elde edildi. Bu termal analizlerin yanısıra, numuneler için bazı mekanik testler de yapıldı. Numunelerin tornado işlenmesi sırasında çıkan çapaklar toplandı ve çapak boylaı ile işlenebilme özellikleri incelendi. Ayrıca numunelere Brinell sertlik, yüzey pürüzlülüğü ve çekme testleri uygulandı. Mikroyapı analizi kapsamında, sıkıştırma basıncı ile mikroyapı özelliklerinin karşılaştırılması için tarama electron mikroskobu ile 28 adet fotoğraf çekildi ve 3 numune metalografik olarak incelendi.

Sonuç olarak, artan sıkıştırma basıncı, eriyik metal ile kalıp arasındaki ısı transfer katsayısını arttırdığı ve döküm numunelerinin mekanik özelliklerini iyileştirdiği bulundu.

TABLE OF CONTENTS

LIST OF FIGURES

LIST OF TABLES

LIST OF SYMBOLS / ABBREVIATIONS

c	Specific heat
h	Heat transfer coefficient
k	thermal conducdivity
m	mass
m_{Al}	Mass of Al metal
m_{ZA-27}	Mass of ZA-27 alloy
m_{Zn}	Mass of Zn metal
P	Squeezing pressure
T	Temperature
T_m	Monotectic temperature
$V_{casting}$	Volume casting
V_{Al}	Mass of Al metal
V_{ZA-27}	Mass of ZA-27 alloy
V_{Zn}	Mass of Zn metal
X	Distance
ρ	Density
ΔT	Temperature difference due to applied pressure
Σ_{uts}	Ultimate tensile strength (N/mm^2)
σ_{ys}	Yield strength (N/mm^2)
$\sigma_{0.2}$	Yield strength
ASTM	American Society for Testing of Materials
AISI	American Iron and Steel Institute
DIN	German Institute for Standardization
MMC	Metal Matrix Composite
ZA	Zinc Aluminum Alloy
ZA-27	Zİnc-27 %wt Aluminum Alloy

1. INTRODUCTION

Squeeze casting is a generic term to specify a fabrication when solidification is promoted under high-pressure within a re-usable die. It is a metal-forming process, which combines permanent mould casting with die forging into a single operation where molten metal is solidified under applied hydrostatic pressure [1].

In the last years, many researchers have carried out research work on the squeeze casting process considering different parameters. A study was focused on the mechanism of strengthening of aluminum and two aluminum-silicon alloys (5% Si and 12%Si), found that the increased tensile strength under pressure was primarily due to the smaller dendrite cell size, smaller silicon particle size, and closer silicon particle spacing resulting from faster solidification rates [2]. Another study involves cast Al alloy or zinc alloy matrix composites reinforced by ceramic particles and graphite flakes (SiC, Si_3N_4 , B_4C Al_2O_3) were fabricated by centrifugal casting and squeeze casting and their mechanical properties were characterized. ZA-27 and ZL-109 alloys were chosen as the matrices of the composites. The particle reinforced composites showed excellent tribological properties with uniform wear characteristics and appreciably decreased friction coefficient and the increased relative seizure resistance [3]. A different work investigated the effect of casting temperature on the properties of squeeze cast aluminum and zinc alloys. In this study, squeeze casting were carried out on a zinc alloy with 4,6% Aluminum with different temperatures. A K type thermocouple is used to measure the die surface temperature and molten metal temperature, while a 25 t hydraulic press with a die set containing a steel mould was used to perform the squeeze casting with a pressure of 62 MPa. Then; tensile, impact and density tests were carried out on the specimens [4]. However, very little works have been reported on the details of heat transfer between the molten metal and die together with mechanical properties especially, in squeeze casting.

Squeeze casting has many advantages such as: parts are produced without gas porosity or shrinkage porosity; feeders or risers are not required and therefore no metal wastage occurs; alloy fluidity (castability) is not critical in squeeze casting as both common casting alloys with the aid of pressure; squeeze castings can have mechanical

properties as good as wrought products of the same composition. Furthermore, the squeeze casting appears to be most effective in that it offers a good suitability for mass production and a relatively simple process for manufacturing near net shape complicated parts [4, 5]. Two different forms of squeeze casting are available: the direct and the indirect methods. In the direct method, the pressure is applied to the entire surface of the liquid metal during freezing, producing castings of full density. In the indirect method, metal is injected into the die cavity by a small diameter piston [4]. The concept of squeeze casting is believed to have originated in Russia nearly a hundred years ago. Both the process has recently been into commercial use in Europe and Japan to produce high quality of engineering components with and without fiber reinforcement [6].

The mechanical and micro structural properties and heat transfer behavior of ZA-27 alloys depend on the squeezing pressure. This work involves the preparation of ZA-27 alloy from ingots; setting up the experimental mechanism; squeeze casting practice under 3 different squeezing pressures; thermal, mechanical and micro structural analyses. The squeezing pressures were selected as 0,1 MPa, 100 MPa and 150 MPa. For thermal analysis, the effect of heat transfer coefficient between molten metal and die was examined. The thermal distribution on the die surface was also investigated. For mechanical analysis, the samples were subjected to tensile test, hardness test, surface roughness and chip length measurement tests. The SEM and metallographic investigations were done for micro structural observation.

2. LITERATURE SURVEY

2.1. Squeeze Casting Method

Squeeze Casting term is used to describe a combined metal forming process in which the pressure is applied to the metal in its semi-solid state to produce finished shapes. This process is also called as 'liquid metal forging', 'squeeze forming', extrusion casting' or 'pressure crystallization', because it is the combination of gravity die casting and closed die forging processes [6].

Squeeze casting combines permanent mould casting with die forging into a single operation where molten metal is solidified under applied hydrostatic pressure. [1] In this process, solidification is carried out under high pressure within a re-usable die and this pressure is several orders of magnitude greater than the melt pressure developed in conventional foundry practice.

2.1.1. Definition

Squeeze casting is a casting process in which metal is solidified ender the direct action of pressure, and essentially a combination of gravity die-casting and closed die forging.

In squeeze casting, the applied pressure and instantaneous contact of molten metal with die surface produce a rapid heat transfer condition that yields a pore free, grained casting with mechanical properties approaching those of wrought product.

The major advantages of squeeze casting process are: (i) melt feed from hot spots into incipient shrinkage pores is achieved much more readily and parts produced are without gas porosity and shrinkage porosity; (ii) feeders or risers are not required and therefore no metal wastage occurs; (iii) alloy fluidity (castability) is not critical in squeeze casting as both common casting alloys and wrought alloys can be squeeze cast to finished shape with the aid of pressure ; (iv) squeeze castings can have mechanical properties as

good as wrought products of the same composition; (v) minimum material and energy utilization are used for process; (vi) the cast structure exhibits more isotropic and improved mechanical properties [4,7]. Squeeze casting also provides formation of a fine-grained equiaxed structure with a small dendrite arm spacing and small constituent particles [8].

Casting is the most economical route to transfer raw materials into readily usable components. However, one of the major drawbacks for conventional or even more advanced casting techniques, e.g., high pressure die-casting is the formation of defects such as porosity. Furthermore, segregation defects of hot tears, A and V segregates and banding could be potential crack initiators during service operation of the as-cast components. New casting techniques have, therefore, been developed to compensate for these shortcomings. Of the many such casting techniques available, squeeze casting has greater potential to create less defective cast components [1].

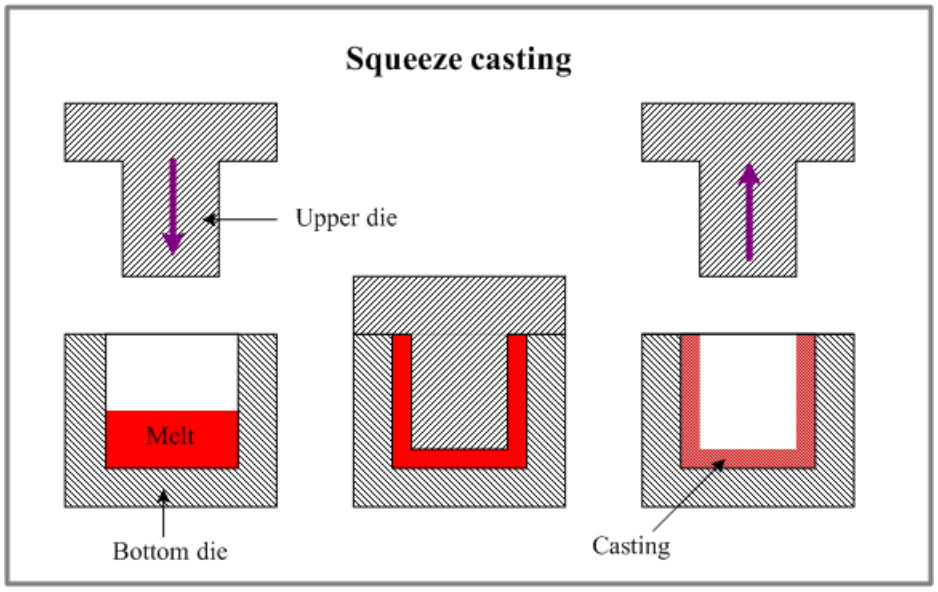

Figure 2.1. Schematic diagram of squeeze casting process [4]

The idea was initially suggested by Chernov in 1878 to apply steam pressure to molten metal while being solidified. However, in spite of its century old invention, commercialization of squeeze casting has been achieved only quite recently and is mainly concentrated in Europe and Japan. It is mainly used to fabricate high integrity engineering

components with or without reinforcement [9]. Hartley reported a technique developed by GKN Technology in UK for the pressurized solidification of Al alloy in reusable dies. In this process a die set is placed on a hydraulic press and preheated, and the exact amount of molten alloy is poured into the lower half of the open die set, the press closed so that the alloy fills the cavity and the pressure maintained until complete solidification occurs (31 - 108 MPa pressure). External undercut forms can be produced, and using retractable side cores, through-holes are possible. Since the as-fabricated components can be readily used in service or after a minor post-fabrication treatment, squeeze casting is also regarded as a net or near net-shape fabrication route [1].

Parallel to commercialization, there are research centers throughout the world that are actively researching further development and exploitation of this net or near net shape fabrication process. This is evidenced by the publication of more than 700 papers in various engineering and scientific journals. These are mainly related to aluminum and magnesium-based alloys with special emphasis on metal matrix composites MMCs. According to Crouch [10], squeeze casting is now the most popular fabrication route for MMC artefacts. The annual 12-15% growth rate of MMCs in the automotive, aerospace, sport and leisure goods and other markets is a clear indication of better usage of advanced manufacturing routes such as squeeze casting [1].

Generally, the SC-fabricated engineering components are fine grained with excellent surface finish and have almost no porosity. They come in a variety of shapes and sizes. The mechanical properties of these parts are significantly improved over those of conventional castings and more sophisticated casting routes of pressure or gravity die-casting. According to Pennington, yield strength is improved by 10-15% and elongation and fatigue strength by as much as 50-80%. Dimensional accuracy is similar to those of die-casting; 0.25 mm in 100 mm to 0.6 mm in 500 mm. It is further claimed that SC-fabricated components have superior weldability and heat treatability. In addition, since squeeze casting may be carried out without any feeding system, runners, gates, etc., and shrinkage compensating units, risers, the yield is quite high with almost no scrap for recycling [1].

Finally, in contrast to forging, squeeze cast components are fabricated in a single action operation with lesser energy requirements.

Factors that influence casting quality listed in decreasing order of importance are the melt quality and quantity, the equipment and tooling, the casting temperature, the tooling temperature, the time delay before pressurization, the pressure level and duration [7]. While pressure is a primary parameter, it is listed last because it is usually eliminated in practice as a quality control variable by providing more than the required press load.

2.1.2. Method Steps

Squeeze casting sequence has four main steps that are: (i) melting the metal and preheating the tooling; (ii) a metered amount of molten metal is transferred into a female die cavity or mould, located on the bed of a hydraulic press; (iii) the male die, or punch, of the appropriate shape is driven into the die cavity to exert a pressure on the metal, while it is solidifying and to form the required shape, and this step is carried out very quickly for rendering solidification of the molten metal under pressure; (iv) the pressure held on the metal until complete solidification. This is not only increases the rate of heat flow, but also most importantly may eliminate macro/micro shrinkage porosity. In addition, since nucleation of gas porosity is pressure-dependent, the porosity formation due to dissolve gases in the molten metal is restricted; (v) after the casting has been solidified completely under the applied pressure, the punch is withdrawn and the shaped solid casting is ejected from the die.

In general, two different methods of squeeze casting are available based upon different approaches to metal metering and movement: ‘direct’ and ‘indirect’ squeeze casting methods. In the direct squeeze casting method, the pressure is applied to the entire surface of the liquid metal during freezing, producing castings of full density. This technique consequently gives the most rapid heat transfer, yielding the finest grain structure. In the indirect squeeze casting process, metal is injected into the die cavity by a small diameter piston and the cast product is not of the superior quality as obtained from the direct squeeze casting process [4]. Another disadvantage of this method is that the material utilization is often inefficient in that a runner and gating system is used and this material has to be removed and cycled [6]. Of the two methods for squeeze casting it appears that the direct process is more common in practice for the production of full integrity castings and metal matrix composite components.

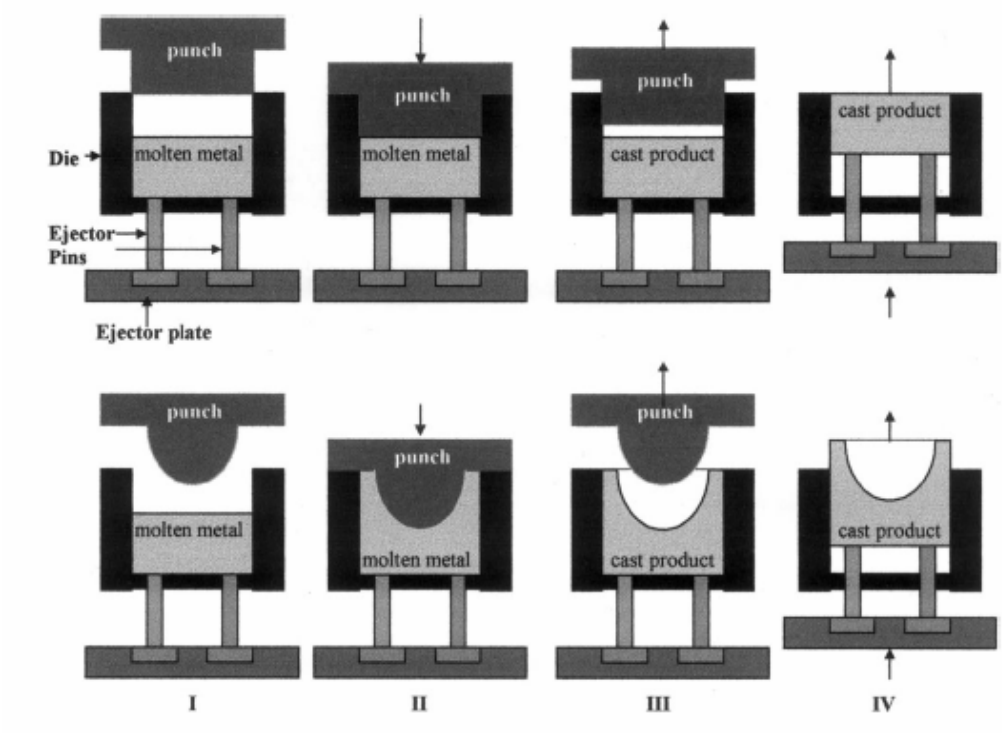

Figure 2.2. Schematic diagram to show two forms of the direct squeeze casting process [1]

2.1.2.1. Melt Quality and Quantity

Melt quality especially in terms of oxide content is more critical in squeeze casting than in gated processes. Because in squeeze casting there are no runners and gates to accommodate any dross that may be present. For both ferrous and nonferrous alloys the oxide content must be minimized whenever possible by a combination of fluxing, skimming and filtering [6].

The quantity of the casting is important for the dimensional accuracy of the casting whenever net-shapes are attempted. Control of final dimensions can be achieved by accurately metering the poured weight or volume of metal [7].

2.1.2.2. Equipment and Tooling

The main elements of the tooling are a punch, a die, and a knock-out pin to eject the casting. The tooling is mounted for use in a hydraulic press. A most crucial aspect in

permanent mould castings such as squeeze casting is the die itself and, most importantly, the design of the die including the selection of a suitable die material, the manufacturing process, appropriate heat treatment and the maintenance practice. Squeeze casting dies are exposed to severe thermal and mechanical cyclic loading, which may cause thermal fatigue, cracking, erosion, corrosion, and indentation. The nature and features of a die are greatly influenced by the particular alloy to be cast. Currently H13 tool steel is a widely used material of constructions but generally die steels should have good hot hardness, high temper resistance, adequate toughness and especially a high degree of cleanliness and uniform microstructure [1].

2.1.2.3. Casting and Tooling Temperature

The temperature at which the molten metal is poured into the die cavity is extremely critical from the standpoints of both casting quality and die life. Too low a casting temperature causes inadequate fluidity in the melt during dir filling and results in incomplete die fill as well as cold laps on the casting surfaces. But on the other hand if, the casting temperature is too high this can cause extrusion of liquid metal through the tooling interfaces and can also result in shrinkage porosity in thick sections of the casting. And the die life is adversely affected by high pouring temperatures [11].

In squeeze casting the temperatures of the die cavity and the punch are usually maintained between 200°C and 300°C. Low temperatures (lower than 150°C) may cause thermal fatigue failures in the dies and also cold laps on the surfaces of the casting. On the other hand, very high tooling temperatures (higher than 400°C) can cause hot spots and shrinkage pores in the casting. Another problem with overheated dies (especially for ferrous applications) is the tendency for welding between the casting and the die [11].

2.1.2.4 Time Delay Before Pressure Application

Optimum results are obtained when the pressure was applied near the zero fluidity temperature of the molten metal. However, it is not practical to pour the melt into the die at or below its liquidus temperature. Consequently, the melt is poured in the superheated condition, and pressurized only after allowing it to cool below the liquidus temperature.

With aluminum alloys, it is frequently necessary to provide a time delay of 10 to 20 seconds before die closure and pressure application [12].

2.1.2.5 Pressure Level and Duration

For squeeze casting operations of most ferrous and nonferrous materials, a minimum pressure level of 70 to 105 MPa is necessary in order not to face shrinkage and gas porosity. However, the geometry of casting dictates the use of higher pressure for controlling porosity formation and die filling. There is a critical pressure for each composition at which density nearly reaches saturation. The saturation values are almost equal to the ideal (theoretical) density of alloy of that composition. This pressure level is also called as 'the critical pressure for density'. There is also critical pressure above which no defects (porosity, shrinkage etc.) are detected (by dye penetrant checking) and this pressure is called 'the critical pressure for defects'. Usually the critical pressure for defects is higher than the critical pressure for density and it dictates 'the minimum pressure level' for a sound casting [13].

In general, a pressure of 105 MPa was necessary to eliminate porosity in alloys with a narrow freezing range ($\Delta T \approx 10°C$), where as 70 MPa was adequate for alloys with extended freezing range ($\Delta T \approx 100°C$). Extended freezing range alloys were found to require less applied pressure because of shorter feed length between the semi-liquid pool and solidifying metal than for narrow freezing range alloys [11].

The pressure level in squeeze casting is usually in the range of 70-105 MPa for simple shapes and rises to 140-210 MPa for thin sections and complex shapes. The shapes and the section thickness of the casting govern the duration of pressure necessary to ensure complete solidification under pressure [11].The timing of pressure application is critical, since if it is applied at a temperature of $T > Tm + \Delta T$, ΔT being the expected increase in Tm due to pressure, the effect of under cooling is negligible and thus increase in the heat-transfer coefficient is the dominant mechanism. If however, the pressure is applied at a temperature $Tm \leq T \leq Tm + \Delta T$, then under cooling would be the dominant mechanism [1].

2.1.3. Disadvantages of Squeeze Casting

Among the disadvantages, the followings mostly common are listed below:

- The oxide level of the melt is more critical than it is in gated casting processes.
- The process needs a close control of tooling temperature and a good timing for pressure application because these parameters highly effect the quality of the casting.
- Squeeze casting is very hard to apply for the narrow freezing range alloys, because of their needs for high overheating temperatures resulting extrusion of liquid metal through tooling interfaces and shrinkage porosity in thick sections.
- Lubrication is very important in order to prevent contact welding resulting from the high pressure and die temperature and to provide good surface finish.
- Squeeze casting needs high capital costs and in squeeze casting the maximum size and weight are limited.

2.1.4. Comparison of Squeeze Casting Method with Other Methods

Although squeeze casting has some disadvantages as listed 2.1.3., there are many advantages of squeeze casting making it the best die casting among the other methods. The major advantages of squeeze casting are as follows [9, 11, 14] listed below:

- Materials having neither gas porosity nor shrinkage porosity are produced.
- The inherent castability of the alloy is of little or no concern since the applied pressure deviate the need for customary high fluidity. Both common casting alloys and ostensibly wrought alloys can be squeeze cast to finished shape.
- Control of microstructure is possible solely by control of the dominant process parameters such as pouring temperature and mould temperature.

- No feeders or risers are required and therefore no metal wastage occurs

- Squeeze casting can have mechanical properties as good as, and in some cases even better than wrought products of the same composition.

- Squeeze casting process also allows fiber performs to be placed in critical areas of the component where high performance is required or it can be used in the production of MMC's with ceramic fiber preforms.

- Labor for molding, trimming of risers and gates and cleaning are eliminated.

- It increases the production rates in comparison with conventional casting techniques.

Table 2.1. Representation of casting quality with respect to the casting technique [1]

	Low Pressure Die Casting	High Pressure Die Casting	Vacuum Die Casting	Thixomoulding	Semi-Solid Forging	Squeeze Casting
Cycle Time						
Surface Finish						
Gas Entrapment						
Shrinkage Pores						
Heat Treatable						
Weldable						
KEY	**PERFORMANCE**					
	GOOD					**POOR**

2.2. Zinc Alloys

A combination of zinc with one or more other metals is called Zinc Alloy. If zinc is the primary constituent of the alloy, then it is a zinc-base alloy. Zinc also is commonly used in varying degrees as an alloying component with other base metals, such as copper, aluminum, and magnesium.

Zinc-base alloys have two major uses: for casting and for wrought applications. Casting includes both die casting and gravity casting, which differs from die casting primarily in that no pressure is applied, except the force of gravity, in forcing the molten metal into the mold.

The great bulk of zinc die casting is carried out with two alloys, commonly identified as alloys 3 and 5. A third alloy has been added and is commonly designated as alloy 7. The entire group in the United States is often spoken of by its original trade name as Zamak alloys and in England as the Mazak alloys.

Aluminum, the major alloying constituent in alloys 3 and 5, is added in amounts of about 4%, which has proved to be the optimum composition from the standpoint of strength, ductility, and stability. The aluminum content also sharply reduces the rate of attack of molten zinc on iron containers. Aluminum also avoids “soldering,” or sticking of the casting to the die. This permits the casting of these zinc alloys in the more productive hot-chamber (plunger) type of die-casting machine.

Alloys 3 and 5 differ primarily in their copper content. Copper additions increase strength and hardness and improve corrosion resistance. The copper content of alloys is held to a specified maximum of 1.25% (in alloy 5) to avoid making the alloy unstable through aging and to avoid reducing the impact strength to a very low value.

Alloy 7 is considered a modification of alloy 3. It has a lower magnesium content, and iron, lead, tin, and cadmium are also held to lower levels. A small amount of nickel is added.

When the alloys are compared, alloy 7 exhibits improved casting properties, making it easier to secure high-quality surfaces for finishing (mostly chromium plating) and to obtain higher production rates [15].

2.2.1. Zinc Alloy Types

Zinc alloy's high strength and hardness, means that it is the ideal alternative to machined, pressed, stamped and fabricated items. At below the types of Zinc Based Alloys are explained [16]:

Zinc Alloy 2 : No. 2 is sometimes referred to as Kirksite. This alloy offers the highest strength and hardness of the family. However, due to the high copper content (3%), changes to the material properties occur with long-term ageing. These changes include slight dimensional growth (0.0014 mm/mm [in/in] after 20 years), lower elongation and reduced impact performance.

Although this alloy exhibits excellent casting characteristics, it has seen limited use by diecasters. Its creep performance is rated higher than the other zinc alloys and it maintains higher strength and hardness levels after long-term ageing.

Zinc Alloy 3: No. 3 Alloy is usually the first choice when considering zinc for diecasting and is the most widely used zinc alloy in North America. Its excellent balance of desirable physical and mechanical properties, superb castability and long-term dimensional stability are the reasons why most diecastings are made from this alloy. No. 3 Alloy also offers excellent finishing characteristics for plating, painting and chromate treatments. In terms of diecasting, it is the standard by which other zinc alloys are rated. Where higher strength is required, the other zinc alloys should be considered.

Zinc Alloy 5: No. 5 Alloy is the most widely used zinc alloy in Europe, with its higher copper content resulting in higher strength and increased hardness at the expense of some loss of ductility (increased elongation) compared to Alloy 3. This reduction in ductility can affect formability during secondary operations such as bending, riveting, swaging or crimping operations and should be carefully considered by the designer.

Because of the wide availability of Alloy 3, component engineers often strengthen components by design modifications instead of using Alloy 5. However, when a measure of tensile performance is needed, alloy 5 castings are recommended.

Creep rates for Alloy 3 and 5 are very similar although Alloy 5 does have better creep resistance, and curves can be used for both alloys. Where temperatures above normal ambient are involved and the component must be designed to accommodate structural loads, Alloy 5 is likely to be a better choice.

Zinc Alloy 7: Alloy 7 is a modification of Alloy 3 resulting in improved casting fluidity, ductility and surface finish. Most Alloy 7 is used for special hardware applications, or when castings require extra formability during subsequent assembly operations such as crimping or staking. The higher fluidity also allows thinner walls to be cast.

Higher fluidity is sometimes desirable especially on components with intricate detail; however it does present special casting considerations. In order to avoid excessive flashing along the tool parting lines, good die fit and close control of casting process parameters is necessary. The high ductility exhibited by this alloy also has an impact on processing, but mainly in secondary operations for flash removal and trimming.

Zinc Alloy ZA-8: The ZA alloys contain significantly more aluminum than the Zamak group of alloys with the numerical designation representing the approximate percentage of aluminum.

ZA-8 was originally developed as a permanent mold alloy having excellent finishing and plating characteristics. It is particularly suitable for decorative applications. Although this alloy does not exhibit quite as good casting characteristics as the other zinc alloys, it offers significantly improved strength, hardness and creep properties. In terms of mechanical performance, this alloy has the highest creep strength of any zinc alloy and the highest strength of any hot-chamber diecast zinc alloy. This is the only ZA alloy that can be hot-chamber diecast.

Zinc Alloy ZA27: Due to the high aluminum content of this alloy, it must be cold-chamber diecast. This alloy has the highest strength, and the lowest density of the ZA alloys. ZA-27 provides the highest design stress capability at elevated temperatures of all the commercially available zinc-based alloys. This alloy also has excellent bearing and wears resistance properties.

Zinc Alloy ACuZinc5: This is an alloy researched and developed by General Motors, which exhibits greatly improved strength, hardness and creep performance due to the high copper and low aluminum contents. This alloy also has excellent bearing properties.

2.2.2. Material Properties of Zinc Alloys

The material properties of ZA alloys as listed below [17]:

Strength: ZA alloys deliver the highest tensile strength among the most widely used non-ferrous alloys and match or exceed that of most cast irons. Yield strength is a major ZA alloy attribute reaching 55,000 psi for ZA-27, that's more than twice that of A380 die cast aluminum, and significantly higher than the strongest plastics. Even ZAMAK 3, the most common alloy has a significant yield strength advantage over A380 aluminum, showing 3 times greater elongation, while maintaining greater hardness and higher stiffness .

Rigidity: Zinc alloys are rigid engineering materials. Their elastic modules are greater than those of aluminum and magnesium alloys, and are an order of magnitude greater than those of plastic. This, combined with their high strength allows the volume of individual castings to be markedly reduced, saving space and weight.

Toughness and Ductility: High impact strength and good ductility are qualities of zinc alloys that are rarely found in most other casting alloys. Ductility is important for bending and crimpling in post-casting assembly operations, while impact strength provides performance in rough environments. Fracture toughness is also greater than for most aluminum alloys and cast irons.

Hardness: ZAMAK alloys provide high hardness and abrasion and wear resistance. Optimum hardness is provided by the ZA family whose Brinell Hardness ranges from 95 to 122 when die cast. These values are much higher than the 70 to 85 BHN displayed by aluminum alloys, and much higher than the hardness values of engineered plastics. Along with high hardness, ZA alloys also exhibit excellent abrasion and wear resistance.

Conductivity: As zinc alloys conduct both heat and electricity, they can be used for heat dissipating devices such as heat sinks. Zinc's excellent casting fluidity permits thinner fin and cooling pin design to better dissipate heat. Zinc's excellent electrical conductivity also provides good EMI, RFI and ESD shielding

Fatigue Strength: This measure of a material's ability to withstand cyclic loading is and important design criterion. Both the ZAMAK and ZA alloys have high fatigue strengths.

Design (Creep) Stress: The allowable design stress, or resistance to creep at room temperature, of ZA alloys is far better than for all but the most esoteric engineering plastics. The room temperature design stress of die cast ZA-27, for example, is 10,000 psi (stress required for the creep of 1% in 100,000 hours). This property allows ZA alloys to be used in applications subject to significant static loading. However, permissible design stress drops with increasing temperature, and a careful review of all constant load applications at temperature is required to determine the suitability of zinc alloys.

Pressure Tightness: Soundness of castings is largely related to product design, tooling layout and process control. Die cast ZAMAK alloys, ZA-8 and ZA-12 are often used for pressure tight applications. For sand and permanent mold casting, ZA-12 is the preferred material. All zinc alloys solidify into a dense strong matrix with excellent pressure tightness.

Corrosion Resistance: Zinc has excellent corrosion resistance under normal atmospheric conditions, and in many aqueous, industrial and petroleum environments. Corrosion resistance can be enhanced by such treatments as plating, chromating, painting and zinc anodizing.

As a summary, the material characteristics of ZA alloys are written below:

- High strength and hardness
- Excellent electrical conductivity
- High thermal conductivity
- Lowest cost raw material
- High dimensional accuracy and stability
- Excellent thin wall capability
- Ability to cold form, which eases joining
- High quality finishing characteristics
- Outstanding corrosion resistance

2.3. Thermal Analysis of Squeeze Casting Process

2.3.1. Modeling of Temperature Measurement Process with a Thermocouple

The principle of thermocouple temperature measurement is based on seebeck effect, which states that an electrical potential gradient is generated from two unlike metals exposed to a temperature gradient in an open electrical circuit. The temperature measurement resulting from the use of thermocouple is in general not necessarily the true temperature. There exists very limited research on modeling the temperature measurement with a thermocouple. In 1998, Rabin and Rittel developed a model for determining the time response of a solid-embedded thermocouple. They suggested that the thermal diffusivity (α) of the thermocouple itself should be at least one order of magnitude higher than that of measured material in order to obtain meaningful results in

thermocouple/material interface, which is at odds with practical situations. Erickson and Houghton (1977) explored the effect of thermocouple on local solidification time during the metal solidification process. They showed that a thermocouple behaves like a heat capacitance, which initially acts as heat sink but finally as a heat source, so that often the local solidification time is artificially increased [18].

There are two basic requirements for accurate temperature measurements. One is that the sensor should be able to accurately track the transient details of the temperature response and the other is that the local temperature field should be disturbed as little as possible by the presence of the sensor.

The measurement of thermocouple is effected by interface thermo resistance, heat conduction coefficient, specific heat, density and thermocouple size.

The interface thermal resistance plays a very important role on the temperature measurement result. If the physical properties of the thermocouple are the same as those of the material and heat transfer mode at the interfaces is heat conduction with material heat conduction coefficient, the thermocouple temperature and true material temperature will equal to each other. Increasing the heat conduction coefficient of the thermocouple, the heat conductance of the thermocouple is bigger than that of the material. So increasing the heat conductance of the thermocouple facilitates temperature tracking in transient situation. The measurement of thermocouple can be improved if size, specific heat and density of thermocouple are decreased.

Based on these facts, the following criterions are recommended for the thermocouple selection if transient temperature measurement is required:

- The specific heat and density of the thermocouple should be smaller than those of material;

- The heat conduction coefficient of the thermocouple should be bigger than that of the material;

- The thermocouple size should be as small as possible;

- The interface thermo resistance should be as small as possible.

2.3.1.1. The Correct Placement of Thermocouples

When producing a casting, the heat flux at the mold/metal interface is an important variable effecting the quality of the casting. In order to calculate the heat flux, the temperature near the mold side of the interface often becomes important [19].

In permanent molds, a hole is typically drilled to make space for the thermocouple. The introduction of the cavity contributes to the distortion of the temperature field. The amount of the distortion differs depending on whether the length the thermocouple is embedded parallel or perpendicular to the isotherms associated with the temperature gradient. The thermocouple, positioned perpendicular to the isotherms, is subjected to the heat flux directly. Concisely, the horizontally placed thermocouple produces errors much less drastic than the error produced by vertically mounted thermocouple [20].

Also, the horizontally positioned thermocouple has the advantage in the control over the position of the thermocouple bead relative to the interface. Often, the distance between the interface and the thermocouple bead becomes an important variable. Therefore, control over that distance is critical when the desired temperature readings must be a certain distance from the interface. When the thermocouple is positioned vertically, the bead may be positioned anywhere inside the perimeter of the base of the hole. Controlling where the bead comes into contact with the base of the hole can be difficult, especially when the depth of the hole is considerable. For that reason, the distance between the bead and the interface becomes questionable as seen in Figure 2.3.

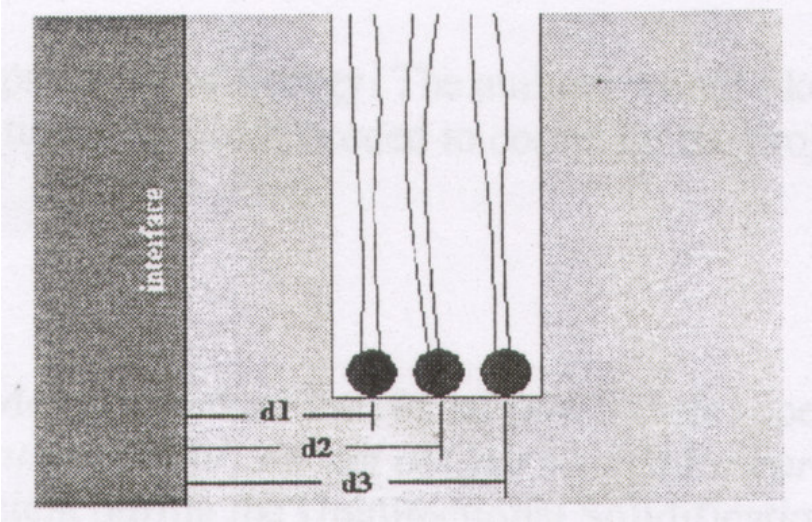

Figure 2.3. Distance between a vertically positioned thermocouple bead and interface [19]

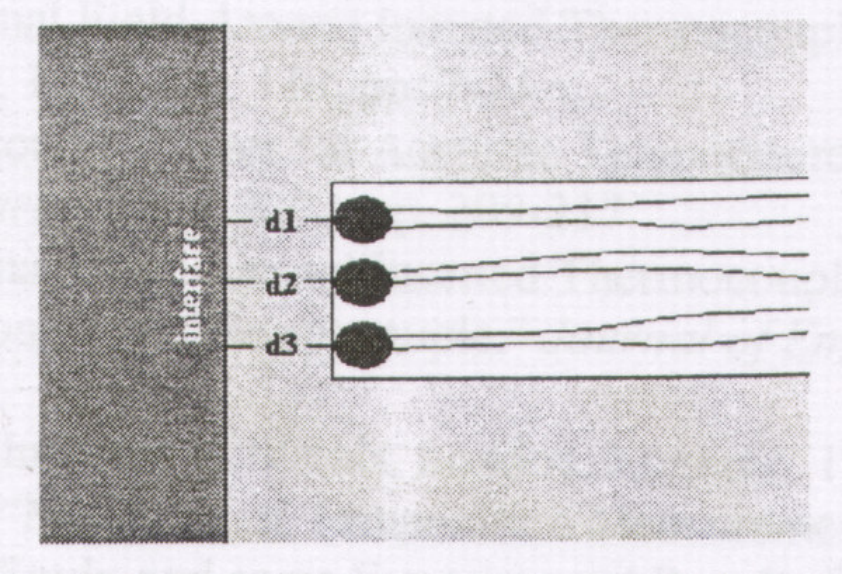

Figure 2.4. Distance between a horizontally mounted thermocouple bead and interface [19]

When the thermocouple is positioned horizontally, however, the distance between the thermocouple bead and the interface is the same regardless of where the bead is located at the base of the hole as seen in Figure 2.4. [20].

Therefore, there are advantages to mounting thermocouples horizontally in permanent mold. The horizontally embedded thermocouple produces a smaller error in temperature measurements and allows more control over the distance between the thermocouple bead and mold/metal interface [20].

2.3.2. Measurement of Heat Transfer Coefficient between Molten Metal and Mold

Inverse methods in heat conduction are used to determine some 'missing information' in the solution of the heat conduction problem. This missing information may be either thermal properties of the material or the heat transfer at the surface of the object. In order to determine the missing information, some supplemental information must be supplied. This supplement information is usually the temperature history at one or more points within the object [21].

An inverse method is used in this investigation to determine the heat transfer from a casting. The method only requires temperature measurements in the mold to determine the heat flux at the interface [21].

For the analysis of a heat transfer problem, an appropriate set of equations is first determined to describe the heat transfer behavior. With the boundary conditions, initial condition, and thermo-physical properties of the materials known, it is possible to obtain the temperature distribution and variation of the whole system. [22].

To make use of the inverse method to determine h, temperature measurements have to be made. To make the analysis of the inverse method easier, a one-dimensional heat transfer system is devised. It requires temperature measurements at least at three points. Two serve as the boundary conditions and the other as the calibration point. Naturally, more temperature measurements make the analysis more accurate. A brief description of the inverse method to analyze the temperature data for h as follows:

$$\frac{\partial}{\partial x}\left(k\frac{\partial T}{\partial x}\right)=\rho c\frac{\partial T}{\partial t} \qquad (2.1.)$$

where k, ρ, c are the thermal conductivity, density and specific heat, respectively.

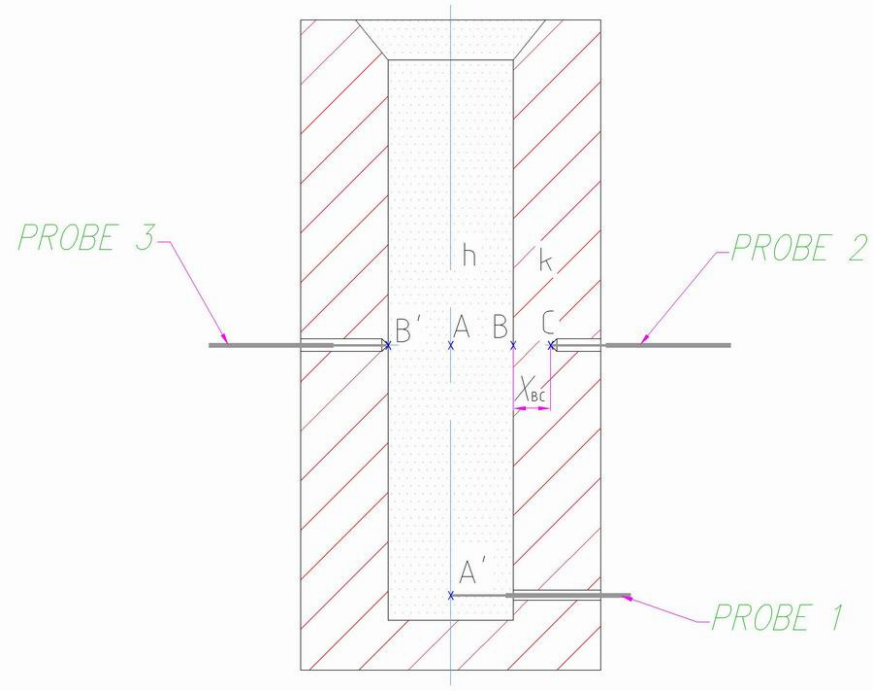

Figure 2.5. Schematic illustration showing the points for heat transfer mechanism

$$Heat\_Conduction @ Point B = Heat\_Convection @ Point B$$

$$-k \cdot A \cdot \frac{dT}{dx} = h \cdot A \cdot (T - T_{\infty}) \tag{2.2.}$$

$$-k \cdot A \cdot \frac{T_C - T_B}{x_{BC}} \cong h \cdot A \cdot (T_B - T_A) \tag{2.3.}$$

$$h \cong -k \cdot \frac{T_C - T_B}{x_{BC}} \cdot \frac{1}{T_B - T_A} \tag{2.4.}$$

The heat transfer coefficient, h, can be calculated provided that the temperature values at points A, B and C; the distance between B and C points and temperature dependent heat conduction coefficient, k, are known.

3. EXPERIMENTAL STUDY

3.1. Materials Used

For casting of ZA27 alloy, high purity Zinc and Aluminum materials were used. Both Al Aluminum and Zinc were commercial grade pure and at ingot state. The Zn and Al ingots were obtained from Körfez Ticaret, Istanbul and Fen İş Aluminum, Gebze respectively. The Al class was Etial 7 (DIN AI99,7) having at least %99.7 purity and the Zn ingot was an import material having %99.95 purity.

Table 3.1. Chemical Composition of the Etial 7 Aluminum

ETIAL – 7	Al	Si	Mn	Fe	Cu	Mg	Cr
	99.72	0.0769	0.0189	0.175	<0.015	<0.036	<0.015
	Ni	Zn	Pb	V	Zr	Sn	Ti
	<0.017	<0.070	<0.078	0.0065	<0.0019	<0.040	0.0057

Figure 3.1. Zinc and Etial 7 ingots (on the left and right respectively)

3.2. Equipments Used

Several equipments were used in different aims to complete the experimental studies. These are listed below depending on their section:

- Material Preparation Equipments
- Casting Equipments
- Temperature Measurement Instruments

3.2.1. Material Preparation Equipments

The Al and Zn ingots were sliced into firstly moderate size pieces and then small pieces by Universal Horizontal Sawing Machine in Ceylan Makina Montaj. The cutting tool material used in this machining process was a high-speed steel (HSS) corresponding to the T42 steel in the AISI standard and Wr Nr 3207-EW9Co10 steel in the DIN standard.

Figure 3.2. Cutting of ingots by Universal Horizontal Sawing Machine

Figure 3.3. Moderate size Zn (on left) and Al (on right) parts

The small pieces were weighted by an electronic scale and were classified in groups depending on their weights.

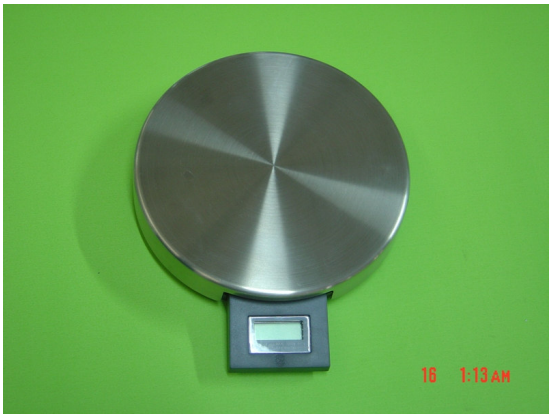

Figure 3.4. Electronic scale

3.2.2. Casting Equipments

3.2.2.1. Furnaces

There are two furnaces which are used for annealing and melting in Materials Laboratory of Boğaziçi University, Mechanical Engineering Department. The melting furnace could be heated up to 1000 ^{o}C while the annealing furnace to 750 ^{o}C. The Al and

Zn parts are melted in the melting furnace. The die and punch are heated up in annealing furnace.

Figure 3.5. Annealing furnace

Figure 3.6. Melting furnace

3.2.2.2. Hydraulic System

The Hydraulic system consists of a hydraulic tank, hydraulic cylinder, pump motor, manuel control arm, pressure regulator and indicator. This system is made by Mert Akışkan Gücü San. ve Tic. A.Ş. and available in Materials Laboratory of Boğaziçi University, Mechanical Engineering Department.

The type of hydraulic cylinder is KHS-Ø100x200. The diameter and stroke of cylinder are 100 mm and 200 mm respectively. These values are necessary for calculating squeezing pressure.

Figure 3.7. Hydraulic system

3.2.2.3. Die and Punch

The die and punch are available in Material Laboratory of Boğaziçi University, Mechanical Engineering Department. The material of dies and punches is industrial type DIN1040 steel. The 2-D and 3-D drawings of die and punch are shown in Figure 3.8 and Figure 3.9 respectively. For 2-D drawings AuroCad 2006 Mechanical Desktop and for 3-D

drawing SolidWorks were used. The die existing in Material Laboratory was modified by some alterations. Firstly the hole located at the middle of bottom part of the die was closed by small a welding spot in order to prevent ZA27 leakage. Then 1 hole with 2 mm. diameter and 2 holes with diameter 2.5 mm. were drilled to locate the thermocouples as seen in Figure 3.11.

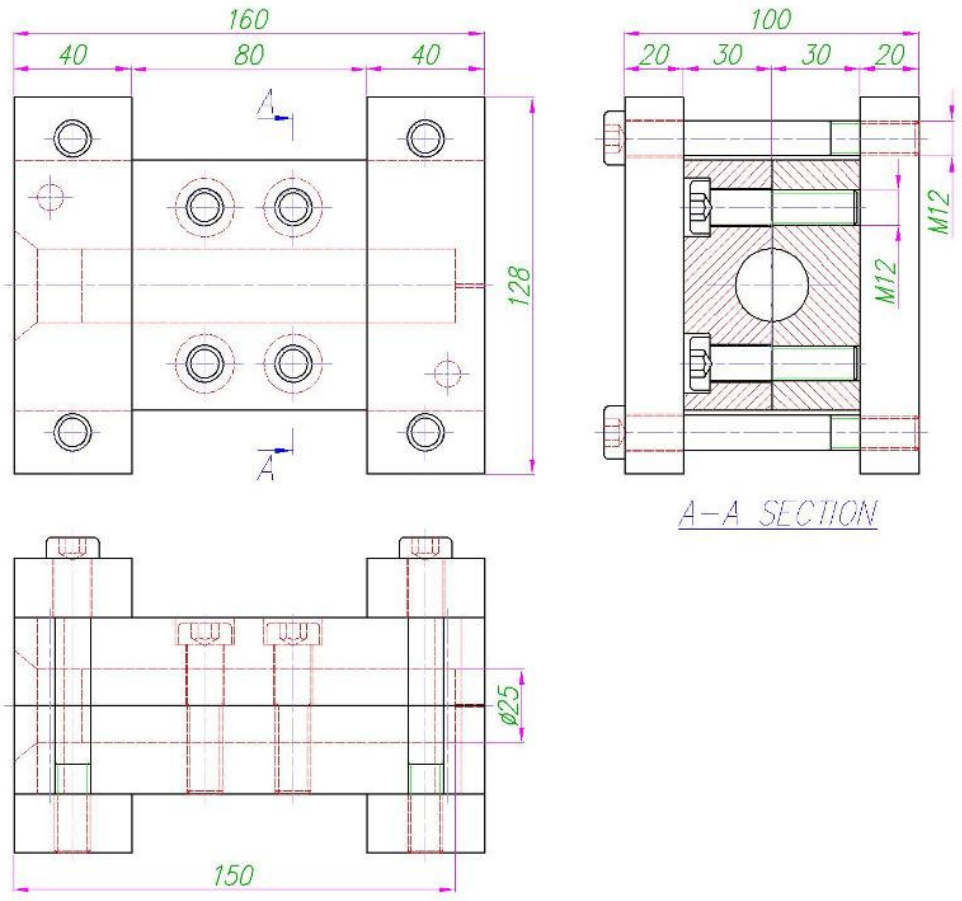

Figure 3.8. 2-D Drawing of the die

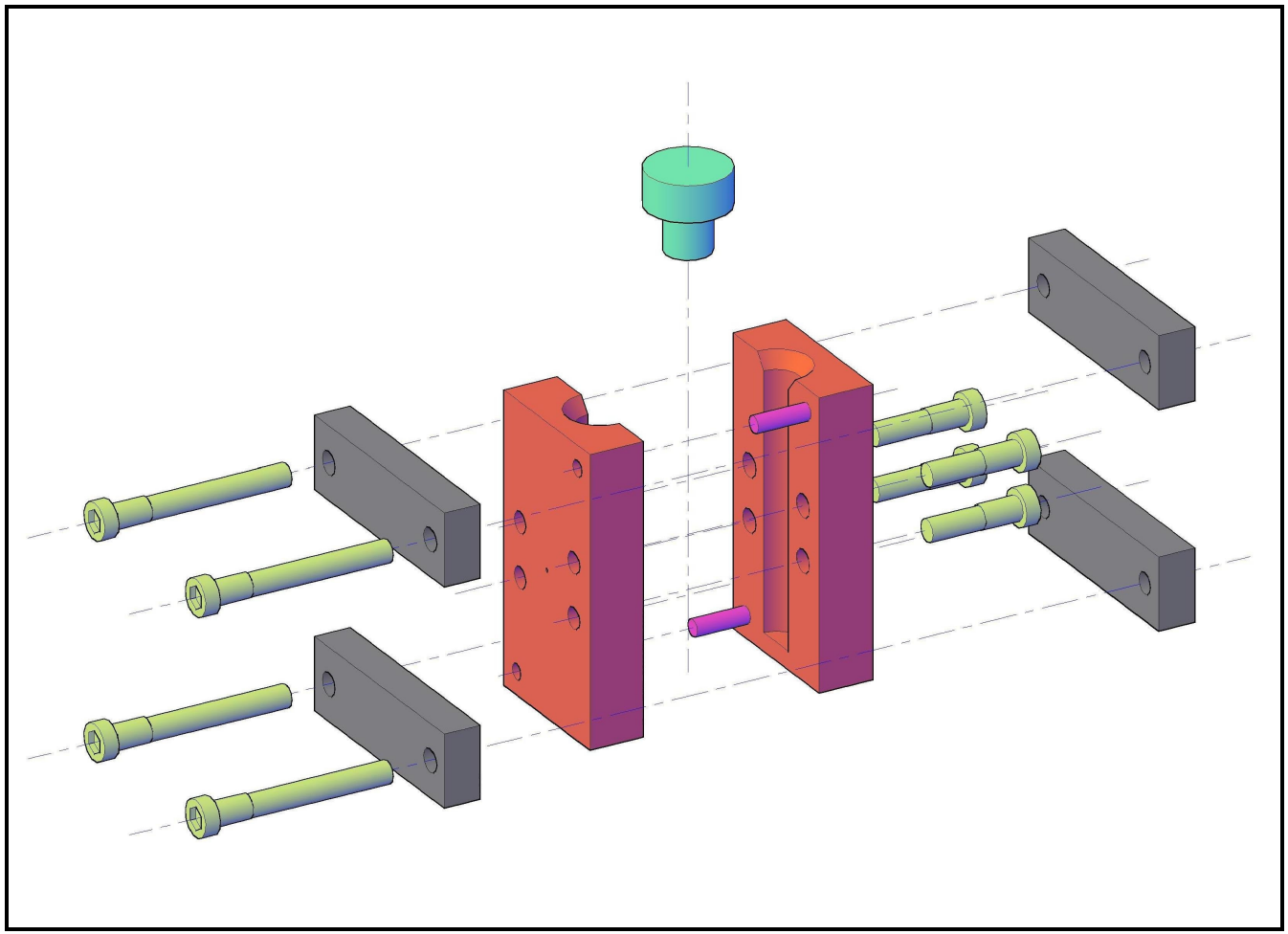

Figure 3.9. Unassembled 3-D drawing of the die and punch

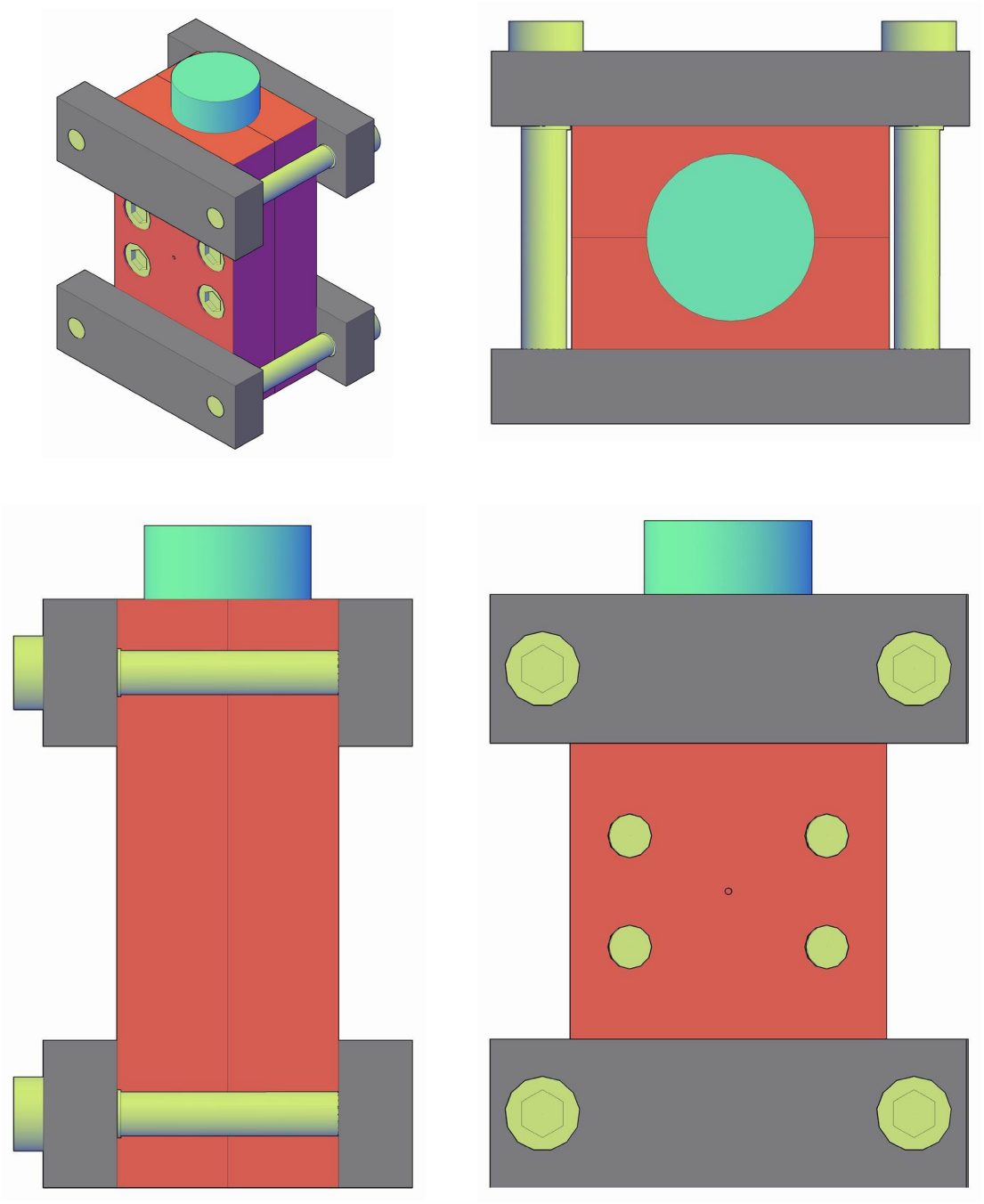

Figure 3.10. Assembled 3-D drawing of the die and punch

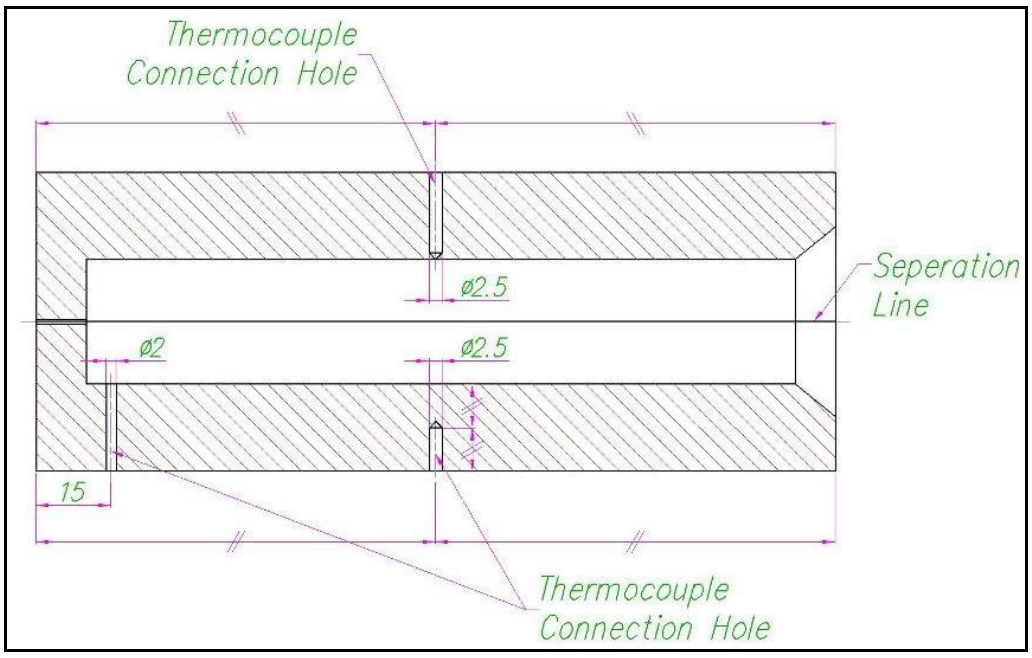

Figure 3.11. Thermocouple connection holes in die

3.2.2.4. Auxiliary Equipments

There are some auxiliary instruments which are Crucible, Stirring Rods and Rock Wool. These instruments were used during casting process.

Crucible is the most necessary and essential equipment for casting. A crucible is a container use to hold metal for melting in a furnace. A crucible is needed to withstand the extreme temperatures encountered in melting metals. The crucible material must have a much higher melting point than that of the metal being melted and it must have good strength. In this study, the crucible was obtained from GAREL Hırdavatçılık San. Ve Tic. A.Ş., Pota Şubesi. It is Diamant brand, "A2" shape and made of Clay Graphite. Graphite is an inert material and does not react to the metals. It is also durable to high temperatures and it does not loose its main composition at high temperatures.

Figure 3.12. Clay graphite crucible

Stirring Rods are made of carbon graphite and used for stirring molten metal. Graphite is good material for stirring because metal does not stick to it, it does not contaminate the metal, and it retards oxidation.

Figure 3.13. Stirring rods

Rock wool sheets and isolator bricks were used as a heat insulator. They have too low heat transfer coefficient so that the heated die and the crucible were put on them instead of directly to the ground. They prevented rapid cooling of die and melt in the die. They also did not allow the heat to transmit from die and crucible to the floor directly as a protection of experiment environment.

3.2.2.5. Safety Equipments

In this experiment, the temperatures were around 800°C for molten metals and 450°C for die and punch. If the molten material is splashed or heated die is touched to human body, it definitely causes serious injuries. In order not to face these accidents, the safety precautions were taken.

A mica visor, a pair of high temperature resistant gloves and leather protector cloths were used for protection of face, hands and body respectively.

Figure 3.14. Safety equipment set

3.2.3. Temperature Measurement Instruments

In this experimental study, high technologic electronic devices were used for thermal analysis. These equipments provided a more accurate and reliable measurement values. The measurements also were carried out faster and easier measurements.

3.2.3.1. Thermocouple

One of these points is in molten metal to measure molten metal temperature and the other two points are at the die to measure the die temperature.

K Type thermocouples were used in order to measure the temperature values at three different points. One of these points was in molten metal to measure molten metal temperature. The other two points were at the interface of molten metal and die and at the mid point of the die. The thermocouple connection hole locations are shown in Figure 3.11. Thermocouples were obtained from Meter A.Ş., Istanbul. K type thermocouples consist of Cr-CrNi wires which are squeezed with MgO powders and surrounded with Inconel 600 as an insulator. This insulation provides an accurate measurement while there is vibration and the wire is bended. The thermocouples, having a diameter of 1 mm and wire length of 50 cm, have a plug transmitting mV.

Figure 3.15. Ceramic insulated K type thermocouple

K type thermocouples are the most popular thermocouple type and offer a wide measurement range with good temperature precision.

3.2.3.2. Data Logger

In order to measure the temperatures and store these during cooling of squeeze cast alloy, Curve-X Data Logger, as a hardware, and Ideal Finish, as software, were used. Curve-X is obtained from Evren Dakro Kaplama, Bursa.

Table 3.2. Technical specifications of Curve-X Data Logger

Temperature Range	0 ^{o}C – 1200 ^{o}C
Accuracy	± 1
Resolution	± 0,3 ^{o}C
Thermal Couple Type	NiCrNi (K Type)
Number of Channels	6 pcs.
Sampling Interval	1 second to 18 hours
Total Memory	20400 data points
Battery Type	9V PP3

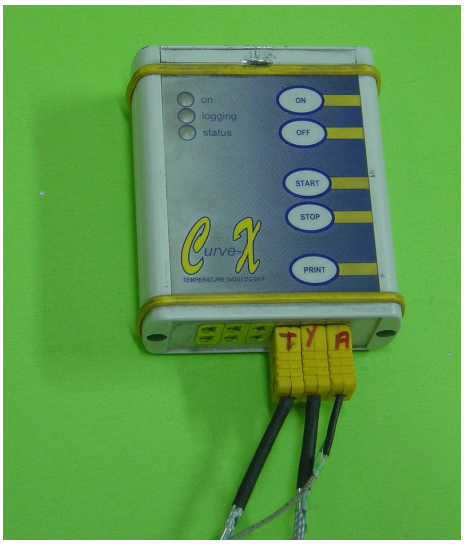

Figure 3.16. Curve-X Datalogger and thermocouple pin connection

The Curve-X is capable of obtaining 6 thermocouples at the same time. After locating the thermocouples to their location, then the pins of thermocouples are connected to the plugs of Curve-X. Then it is pressed on start button and the Curve-X starts to store the datas coming from thermocouples in given each time interval. After reaching to desired measuring time, it is pressed on stop button and Curve-X stops to store datas. Then Curve-X is connected to a PC via a serial port.

Figure 3.17. Temperature measurement set

The Curve-X Data Logger is supplied with Ideal Finish, an advanced temperature monitoring software package. With two user levels, basic and advanced, Ideal Finish offers user-friendly report functions for standard production work as well as advanced calculations for in-depth analysis of the casting processes. Detailed graphic representations and customizable reports help to make the right decisions to optimize the production line.

3.2.3.3. Infrared Camera

Infrared cameras are used to measure surface temperature of an object without touching it. Depending on the type of the lenses, the distance between the camera and object can be modified. These cameras are used in many industrial applications such as electrical systems, mechanical systems, refractory materials, vapor systems, construction materials and Research& Development applications.

In this experiment, an infrared thermal camera, FLIR brand, was rent from Sentez Optik Elektronik ve Endüstriyel Cihazlar Mühendislik Tic. Ltd. Şti., giving infrared

problem solutions service for two working days. The company also sent the operator of the camera as a supervisor to use the camera.

Table 3.3. Specifications of infrared camera

SPECIFICATIONS of INFRARED CAMERA	
Field of view/min focus distance	24° x 18° / 0.3 m
Spatial resolution (IFOV)	1.3 mrad
Electronic zoom function	2, 4, 8, interpolating
Focus	Automatic or manual
Digital image enhancement	Normal and enhanced
Detector type	Focal plane array uncooled microbolometer; 320 x 240 pxls.
Spectral range	7.5 to 13 µm
Thermal sensitivity @ 50/60Hz	0.08° C at 30° C
Temperature ranges	-40° C to +120° C (-40° F to +248° F), Range 1 0° C to +500° C (+32° F to +932° F), Range 2 +350° C to +1500° C (+662° F to +2732° F), Range 3 Up to +2000° C (+3632° F), optional
Accuracy (% of reading)	± 2° C or ± 2%
Emissivity corrections	Variable from 0.1 to 1.0 or select from listings in pre-defined material list
Measurement features	Automatic corrections based on user input for reflected ambient temperature, distance, relative humidity, atmospheric transmission, and external optics

Figure 3.18. Infrared camera

The infrared camera is able to capture both photos in each given time period and thermal movie. In our experiment, both functions were used; photos and movies during casting were obtained.

3.2.3.4. Infrared Thermometer

Infrared thermometers are used to measure temperature at a point on an object without touching it. The measuring distance range depends on the type of the thermometer. These thermometers are used in many applications varying from measuring the temperature of a machining tool in mechanical area to measuring the body temperature of babies in medical area. In our experiment, an infrared thermometer was used to measure the die temperature before pouring the molten alloy into die. It was also possible to measure it by thermocouples but infrared thermometer was easier, more safety and quicker.

Figure 3.19. Infrared thermometer

3.3. Squeeze Casting Practice

3.3.1. Preparing of Materials for Casting Process

The Al and Zn ingots were sliced into firstly moderate size pieces and then small pieces by Universal Horizontal Sawing Machine. The small pieces were weighted by an electronic scale and were classified in groups depending on their weights. For different weight intervals a separate bag was used for classification which is essential to gain time during preparation of Al and Zn amounts for casting to get the mass concentration of ZA-27.

Table 3.4. Number of Al and Zn sliced parts in classifying range

Range (grams)	Number of Part [Aluminum]	Number of Part [Zinc]
0 – 5	36	32
5 – 10	25	37
10 – 20	45	38
20 – 30	40	35

30 – 40	38	54
40 – 50	41	48
50 – 60	55	34
60 – 70	54	46
70 – 80	34	34
80 – 90	32	24
90 – 100	21	27
100 – 120	8	19
120 – 140	4	15
140 – 160	-----	13
160 – 200	-----	4

After classification of small metal parts, the packages were prepared for one casting experiment by the calculation below:

$$V_{Al} + V_{Zn} = V_{casting} \tag{3.3.1}$$

The densities of Aluminum and Zinc are 2,7 gr/cm^3 and 7,14 gr/cm^3 respectively. The volume of the mould is 73 cm^3. ZA-27 contains %27 Al and %73 Zn by mass. It could be represented as below:

$$\frac{m_{Al}}{m_{ZA-27}} = \frac{27}{100} \tag{3.3.2}$$

By substituting $m = d \times V$ in equation 3.3.2 we get:

$$\frac{2,7 \cdot V_{Al}}{7,14 \cdot V_{Zn} + 2,7 \cdot V_{Al}} = \frac{27}{100} \tag{3.3.3}$$

$$V_{Zn} = \frac{7,3}{7,14} V_{Al} \tag{3.3.4}$$

By substituting (3.3.4) in (3.3.1) we get:

$$V_{Al} + \frac{7,3}{7,14} V_{Al} = 73 = V_{mould} \tag{3.3.5}$$

By solving (3.3.5) all unknowns are found as below:

Table 3.5. Weight and volume values of Al, Zn and casting

	Aluminum	Zinc	Casting
Volume (cm^3)	36,1	36,9	73
Mass (gr)	97,5	263,5	361

During casting the total volume of the molten materials should be more than the volume of the mold. So, the mass amount of Al and Zn were taken 25% -26 % more than that is shown in Table 3.5. for preparation of ready packages for casting. The amount of Al and Zn were taken as 123 gr. and 332 gr. respectively and each ready package was prepared with these amounts.

Figure 3.20. Weighing of Al and Zn for ready packages

Figure 3.21. Ready packages

3.3.2. Casting of Unsqueezed ZA 27 Alloy

Firstly the two furnaces, annealing and melting furnaces, were switched on. The annealing furnace was set to 550°C and started. The die was disassembled and two sides of the die cavity were cleaned by a wire brush and all the dusts were removed. Then the die was assembled and put into annealing furnace. The melting furnace was set to 800°C and started.

Setting temperature values of furnaces is an important subject. In order to decrease the heating time of the die or melting time of the aluminum in the crucible, heat flux from the furnaces to the crucible or die must be increased. The melting temperature of the aluminum is 660°C and there is also an additional transformation heat to change the aluminum from solid to liquid phase. Considering this transformation heat, it is needed more heat flux which can be achieved by a furnace set to higher temperature values. The higher temperature means higher heat flux from the furnace to the die or crucible. In order to do all mentioned above, the melting furnace was set to 800°C and annealing furnace was set to 550°C.

The crucible was cleaned with a wire brush. One of the early prepared ready package including right mass amounts of Al and Zn to get ZA-27 is opened and Al slices were put into the crucible. The crucible was put into melting furnace and furnace cover was closed.

When the aluminum slices inside the crucible were melt, mica visor, gloves and protecting cloth was put on and the crucible was taken out from the furnace on an isolator brick. The zinc slices, from already opened ready package, were put into crucible and the crucible was located into furnace again. The crucible was waited at least until melting of all zinc slices.

Figure 3.22. Taking out the crucible from melting furnace

Meanwhile on the other the die in the annealing furnace was temporarily taken out of the furnace and the temperature of the die was checked by infrared thermometer whether it was reached to 325°C or not. If it is not, it is needed to heat more. The die was taken out and put on isolator brick when it reached to 325°C. The infrared camera is located to capture whole view of die and pouring process. The three thermocouples were located to the holes on the die and connected to Curve-X Data Logger. Curve-X and infrared camera were started to record.

Figure 3.23. Connection of thermocouples to Curve-X and die

Figure 3.24. Recording of thermal distribution of die outer surface

The die temperature was checked periodically by infrared thermometer whether the temperature was decreased to 290°C or not. The crucible was taken out and put on isolator brick when the die's temperature dropped to 290°C. The molten ZA-27 was stirred by stirring rods. The slags covering top surface of molten ZA-27 were cleaned.

Figure 3.25. Stirring of molten metal in crucible

When the die temperature was 285°C, the molten ZA-27 was poured into die cavity by holding the crucible with tongs.

Figure 3.26. Pouring molten metal into the die

Figure 3.27. Molten ZA-27 alloy just poured

After 8-10 minutes passed from pouring, the infrared camera and Curve-X Data Logger were stopped, the thermocouples were removed from the die, the die was disassembled and the specimen was taken out by holding with tong. The specimen was kept in rock wool to provide a slow cooling rate and avoid structural tension.

Figure 3.28. Specimen while taken out from the die

There are two essential points for pouring the molten metal. One of them is that the pouring process must be continuous and should not be interrupted. Any interruption causes nonhomogenous structure including air gaps. The second point is the volume of the poured molten metal. When molten metal is poured into the die, it shrinks. So, the final length of specimen becomes shorter. In order to avoid shrinkage problem, the poured molten metal volume should be more than the volume of die cavity.

3.3.3. Casting of Squeezed ZA-27 Alloy

In squeeze casting, the hydraulic cylinder set was used. This set consists of one hydraulic cylinder, hydraulic pump and oil tank. The diameter of the hydraulic cylinder is 100 mm . There is an indicator showing the pressure value. The desired pressure level is adjusted by a screw on the manual control arm.

Figure 3.29. Hydraulic cylinder set

In this experiment, squeeze casting was performed by 100 MPa and 150 MPa pressures. These are the pressures applied on the molten metal which was poured in the die cavity. Firstly, the indicator was set to a pressure value which would be applied on the molten metal by a calculation depending on the diameter sizes of hydraulic piston and punch. This calculation is based on the applied force by cylinder is directly transmitted to

the punch and also molten metal. The applied force is same for the whole system as written in Equation 3.3.6.

$$F_{Cylinder} = F_{Punch} \tag{3.3.6}$$

$$P_{Cylinder} \times A_{Cylinder} = P_{Punch} \times A_{Punch} \tag{3.3.7}$$

$$P_{Cylinder} \times \frac{\pi \cdot D_{Clinder}^2}{4} = P_{Punch} \times \frac{\pi \cdot D_{Punch}^2}{4} \tag{3.3.8}$$

$$P_{Cylinder} = P_{Punch} \times \left(\frac{D_{Punch}}{D_{Cylinder}} \right)^2 \tag{3.3.9}$$

Table 3.6. Squeezing Pressure Values

Diameter of Hydraulic Cylinder	Diameter of Punch	Pressure 1 on Molten Metal	Pressure 2 by Hydraulic Cylinder
100 mm.	25 mm.	100 MPa	63,5 kg/cm^2
100 mm.	25 mm.	150 MPa	95,5 kg/cm^2

Pressure 1 values are the desired pressure values. Using the diameter values and Equation 3.3.9., the pressure adjusted by a screw on the manual control arm to Pressure 2 values.

In the experiment, for 100 MPa and 150 MPa desired pressure values, the hydraulic cylinder was set to 63,5 kg/cm^2 and 95,5 kg/cm^2 respectively

The all practice, made for unsqueezed ZA-27 alloy, was repeated again. This time punch also was heated together with the die.

The die temperature was checked periodically by infrared thermometer whether the temperature was decreased to 290°C or not. The crucible was taken out and put on isolator

brick near the hydraulic cylinder when the die's temperature dropped to 290°C. At the same time, the punch was also taken out from the annealing furnace and put near to die. A tong was put near to die to hold the punch without any time delay. The molten ZA-27 was stirred by stirring rods. The slags covering top surface of molten ZA-27 were cleaned. When the die temperature was 285°C, the molten ZA-27 was poured into die cavity by holding the crucible with tongs. After pouring, the die was immediately located on to the press table with the biggest size tongs. The punch was held with smaller tongs and it was put onto the die cavity. The lever of squeeze casting hydraulic cylinder was immediately pushed on the top surface of the punch. So, the punch was pressed on molten metal. At the same time with pushing lever, a chronometer was started in order to apply the pressure on the molten metal for 103 seconds. By pressing, the specimen was started to squeeze. After 103 seconds the lever was pulled back, the cylinder went up and pressing on molten metal was ceased.

Figure 3.30. Data collection by infrared camera and Curve-X

After 8-10 minutes passed from pulling the lever back, the infrared camera and Curve-X Data Logger were stopped, the thermocouples were removed from the die, the die was disassembled and the specimen was taken out by holding with tong. The specimen was kept in rock wool to provide a slow cooling rate and avoid structural tension.

If the punch is drawn into the die too much or too less, the squeeze casting becomes unsuccessful. Then the lever was pulled back, the thermocouples were removed, the die was disassembled and the specimen was removed. The two parts of die was cleaned by wire brush, the die was assembled and put into annealing furnace again. The allowable entering degree of the punch is middle. The punch should draw into die until to the middle of its range.

3.4. Thermal Analysis

The thermal analysis was carried out by two methods. In the first method the temperature values at three different points were measured by thermocouples and Curve-X. In the second method, the temperature value distribution on the die surface was obtained by infrared camera.

3.4.1. Temperature Measurement and Cooling Curve Determination

In this experiment, three thermocouples were put into three different points at die. One of these points was in molten metal to measure molten metal temperature. The other two points were at the interface of molten metal and die and at the mid point of the die. The thermocouple connection hole locations and thermocouple end point locations are shown in Figure 3.11. and Figure 3.31. respectively.

The thermocouples are connected to Curve-X Data Logger. Curve-X is able to store temperature values in each given time interval. This time interval was set one second in this experiment. So, each second Curve-X stored one measured temperature value from each thermocouple. By the integrated software program to Curve-X, named Ideal Finish, these temperature values were listed in a list and temperature vs. time graphics were drawn. These graphics are called cooling curves. In Ideal Finish software, when mouse point is moved to any point on the cooling curve, the time and temperature values belonging that point is written on the screen. It is also possible to zoom in and zoom out at these curves. This property allows the users to get information about sudden changes. There are two working platforms, advance and basic, of Ideal Finish. In this experiment, advance working platform always was used since it provides more facilities to user.

The three probes used for this experiment was given number from 1 to 3. These probe numbers, as seen in Table 3.7., indicate the location of the probes and the location and correspondent number did not change for the whole project.

Table 3.7. Probe numbers and locations

Probe No 1	In molten metal
Probe No 2	Midpoint of the die
Probe No 3	Interface of molten metal and die

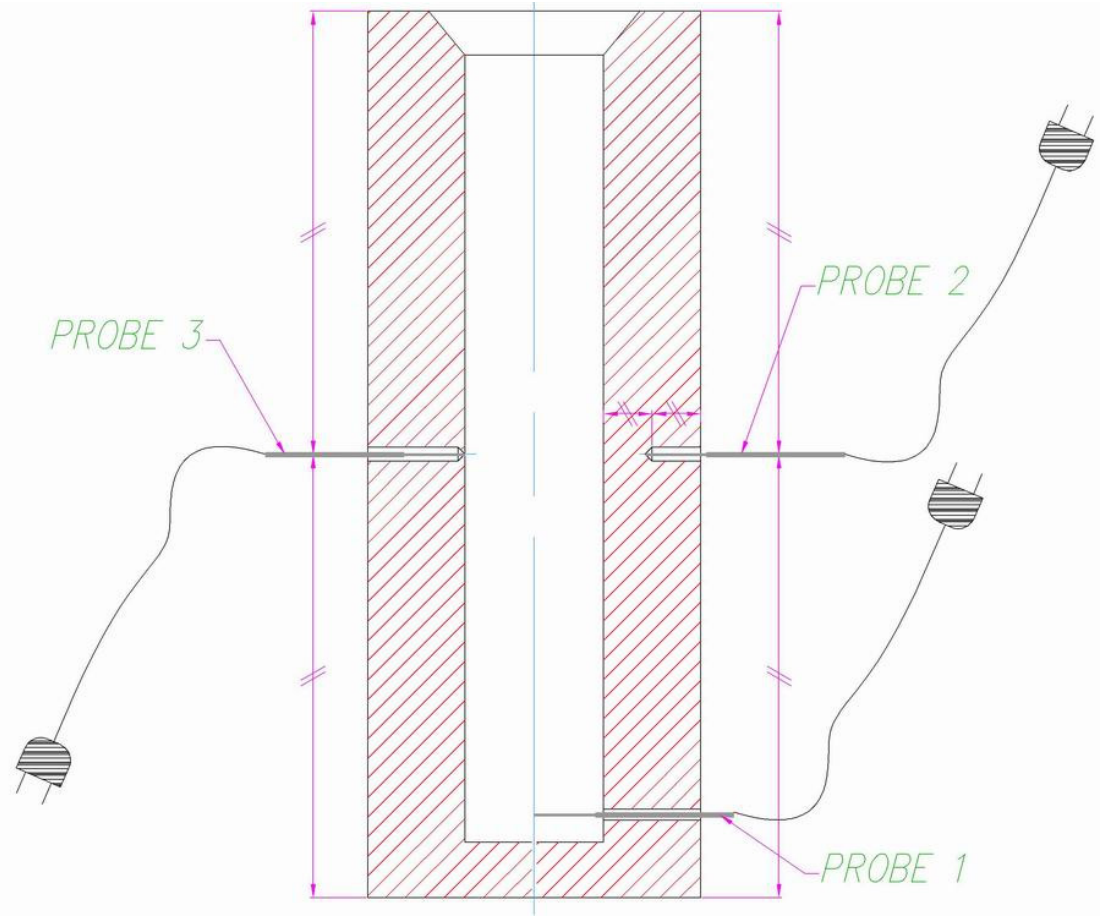

Figure 3.31. Thermocouple end point locations

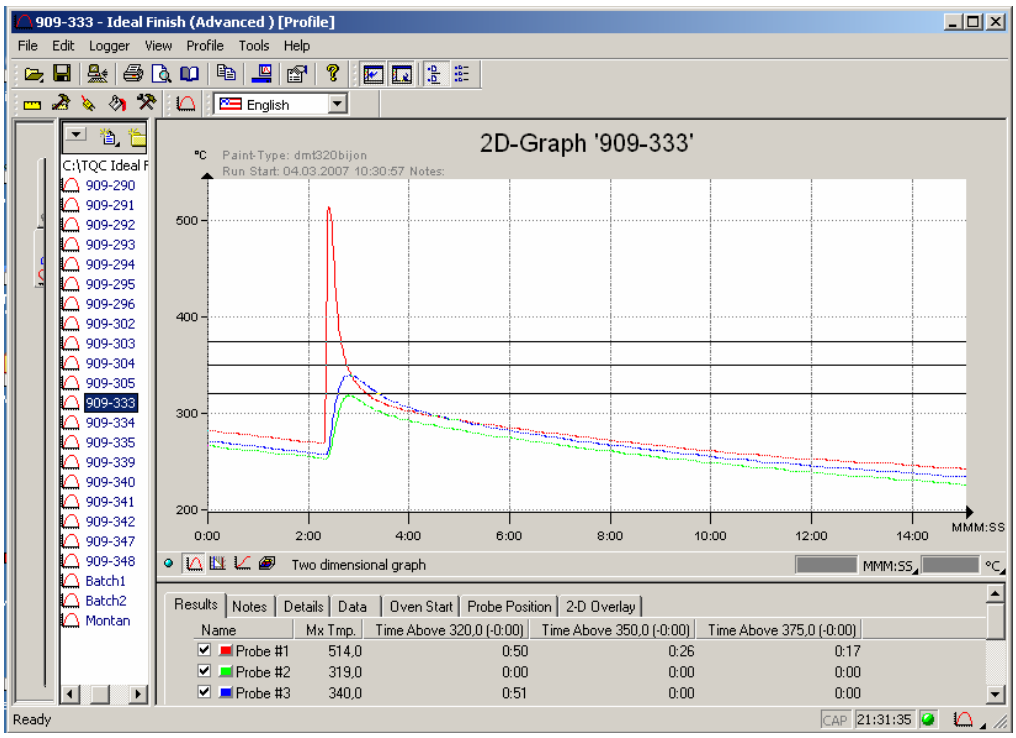

Figure 3.32. Cooling curve for specimen 10 (P=0,1 MPa) by Ideal Finish©

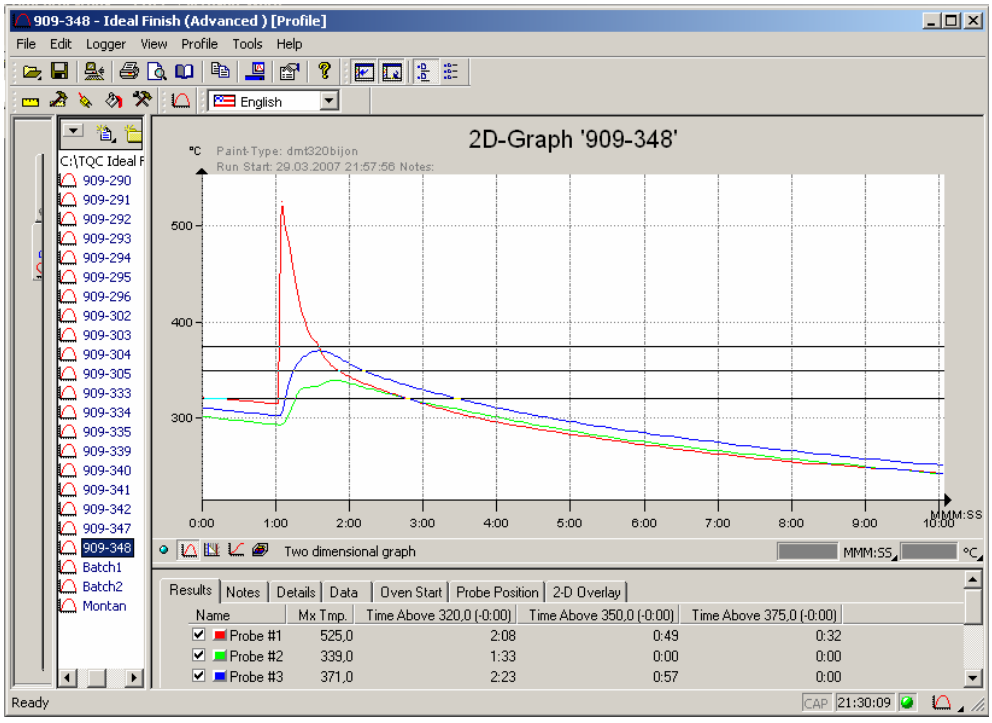

Figure 3.33. Cooling curve for specimen 17 (P=150 MPa) by Ideal Finish©

3.4.2. Die Surface Temperature Distribution Analysis

In this experiment, an infrared camera was rented from Sentez Optik Elektronik ve Endüstriyel Cihazlar Mühendislik Tic. Ltd. Şti. Its brand was FLIR Thermal Systems. The company also assigned one supervisor to operate the camera. The operator located the camera to a point having a good view of die. He also adjusted all settings and started the camera to record. A software program, named Irwin Image, was also given by the operator. This software lets loading picture files taken during casting process and work on them. By clicking any point on the picture, taken by infrared camera, this software indicated the temperature value of clicked point.

For the specimen no 11, the temperature values, at twelve different points on the same line was lying at the diagonal of die, were collected by Irwin Image for time intervals. The diagonal line and the twelve points lying on it are seen in Figure 3.34.

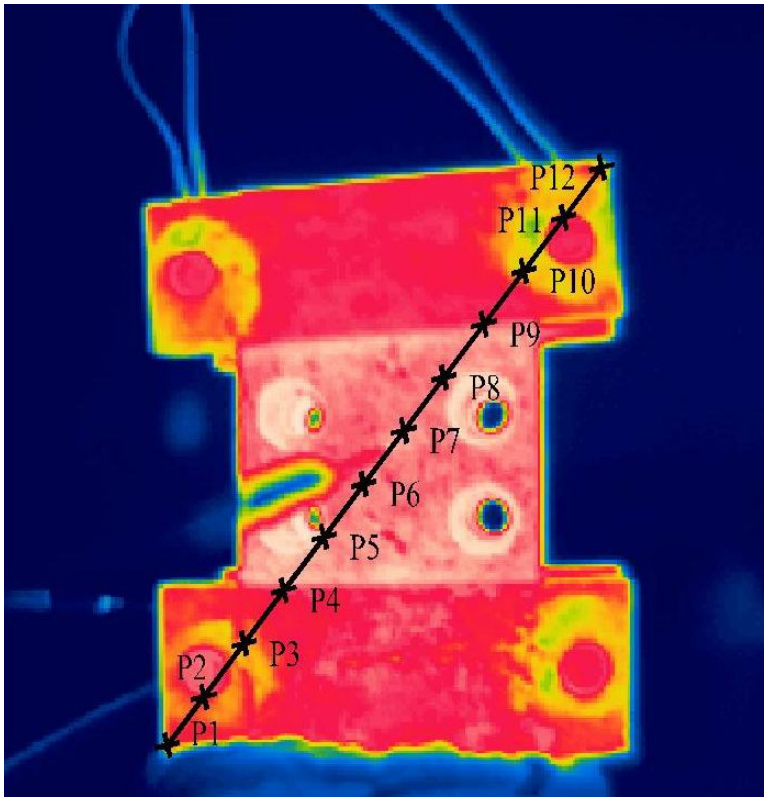

Figure 3.34. Diagonal line with twelve points lying on it

These time dependent values were inserted in Microsoft Excel© and the related graphics were obtained. Beside this examination, for the specimen no 13, the maximum and minimum die surface temperature values also were investigated. The related graphics were drawn considering the time of pouring metal and starting squeezing. The temperature changing after pouring molten metal and starting squeezing was observed in these graphics.

The working principle of infrared cameras is the thermal diversities on a surface. If the temperature values on the surface are almost same, then the colour scale become too narrow and the coloured images, taken by infrared camera, represents almost same colour. It becomes difficult to observe the colour changes in the images. In this experiment, the die was 285 °C at the beginning of molten metal pouring. 285°C was quite high temperature value comparing the molten metal temperature just after pouring had started. So, the temperature changes were not observed very clearly. In order to see the temperature changes better, the casting experiment were carried out with cold die one time instead of preheated. At this time, pouring a molten metal having a temperature over 600°C was poured into a die having 19°C temperature value that was room temperature. So, the temperature differences were too high that the colour changes, in the thermal camera images, were observed very clearly. The thermal images of the experiment with cold die are shown in Appendix A.

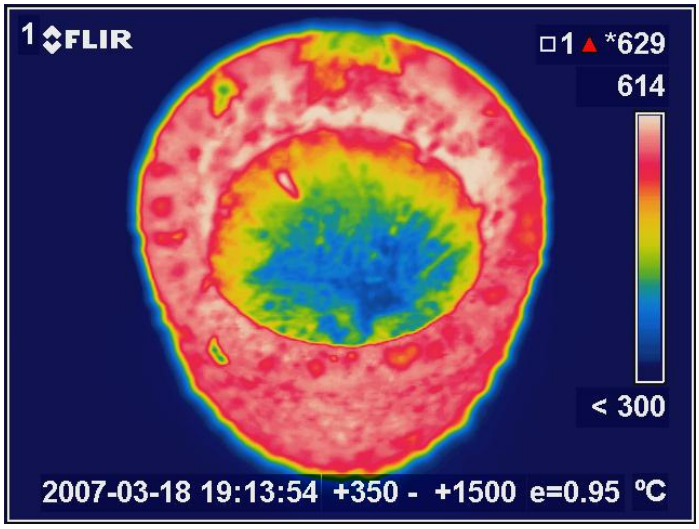

Figure 3.35. Thermal photo of crucible before pouring the molten metal to die cavity

In the figure 3.35, the thermal distribution of crucible surface is seen. The blue color region is around 300-400 °C. In fact this blue region is the surface of molten metal and supposed to have higher temperature. This is a result of cooled slag layer on the molten metal surface.

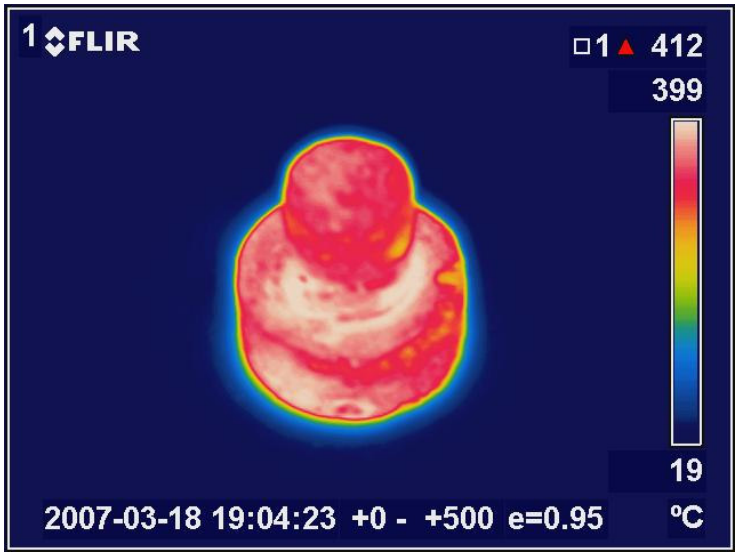

Figure 3.36. Thermal photo of the punch

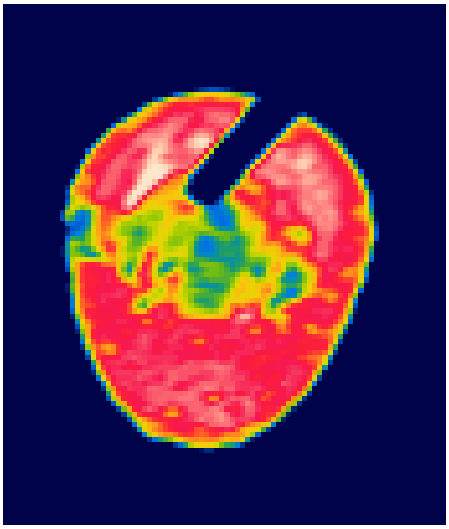

Figure 3.37. Thermal photo of stirring molten metal by stirring rods

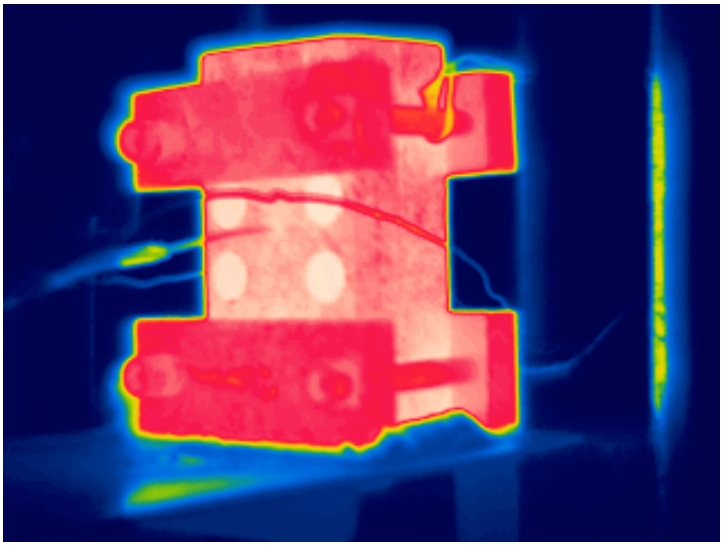

Figure 3.38. Thermal photo of the die just before pouring molten metal

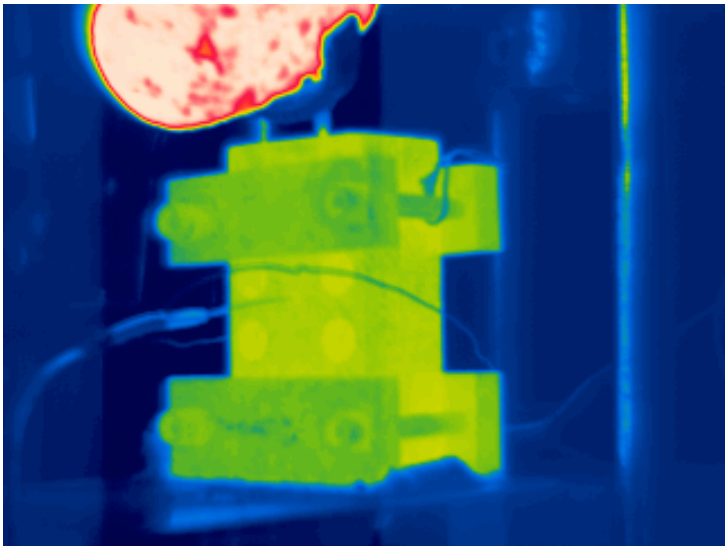

Figure 3.39. Thermal photo of pouring molten metal into the die cavity

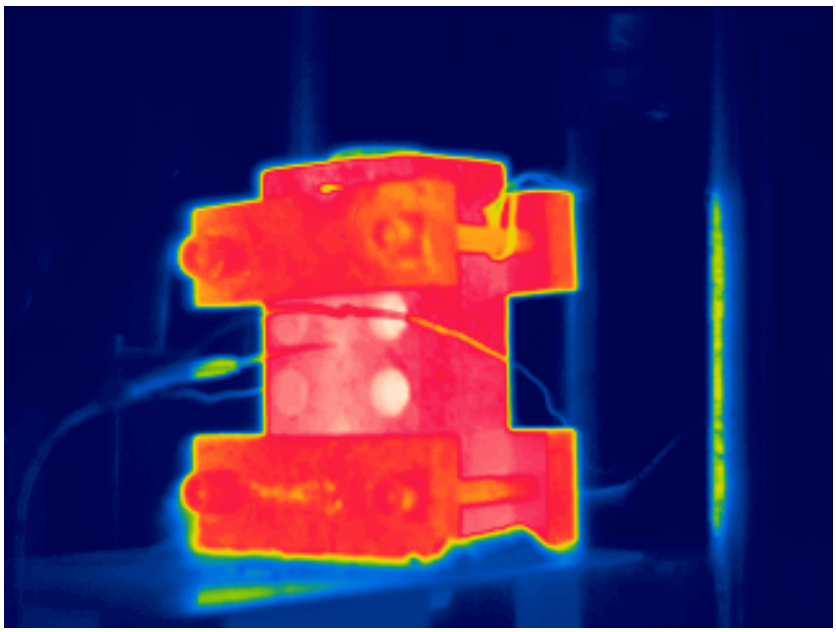

Figure 3.40. Thermal photo of the die just after pouring molten metal

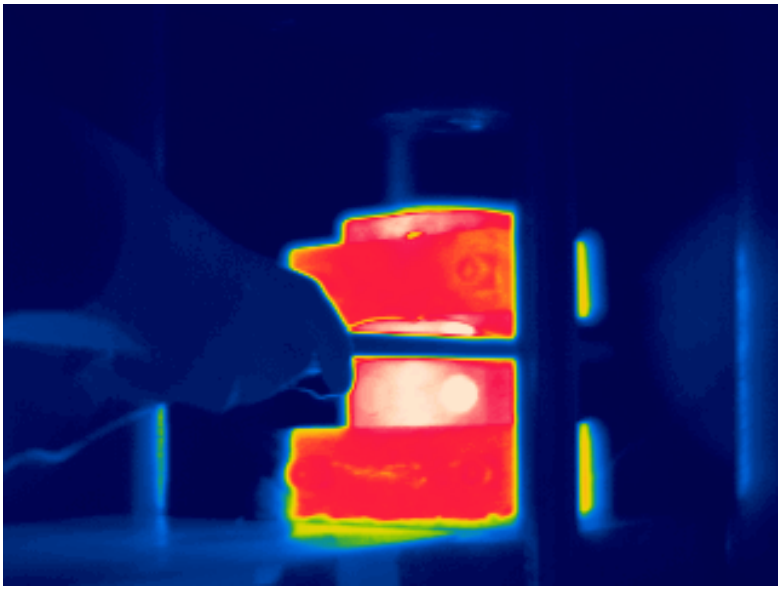

Figure 3.41. Thermal photo of locating the die under hydraulic cylinder

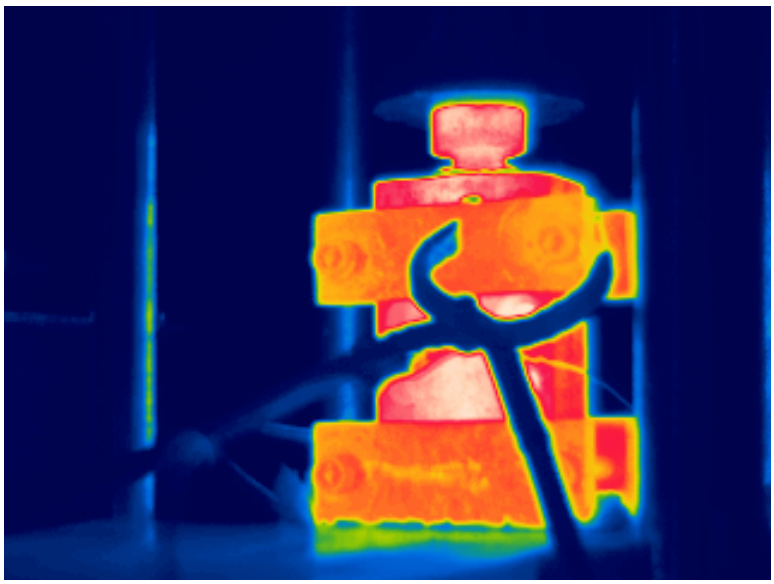

Figure 3.42. Thermal photo of locating punch and starting squeezing

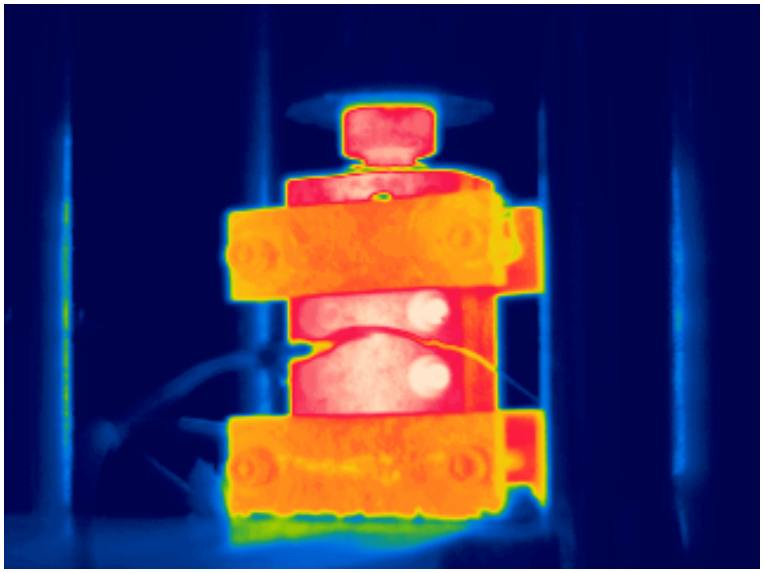

Figure 3.43. Thermal photo during squeezing

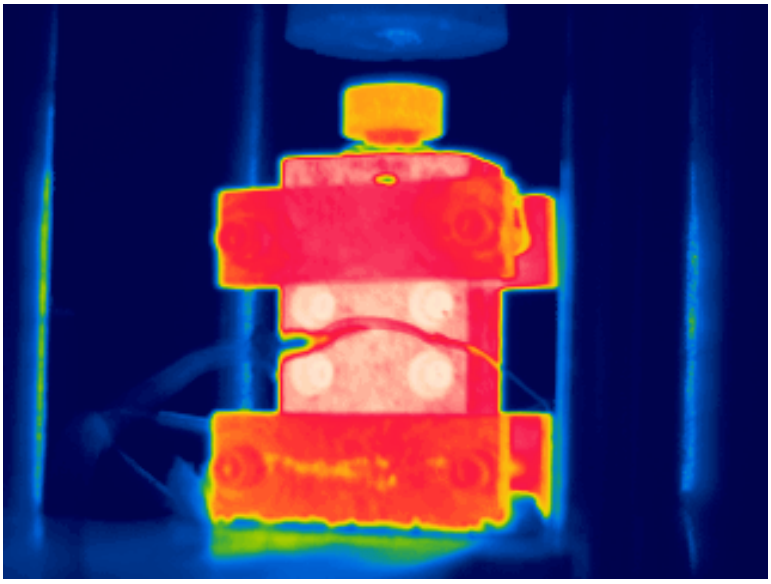

Figure 3.44. Thermal photo of the die after squeezing

FLIR infrared cameras have two temperature sensing scale. One of them is less than 500 °C, and the other one is between 501 – 1500 °C. If 0-500 °C degree scale is chosen then the objects having surface temperature greater than 500°C are not sensed and recorded by the camera. In the same way if 501-1500 °C degree scale is chosen, then the objects having surface temperature less than 501 °C are not sensed and recorded. In Figure 3.39, the die is not seen in colours but the crucible is seen in colours. This is due to choosing 501-1500 °C scale. At that figure, surface temperature of the die was around 285 °C while it was around 650 °C at crucible It means that the die surface temperature was less than 500 °C and the crucible surface temperature was greater than 500 °C.

3.5. Material Property Analysis

3.5.1. Chip Length Measurement

Almost all of the specimens at each squeeze casting pressure were subjected to chip length analysis since chip length is one of the main indicator of the machinability of the material. The specimens were machined by lathe with a high speed steel cutting tool. Four different turning speeds were used for cutting. The axial movement speed of the tool was kept as constant for four different turning speeds. The turning speeds were 180 rpm, 355 rpm, 710 rpm, and 1000 rpm. When the turning speed is increased, then automatically the axial movement speed of tool is increased. So, in order to keep axial speed constant, the gear of lathe was changed for each turning speed. In the experimental practice, firstly the lathe was started to turn with 180 rpm. At that turning speed, the tool moved 42 mm in 1 minute in axial direction. This displacement was measure by a digital position meter integrated on lathe machine. This axial movement speed was obtained also for the other three turning speeds which are 355 rpm., 710 rpm and 1000 rpm.

Table 3.8. Turning and Axial Speeds of Lathe

Turning Speed	Gear	Axial Movement Speed
180 rpm	A3	42 mm / min
355 rpm	B1	42 mm / min
710 rpm	B3	42 mm / min
1000 rpm	B1	42 mm / min

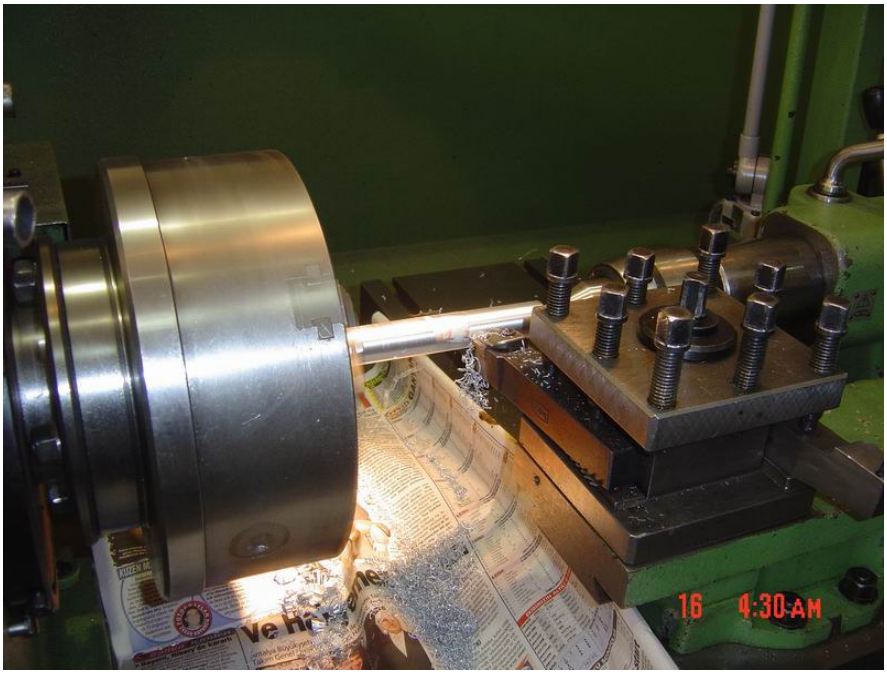

Figure 3.45. Chip collection

For all parts, firstly a cleaning pass was applied by lathe. The lengths of the specimens were measured. The pass depth was set as 1mm. for all specimens. Then 1/4 of the length of specimen was machined at 180 rpm. From 1/4 to 1/2 of the length, the specimen was machined at 355 rpm. From 1/2 to 3/4 of the length, the specimen was machined at 710 rpm. The last quarter of the length of specimen was machined at 710 rpm. For all speeds, the chips were collected and put into different nylon bags. The part number and turning speed values; and also date of experiment were written on the nylon bags for classification. It was too essential to prevent the chips from braking off while collecting them.

Figure 3.46. Chip collection in nylon bags

After collecting all chips, their lengths were measured by the help of ruler and smallest pliers. All collected data was recorded and evaluated based on turning speed of lathe.

3.5.2. Surface Roughness Measurement

Surface topography is of great importance in specifying the function of a surface. A significant proportion of component failure starts at the surface due to either an isolated manufacturing discontinuity or gradual deterioration of the surface quality. Typical of the former is the laps and folds which cause fatigue failures and of the latter is the grinding damage due to the use of a worn wheel resulting in stress corrosion and fatigue failure. The most important parameter describing surface integrity is surface roughness. In the manufacturing industry, surface must be within certain limits of roughness. Therefore, measuring surface roughness is vital to quality control of machining work piece.

The roughness of a surface can be measured in different ways which are classified into three basic categories

- Statistical descriptors that give average behavior of the surface height. For example, average roughness Ra; the root mean square roughness Rq; the skewness Sk and the kurtosis K.

- Extreme value descriptors that depend on isolated events. Examples are the maximum peak height Rp, the maximum valley height Rv, and the maximum peak to valley height Rmax..

- Texture descriptors that describe variations of the surface based on multiple events. An example for this descriptor is the correlation length.

Among these descriptors, the Ra measure is one of the most effective surface roughness measures commonly adopted in general engineering practice. It gives a good general description of the height variations in the surface. The following figure shows a cross section through the surface , a mean line is first found that is parallel to the general surface direction and divides the surface in such a way that the sum of the areas formed above the line is equal to the sum of the areas formed below the line. The surface roughness Ra is now given by the sum of the absolute values of all the areas above and below the mean line divided by the sampling length. Therefore, the surface roughness value is given by equation 3.5.1.

$$Ra=(|\text{area abc}|+|\text{area cde}|)/f \qquad (3.5.1.)$$

where f is the feed.

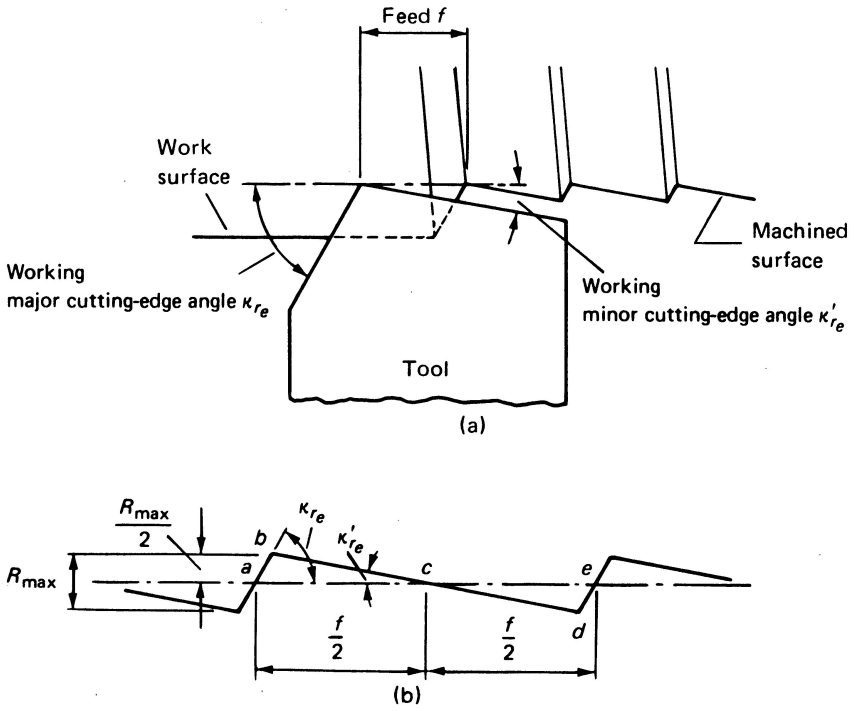

Figure 3.47. Surface roughness geometry [18]

Figure 3.48. Surface roughness measurement machine in KOSGEB - Istanbul

Inspection and assessment of surface roughness of machined workpieces can be carried out by means of different measurement techniques. These methods can be ranked into the following classes:

- Direct measurement methods
- Comparison based techniques
- Non contact methods
- On-process measurement

In this experiment, some of the specimens, from each squeeze casting pressure, were subjected to surface roughness test. Firstly all the specimens were machined by lathe as a cleaning pass of 0,5 -1 mm. Then, they were machined by lathe as 1 mm. pass at 1240 rpm turning speed. The surface roughness tests were done in KOSGEB-IMES in Istanbul.

3.5.3. Brinell Hardness Test

Hardness is a measure of the resistance of a metal to permanent (plastic) deformation. The hardness of a metal is measured by forcing an indenter into its surface. The indenter material, which is usually a ball, pyramid, or cone, is made of a material much harder than the material being tested. For example hardened steel, tungsten carbide, or diamond are commonly used materials for indenters [23].

The hardness of a metal depends on the ease with which it plastically deforms. Thus a relationship between hardness and strength for a particular metal can be determined empirically. The hardness test is much simpler than the tensile test and can be nondestructive. For these reasons, the hardness test is used extensively in industry for quality control [23].

Brinell hardness is determined by forcing a hardended steel or carbide sphere of a specified diameter under a specified load into the surface of a material and measuring the

diameter of the indentation left after the test. The Brinell hardness number, or simply the Brinell number, is obtained by dividing the load used, in kilograms, by the actual surface area of the indentation, in square millimeters. The result is a pressure measurement, but the units are rarely stated.

The Brinell hardness test method consists of indenting the test material with a 10 mm diameter hardened steel or carbide ball subjected to a load of 3000 kg. For softer materials the load can be reduced to 1500 kg or 500 kg to avoid excessive indentation. The full load is normally applied for 10 to 15 seconds in the case of iron and steel and for at least 30 seconds in the case of other metals. The diameter of the indentation left in the test material is measured with a low powered microscope. The Brinell harness number is calculated by dividing the load applied by the surface area of the indentation.

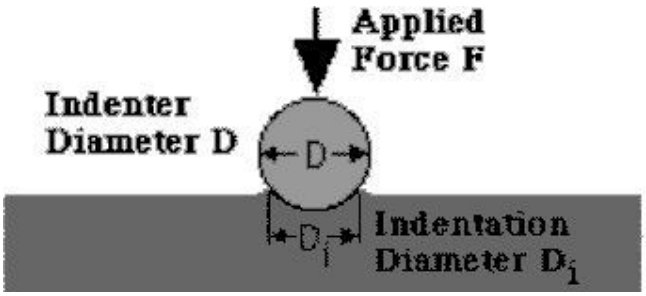

Figure 3.49. Schematic illustration of Brinell testing method

$$BHN = \frac{2F}{\pi \cdot D \cdot (D - \sqrt{D^2 - D_i^2})} \qquad (3.5.2.)$$

The specimens were also used for hardness determination in KOSGEB in Istanbul. Brinell method was carried out with 62.5 kg. pressing force, 2.5 mm. ball diameter and 15 seconds pressing time. The ball material is Wolfram Carbide. The left sides of the specimens were machined to get a fine and smooth surface with circular section. This surface was subjected to hardness test.

Figure 3.50. Brinell testing machine in KOSGEB - Istanbul

Figure 3.51. Magnified vision of the track formed by Ø2,5 mm. Wolfram Carbide ball

Figure 3.52. Samples were subjected to Brinell Hardness Test

3.5.4. Tensile Testing

Tensile testing is used to evaluate the strength of metals and alloys. In this test a metal sample is pulled to failure in a relatively short time at a constant rate. Figure 3.53 illustrates schematically how the sample is tested in tension.

The force (load) applied on the sample being tested is plotted by the instrument on moving chart graph paper, while the corresponding strain can be obtained from a signal from an external extensometer attached to the sample and also recorded on the chart paper

The force data obtained from the chart paper for the tensile test can be converted to engineering stress data, and a plot of engineering stress vs. engineering strain can be constructed.

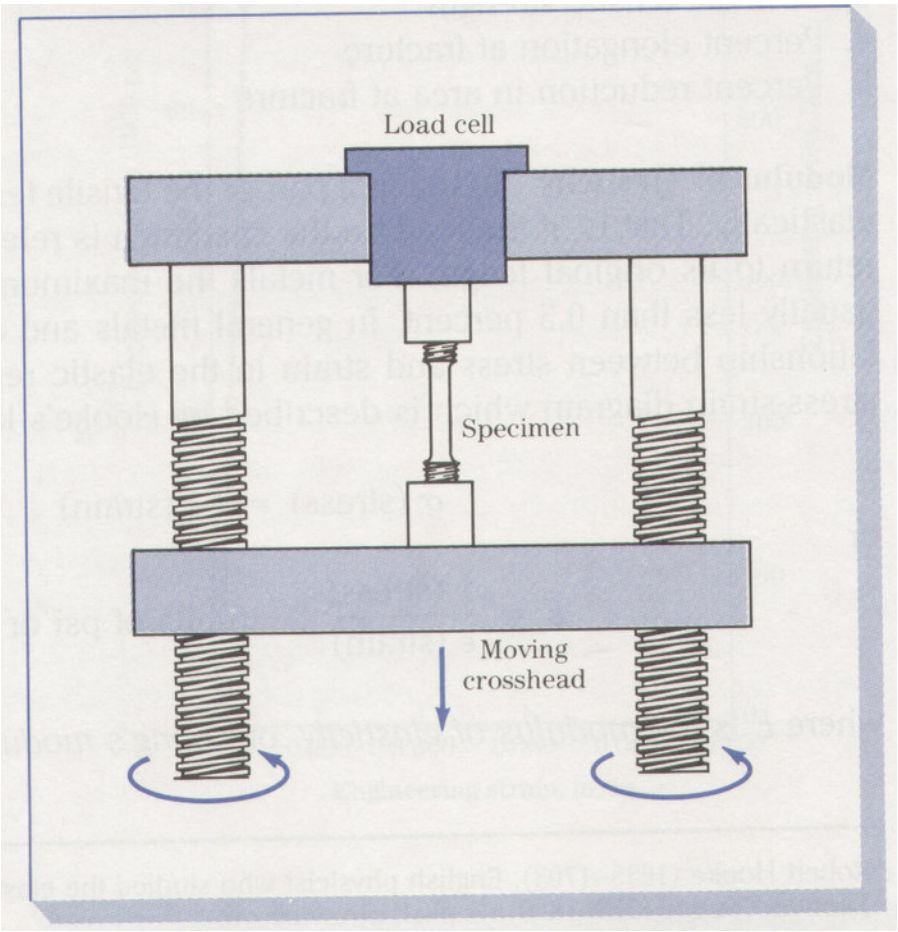

Figure 3.53. Schematic illustration showing how the tensile machine operates

The mechanical properties of metals and alloys which are of engineering importance for structural design and which can be obtained from engineering tensile test are:

- Modulus of elasticity
- Yield strength at 0.2 percent offset
- Ultimate tensile strength
- Percent elongation at fracture
- Percent reduction in area at fracture

In this experiment, three specimens, from each squeeze casting pressure, were subjected to tensile testing in KOSGEB Istanbul. Specimens were machined to a standard for the tensile testing according to ASTM E8 standard in Ceylan Makina Montaj. The tensile test was applied to the specimens by a tensile test machine named DARTEC RF-91146 Universal Tensile & Press Test Machine. It had a capacity of 1200 kN.

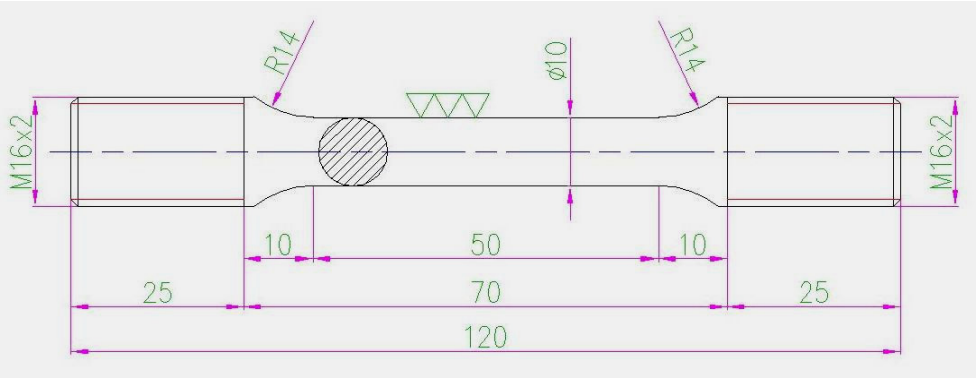

Figure 3.54. Technical drawing of machined tensile test specimen

The experimental procedure of tensile testing is as follows:

- Specimens were machined in Ceylan Makina Montaj, according to ASTM E8 standards. The two ends of the part were treaded M16x2 to match with specimen holder. The length of tread, gage diameter, gage length and total length of the specimens were 25, 10, 60 and 130 mm respectively.

- The testing machine had already been set up and calibrated by the lab assistant.

- The specimen was mounted to the bottom grip and upper grip respectively.

- After all controls, the operator pressed on start button.

- By giving preload, tensile machine firstly eliminated the space between machine heads.

- Machine started to stretch the specimen and after a while a cracking sound was heard and the specimen cracked. The heads were separated and two parts of the specimen were taken out from the grips by unfastening the treads.

- The two parts was wrapped with a clean handkerchief and put in a nylon bag on which the code of the specimen had already been written. The air inside this nylon bag was vacuumed by suctioning orally and the damage of air to the fractured surface was prevented. To keep the fractured surface stable and undamaged is very essential for having accurate results from SEM analysis.

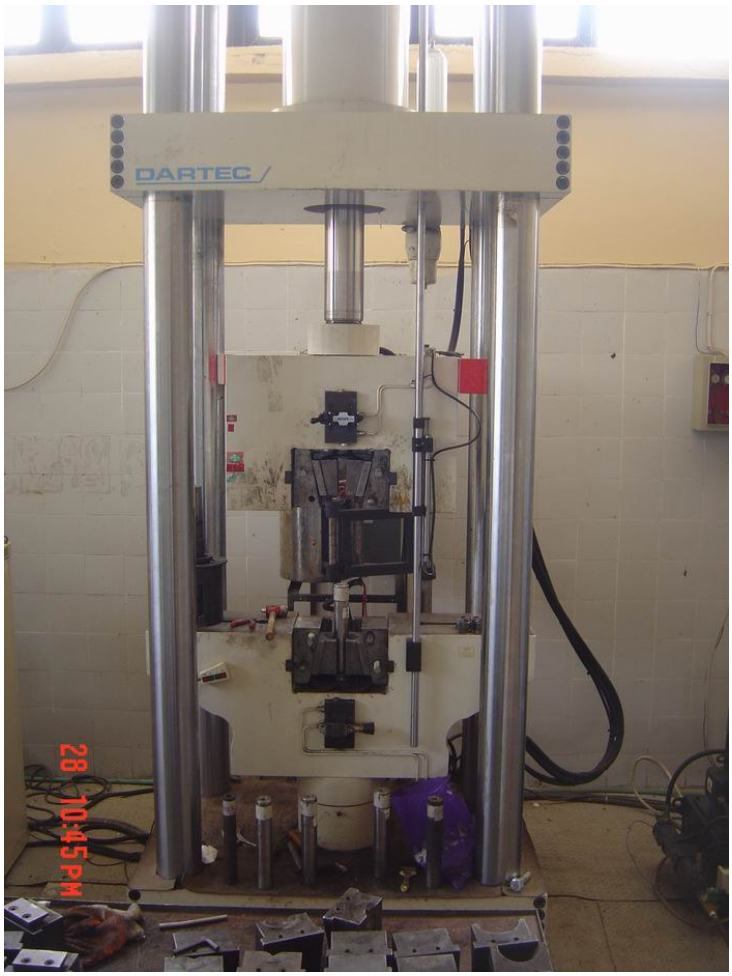

Figure 3.55. Tensile testing machine in KOSGEB - Istanbul

Figure 3.56. The specimen connected to upper and bottom grip in KOSGEB - Istanbul

3.6. Microstructural Examination

3.6.1. Investigation with Scanning Electron Microscope

Eight specimens which had been squeezed by different pressures were investigated by Scanning Electron Microscope in Material Institute at MAM Tübitak Gebze. After tensile testing of eight specimens in KOSGEB Istanbul, one part of each broken pair was cut by a fret saw from fifteen millimeters away the fracture surface. The surfaces, which were cut by saw, were also polished by sand paper. On the other hand, the fracture surfaces were not touched to any object. These eight small specimens were wrapped by a clean towel carefully without touching the fracture surface and then located in small nylon bags. The air inside these bags was vacuumed to prevent the oxidation effects of air on fracture surface.

In MAM Tübitak Gebze, these eight small specimens were separated into two groups involving four specimens in each. Four specimens in same group were inserted in SEM together on a same adaptor as it is seen in Figure 3.57.

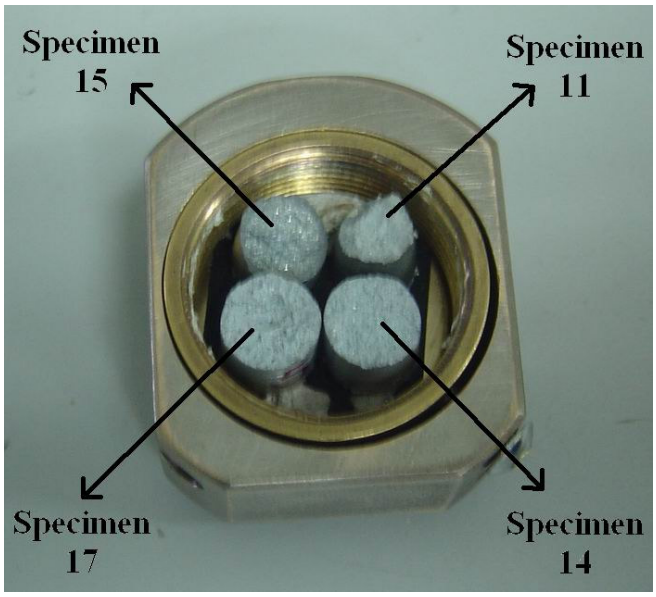

Figure 3.57. Four specimens mounted on a adaptor

Four specimens were mounted on the adaptor by a carbon tape having electrical conductivity. Then the adaptor was inserted in Scanning Electron Microscope.

Figure 3.58. Inserting of adaptor in SEM

Figure 3.59. Scanning Electron Microscope in MAM Tübitak Gebze

For eight specimens, totally 28 photographs were taken by SEM with different magnifications such as 30X, 100X, 250X and 500X. Beside this, four specimens were also subjected to sectional chemical analysis for investigating the both weight and atomic percentages of Zn and Al elements on fracture surface.

3.6.2. Metallographic Investigation

Metallographic observation for three specimens which had been squeezed with different pressures, were done in Material Institute at MAM Tübitak Gebze. The specimens 11, 14 and 17, which had been squeezed 0,1 MPa, 100 MPa and 150 MPa respectively, were used for this analysis. After SEM analysis, three specimens were located on a capsule that was dipped in a bakelite mold preparation machine which is seen in Figure 3.60. The capsule was filled with molding bakelite powder. Then the capsule was heated up to 180°C for melting the powder. When the bakelite powder was melted, it surrounded the three specimens. The inside of capsule was cooled by water indirectly and finally a cylindrical sample involving three specimens surrounded by bakelite was obtained as in Figure 3.61.

Figure 3.60. Bakelite mold preparation machine

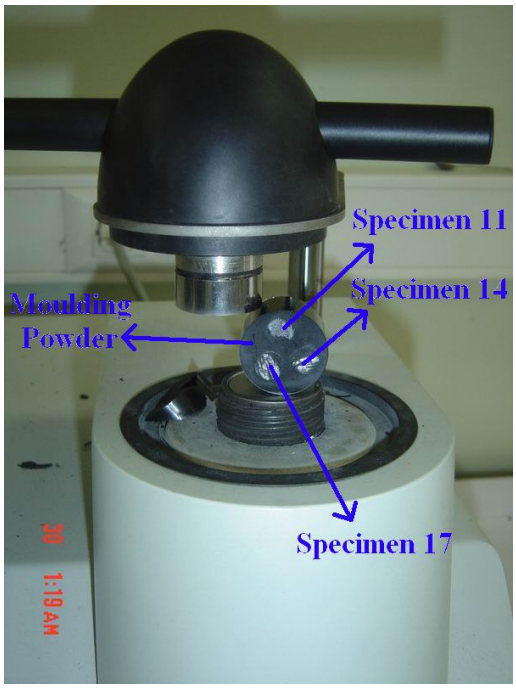

Figure 3.61. Cylindrical sample involving three specimens surrounded by bakelite

Using this bakelite, the samples were easily handled. After this hot molding, the fine sanding process was subjected to the sample. The sample was sanded starting from low grids to high grids. 600, 1200 and 2500 grids emery papers were used in given order. Then as a final step of fine sanding, 3 micron diamond broadcloth was used for sanding. After these operations, polishing step was started and the sample was polished by broadcloth involving colloidal 0.05 micron silica solution. Then the sample was washed by ethyl alcohol and dried by a heat blower. Finally the sample was ready to be investigated by light microscope.

After this observation, HF solution, involving 5% HF and 95% water, as an etcher was used for etching the sample. By a small tweezers the bakelite sample was hold and dipped into HF solution for five seconds. Then it was taken out, washed with water and dried. Drying was important to prevent the oxidation effects of water on the micro structure.

The reason of the metallographic observation with etching and without etching was to observe the porosities and dendritic structure. The solid and porous regions are seen better before etching while it is better to observe the dendritic structure after etching.

In this experiment, two magnification scales that were 25X and 100X were used to investigate three specimens before and after etching. Totally twelve photographs were taken for the investigation.

4. RESULTS AND DISCUSSIONS

4.1. Variation in Heat Transfer

The cooling curves were examined for all specimens and the heat transfer coefficient between the molten metal and die was examined for three specimens which were 10, 13 and 15. The temperature values obtained from three thermocouples every second recorded by the software named Ideal Finish. In order to make mathematical calculations, these temperature values were written into Microsoft Excel©. Then temperature dependent heat transfer coefficient values were calculated using the Formula 2.4.

As it is seen that in the Figures 3.32 and 3.33, the cooling curves have the same manner. In the beginning at all three points, the temperature values were decreased until pouring the molten metal. When pouring was started, the temperature value measured by Probe No 1 was increased rapidly and reached its pick point. Then the heat transferred from molten metal to the die so the temperature values measured by Probe No 1 started to decrease. This resulted in a slow increase in the temperature values measured by Probe No 2 and Probe No 3. Probe No 2 and Probe No 3 started to decrease after they have been reached to their pick point. After that time, the temperature values at all three points started to decrease. These heating and cooling behaviors were obtained as same for all specimens.

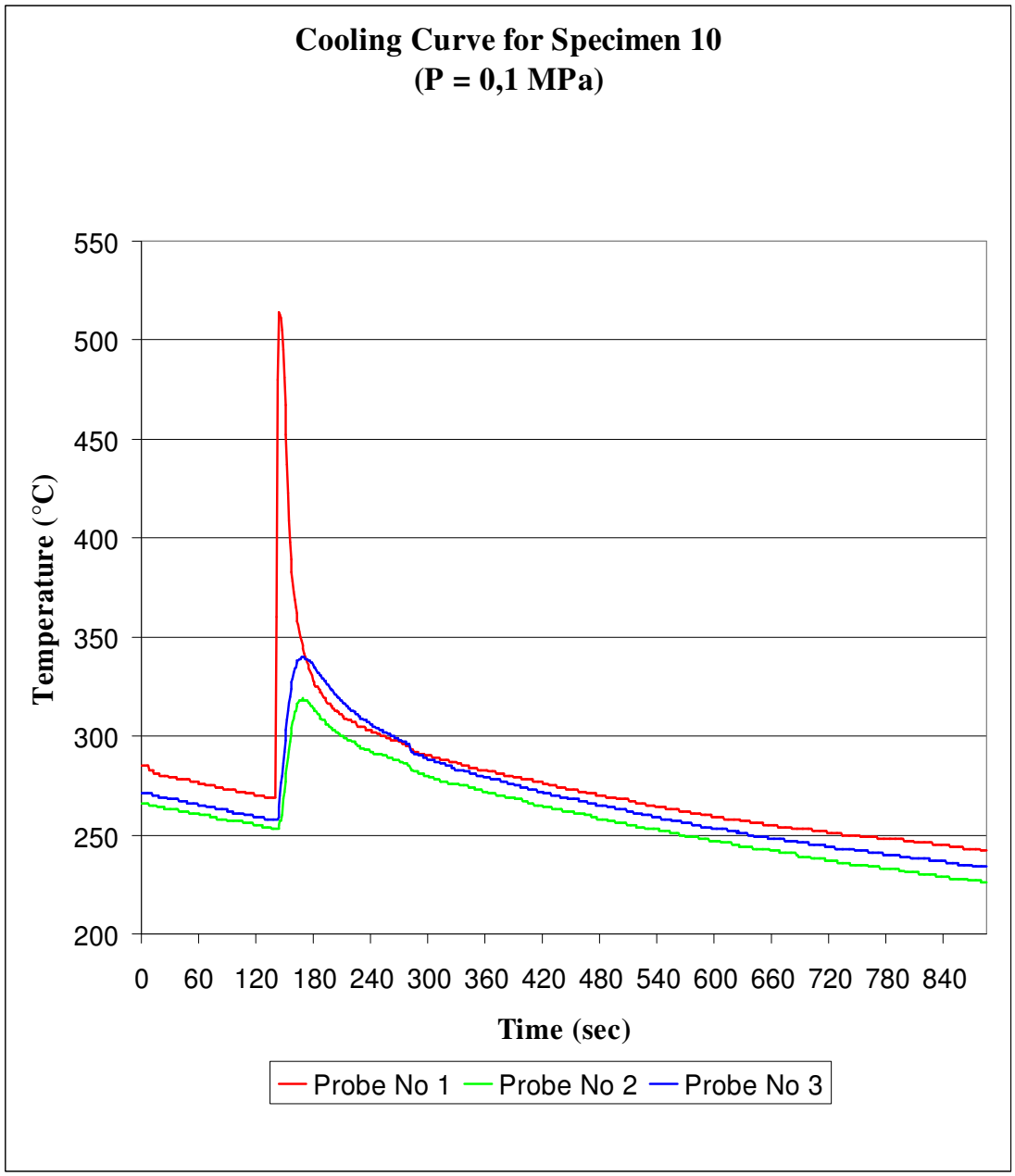

Figure 4.1. Cooling curve for specimen 10 (P=0,1 MPa) by Microsoft Excel©

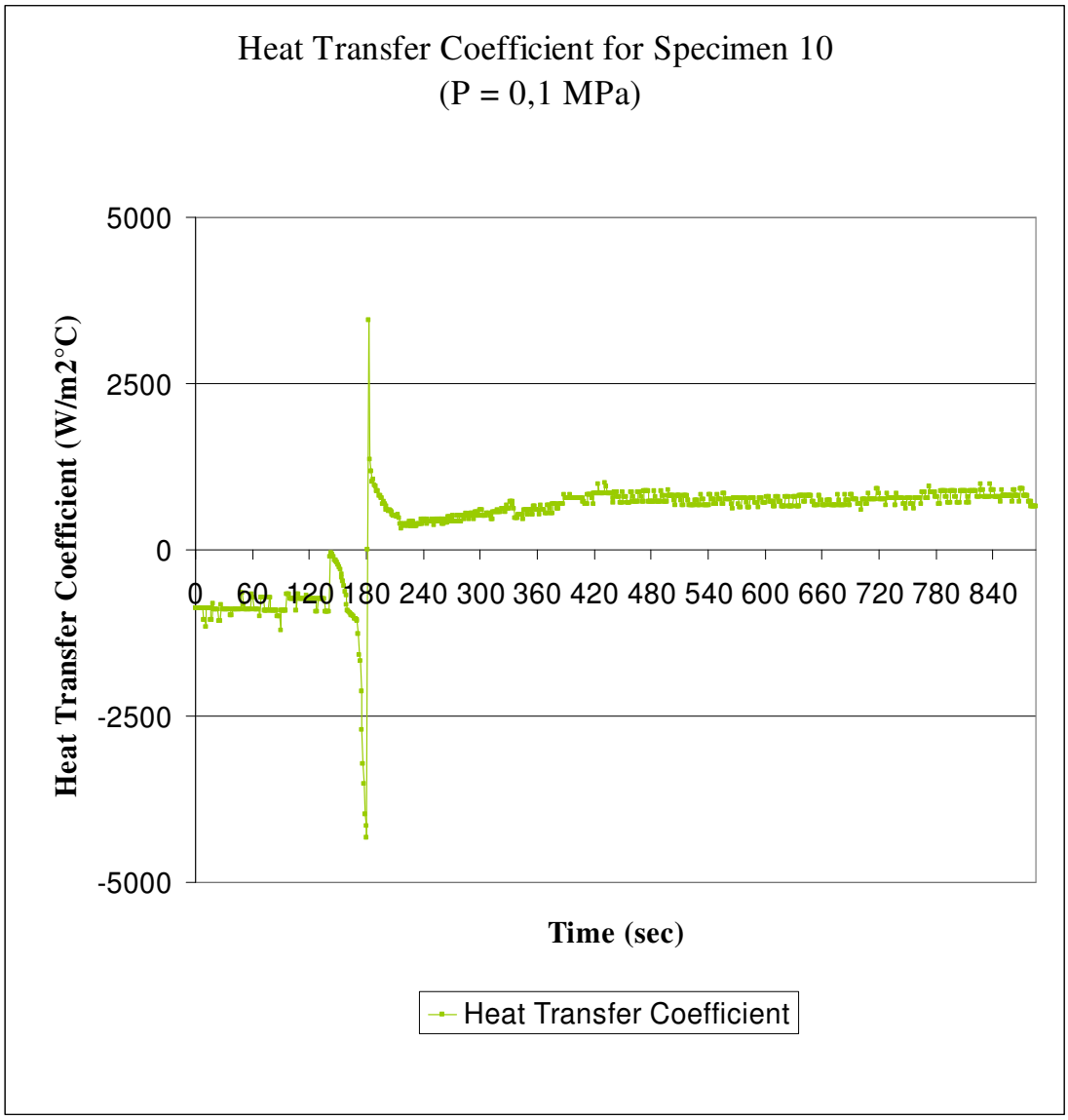

Figure 4.2. Heat transfer coefficient for specimen 10 (P=0,1 MPa)

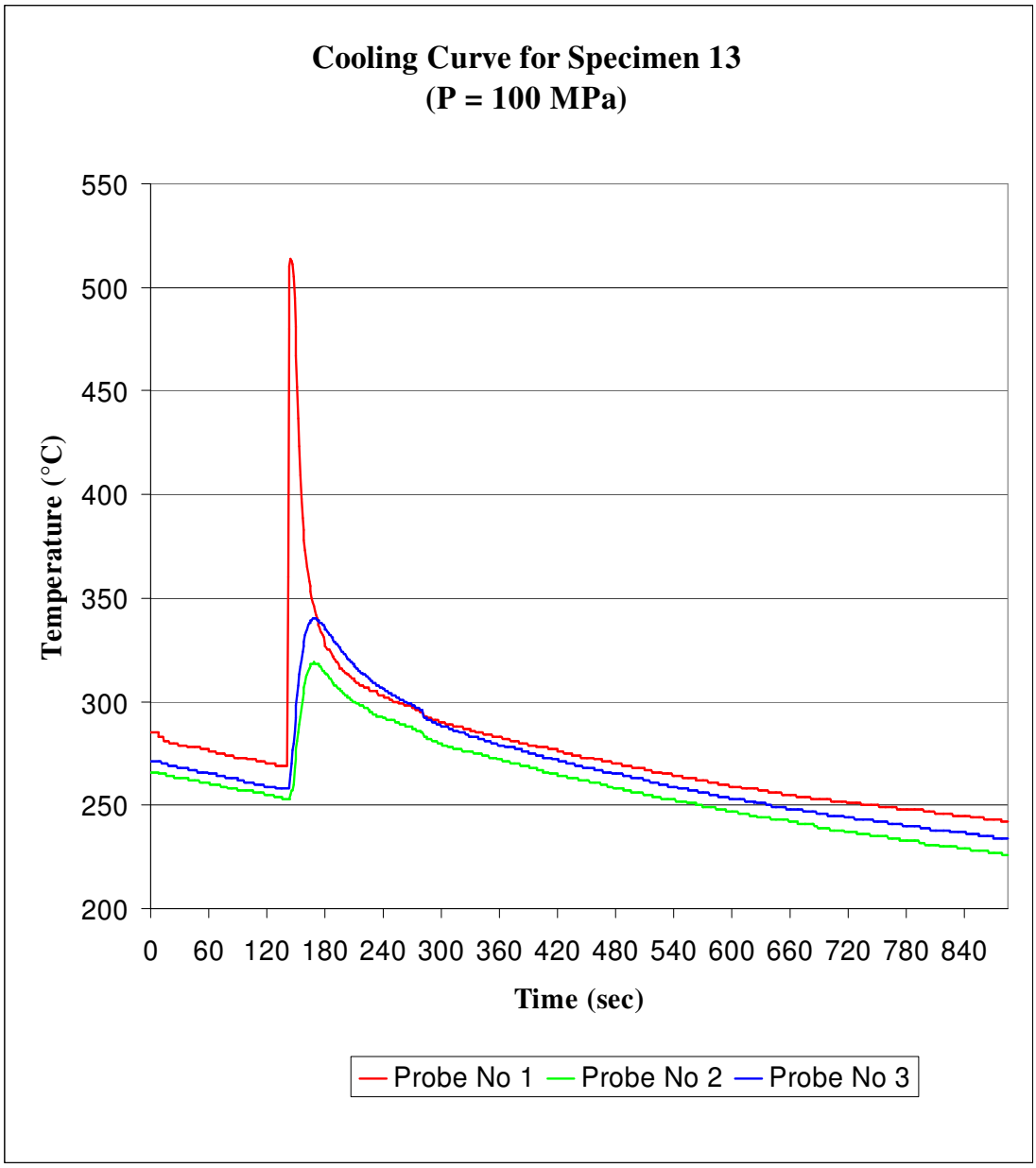

Figure 4.3. Cooling curve for specimen 13 (P=100 MPa) by Microsoft Excel©

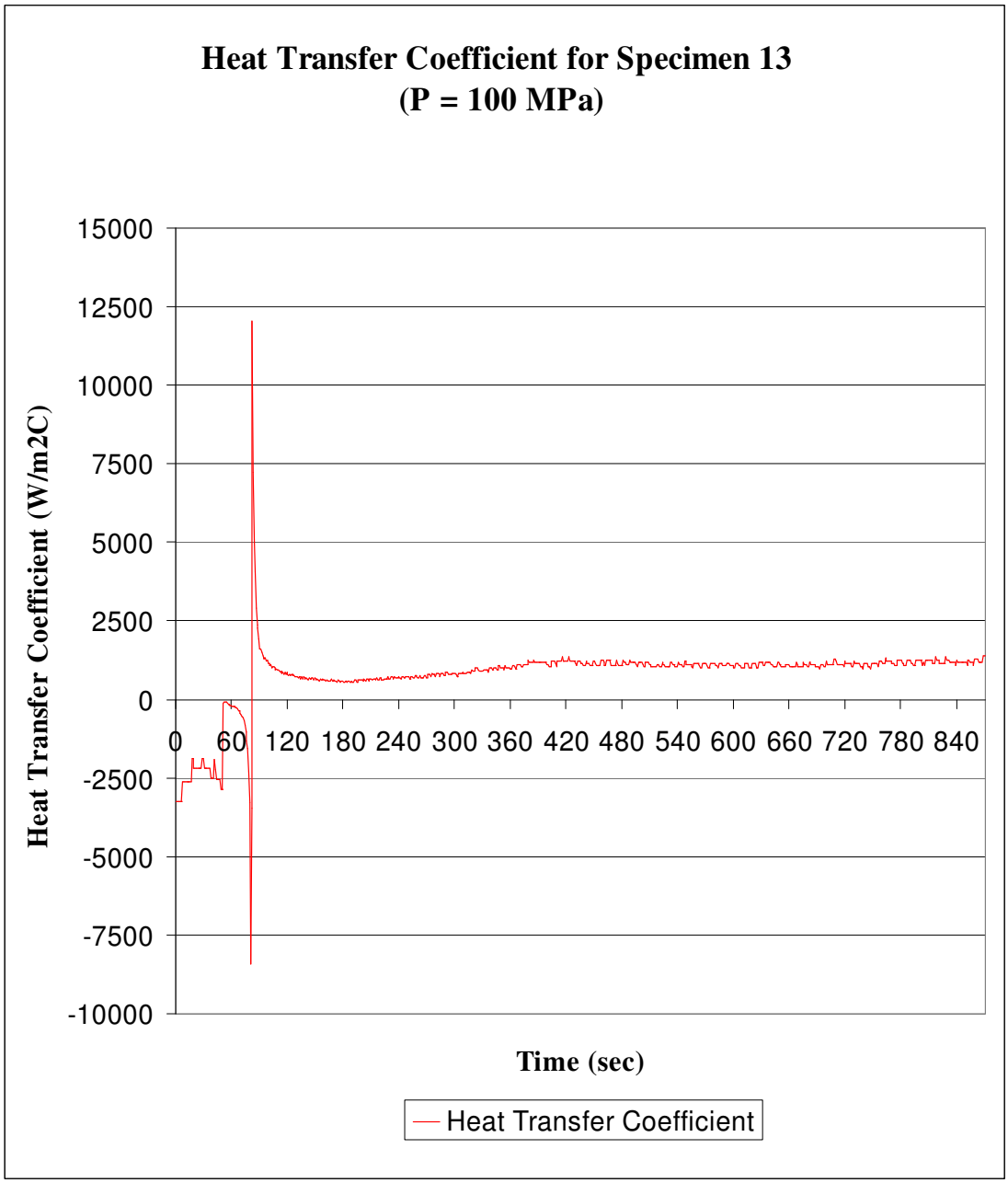

Figure 4.4. Heat transfer coefficient for specimen 13 (P=0,1 MPa)

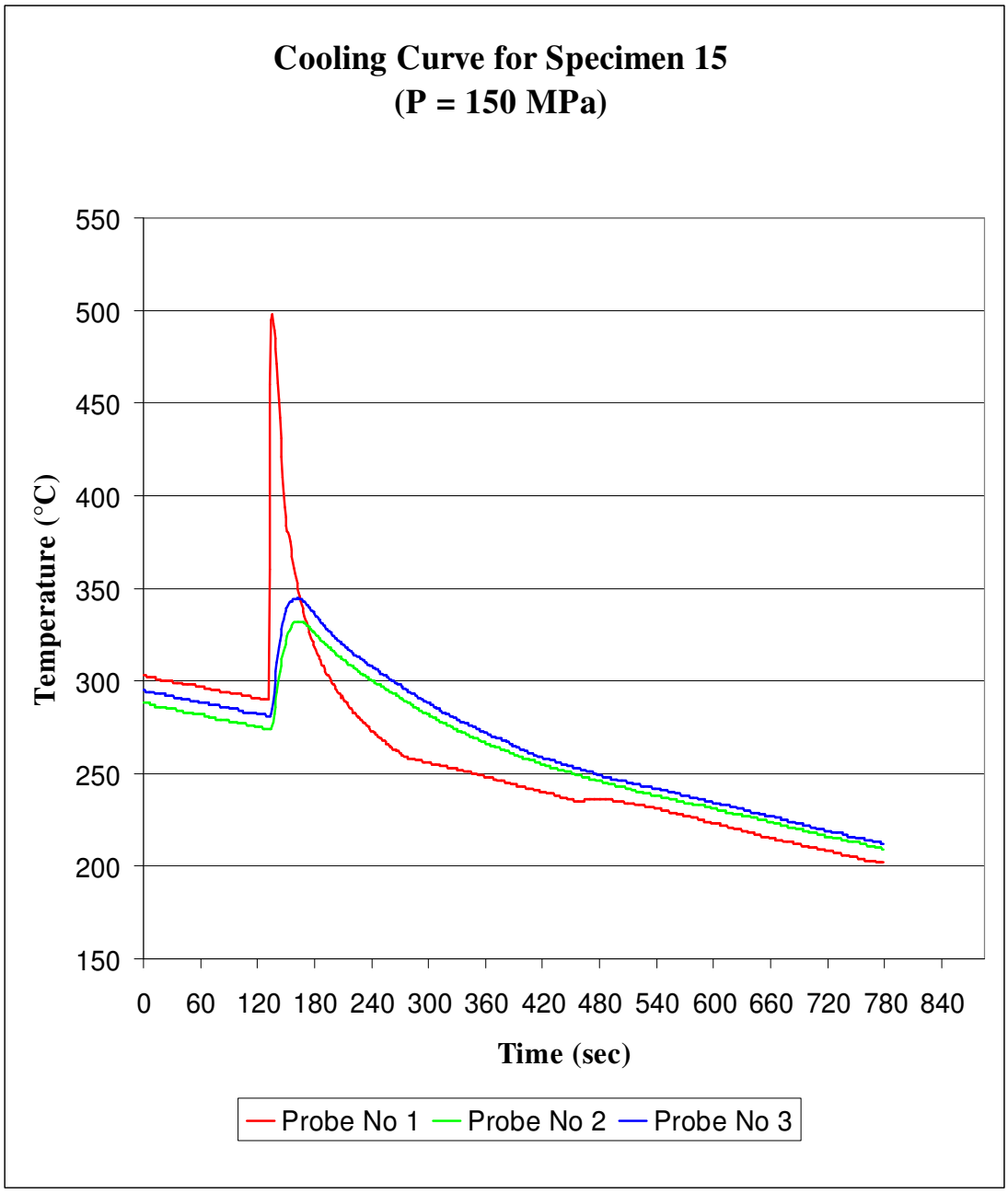

Figure 4.5. Cooling curve for specimen 15 (P=150 MPa) by Microsoft Excel©

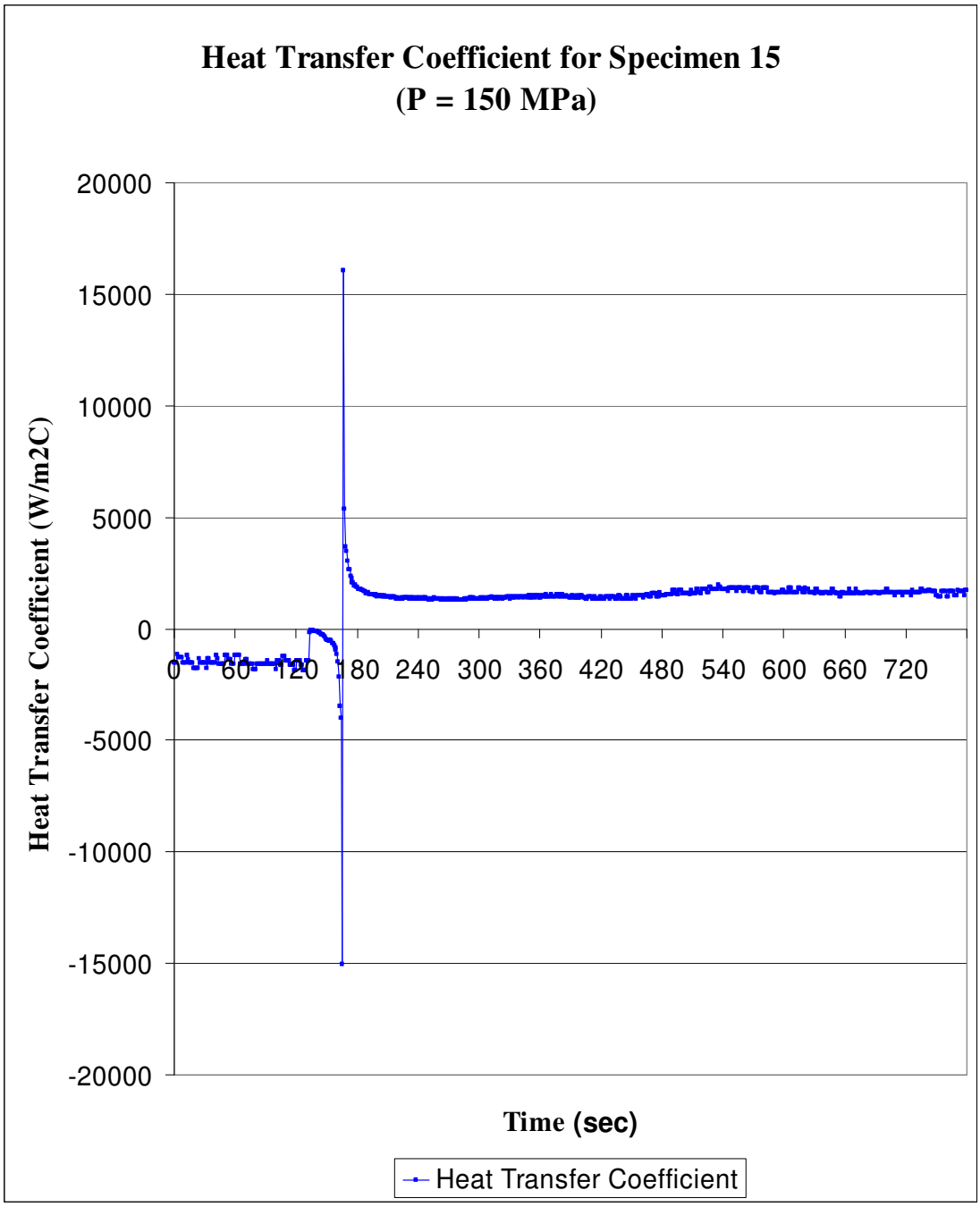

Figure 4.6. Heat transfer coefficient for specimen 15 (P=150 MPa)

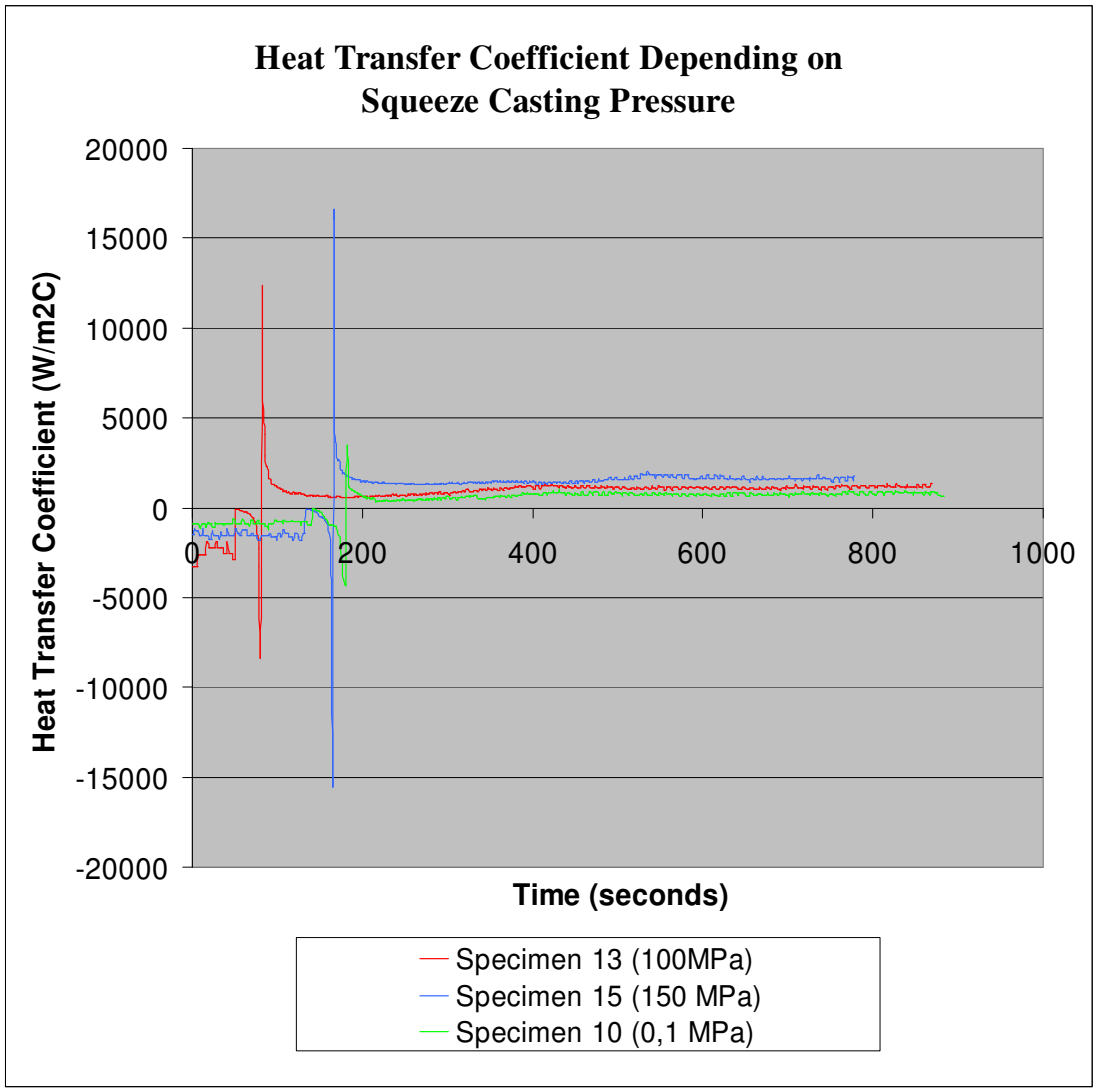

Figure 4.7. Time dependent heat transfer coefficients

As it is seen in the Figure 4.7., an increase in squeeze casting pressure results in increase in heat transfer coefficient between the molten metal and die. At the pouring time, the heat transfer coefficient becomes maximum and then it starts to decrease. Finally, it becomes stable. Heat transfer coefficient values at the peak point and in the stable region are also dependent to squeezing pressure. As the pressure is increased, both of these values are also increased. For the squeeze casting with 0,1 MPa, 100 MPa and 150 MPa pressure values, the heat transfer coefficient value varied between 240 to 1160 $W/m^{2}°C$; 420 to 3200 $W/m^{2}°C$ and 755 to 5100 $W/m^{2}°C$ respectively. The stable region heat transfer

coefficient values are 710 W/m^2°C, 1100 W/m^2°C and 1600 W/m^2°C for the specimens with the squeezing pressure 0,1 MPa, 100 MPa and 150 MPa respectively.

K.N. Prabhu, S.A. Kumar and N. Venkatraman have examined the heat transfer coefficient between the molten metal and mold at atmospheric pressure. The molten metal was Al-Cu-Si Alloy (LM-21) and the mold material was cast iron. They have observed that the heat transfer coefficient values varies from 1000 W/m^2°C to 4200 W/m^2°C [24].

The behavior of heat transfer coefficient value between the molten metal and mold depending on squeeze casting pressure were examined by Himadri Chattopadhyay. He made his experiments using A-356 as molten metal with squeeze casting pressures 25 MPa, 50 MPa and 100 MPa and has came to a result that an increase in squeezing pressure increases the heat transfer coefficient [25].

Finally, it is possible to state that heat transfer coefficients between molten metal and casting generally rise to a rapid peak and than decrease with time during solidification; and are increased with squeezing pressure.

4.2. Variation in Surface Temperature of the Mold

The temperature values at twelve different points on the die surface for the specimen 11 are seen in the Table 4.1. The locations of points are seen in Figure 3.34. The points lie on same line which pass two corner and center of molud. These temperature values were recorded by infrared camera and obtained by Irwin Image. The values were inserted to Microsoft Excel for graphical observation. Figure 4.8. shows the temperature changes of these twelve points by graphically.

Table 4.1. Temperature values of twelve points on the die surface during the casting of specimen 11

Time	Point 1	Point 2	Point 3	Point 4	Point 5	Point 6	Point 7	Point 8	Point 9	Point 10	Point 11	Point 12
0	196	217	179	247	253	231	224	239	236	154	201	204
13	198	217	179	243	253	230	219	224	236	145	200	191
15	195	226	177	244	263	239	228	234	232	150	210	193
16	199	218	177	244	263	240	252	239	237	155	216	200
26	201	228	197	260	300	289	283	284	256	152	215	200
36	194	225	181	273	294	301	303	291	271	147	214	196
52	200	219	177	276	294	283	295	290	276	156	216	204
56	192	230	173	281	294	289	286	291	280	146	213	199
66	200	217	178	280	298	285	267	285	270	147	212	197
76	201	215	182	276	290	272	273	276	266	150	212	197
116	197	231	175	271	282	263	233	271	269	156	212	196
166	197	216	181	264	281	253	232	262	253	150	211	195
216	196	231	176	259	269	253	226	252	245	155	210	195
266	206	210	179	256	263	243	221	241	252	154	208	191
306	200	208	178	253	258	240	225	241	237	152	206	188
356	182	210	175	247	256	238	216	241	242	150	205	187
406	179	217	174	245	255	231	212	232	237	142	202	185
456	186	210	174	240	247	222	208	223	226	149	200	180
506	188	213	171	235	244	224	197	224	212	140	198	178
556	183	201	166	232	244	212	192	220	218	143	195	175

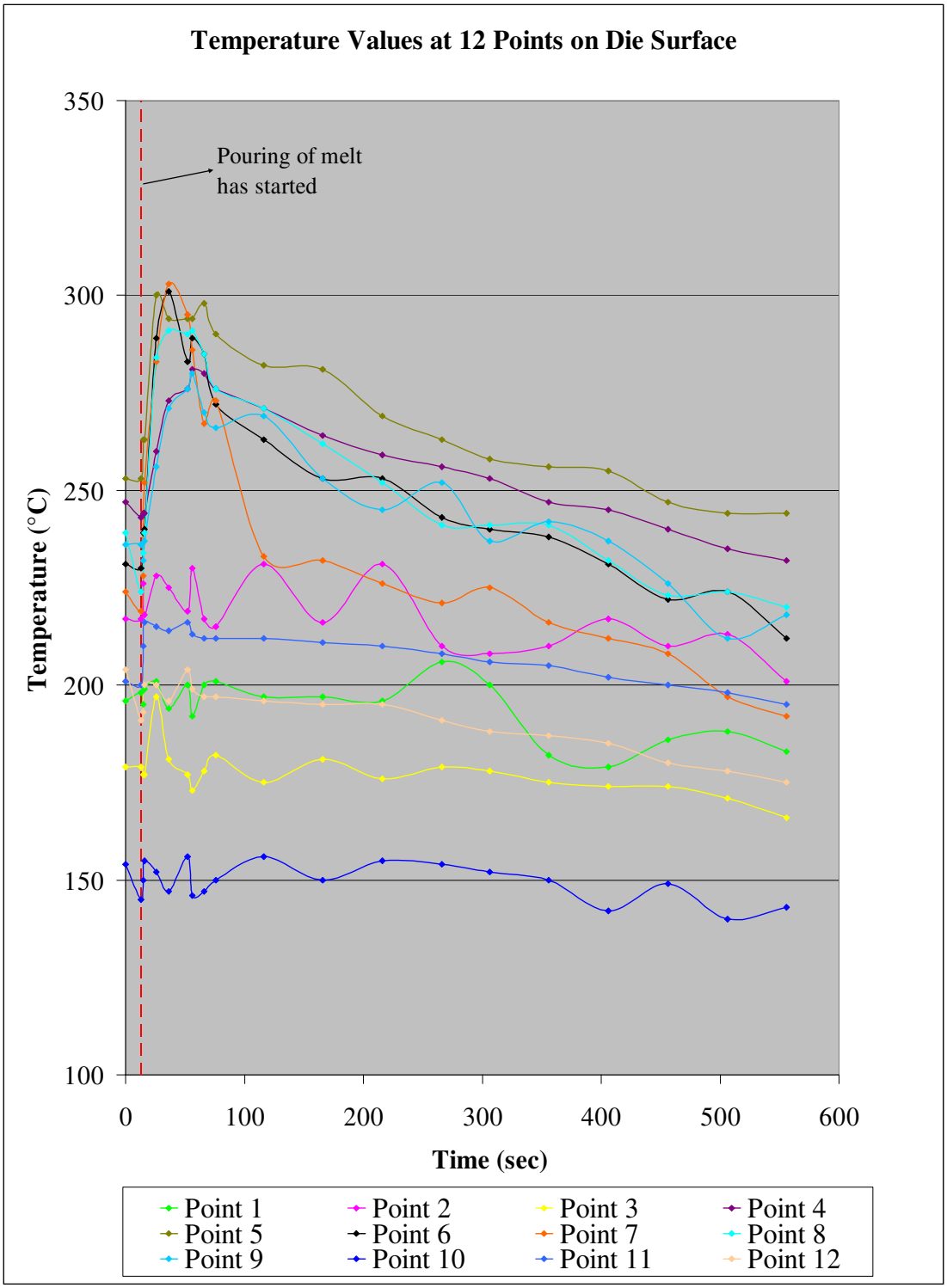

Figure 4.8. Die surface temperatures for specimen no 11

As it is seen in the Figure 4.8., the temperature values almost at all points out of twelve points on the die surface increases by pouring melt and then all of them follows a decreasing manner. The temperature values at the points near to the middle of die are bigger than the points at the corner of die surface.

The maximum and minimum temperature values on the die surface for the specimen 11 were obtained by a coloured scale produced by Irwin Image and recorded as seen in Table 4.2. Irwin image is able to give maximum and minimum temperature values on a surface with a coloured scale as seen in Figure 4.9.

Table 4.2. Maximum and minimum temperature values on die surface for specimen no 11

Time [sec]	Max. Temperature on Die Surface [°C]	Min. Temperature on Die Surface [°C]
0	259,2	140
13	245	135
15	269,6	201
16	272,9	210
26	322	205
36	326,4	213
52	322	195
56	318,1	182
66	311,6	166
76	303,6	154
116	294,3	145
166	286,2	117
216	279,4	109
266	273	102
306	267,3	100
356	261,8	94
406	257,1	92
456	252,6	90
506	248,5	88
556	244,5	85

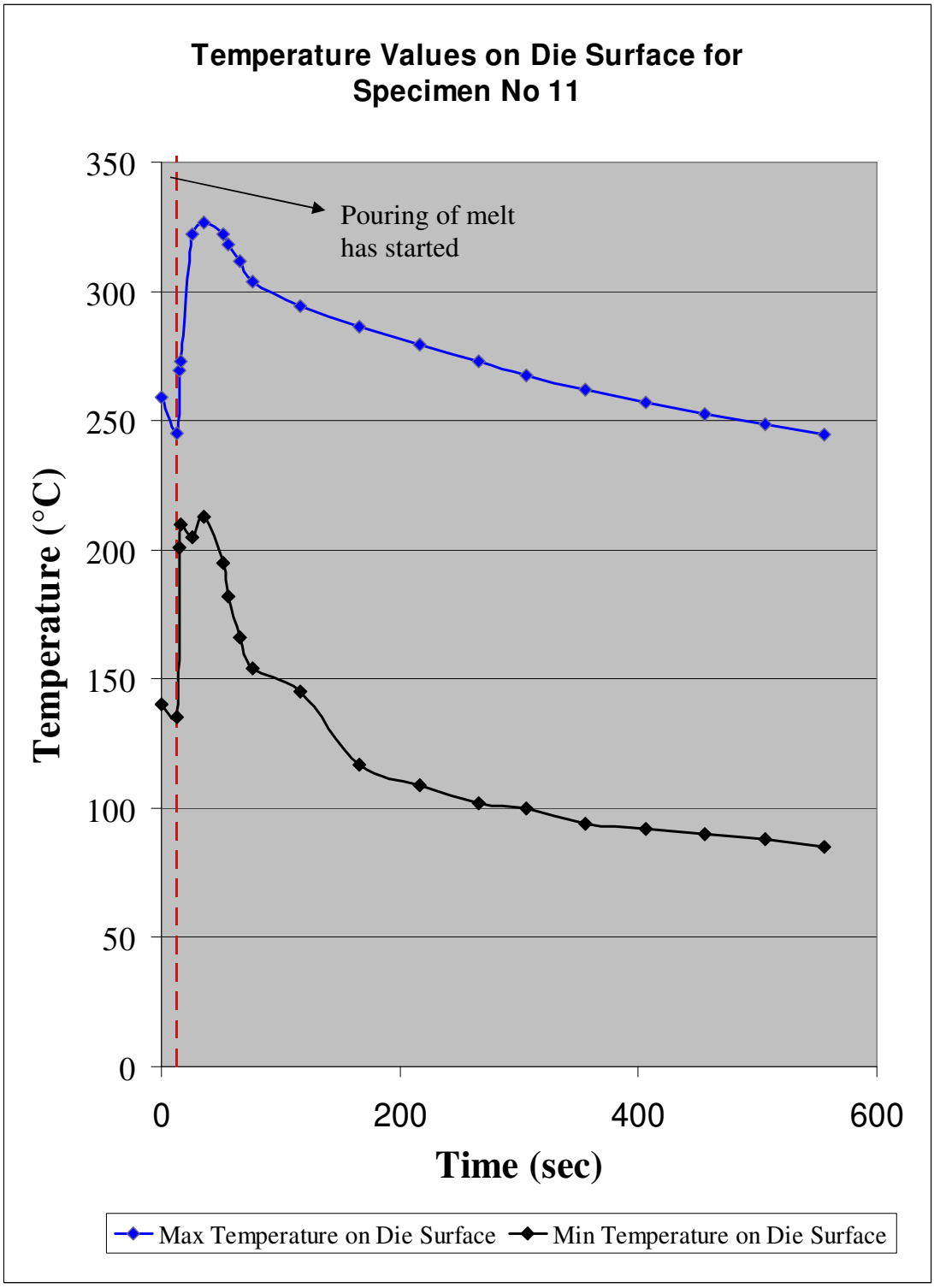

Figure 4.9. Maximum and minimum surface temperatures for specimen 11

In order to examine the effect of squeezing on die surface temperature distribution the analyses above were carried out for specimen no 13 which had been squeezed under 100 MPa. The temperature values and related time dependent graphic were seen in Table 4.3. and Figure 4.10. respectively.

Table 4.3. Maximum and minimum temperature values on die surface for specimen no 13

Time [sec]	Max. Temperature on Die Surface [°C]	Min. Temperature on Die Surface [°C]
0	318,5	246
4	318	245
366	268	217
371	300	225
376	292	232
386	318	211
390	327	205
395	328,8	224
400	326	213
405	324,5	208
410	321,9	205
415	319,7	210
420	317,5	209
458	305	218
487	300	217
496	298	205
633	275	207
656	273	201
777	259	205
804	256	198
914	247	202
1006	240	205
1052	237	204
1085	234	201

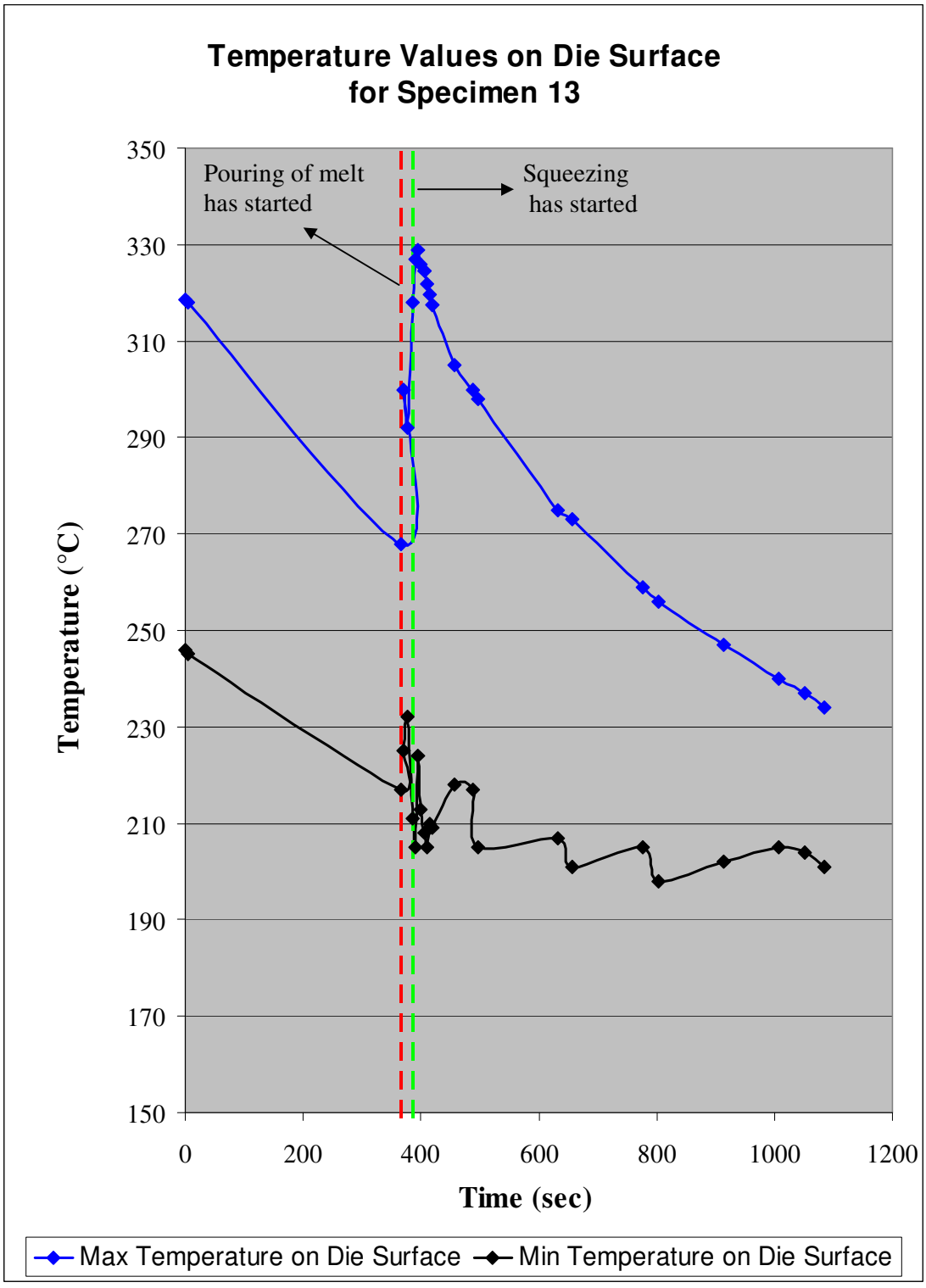

Figure 4.10. Maximum and minimum surface temperatures for specimen 13

As it is seen in Figure 4.10., the values of maximum and minimum temperatures on the die surface were increased just after pouring of ZA-27 melt at t = 366. Then the temperature values started to decrease. Starting squeezing at t = 386, these values increased a little and after a pick point started to decrease again. By squeezing the heat transfer coefficient between the molten metal and the die was increased and the temperature values which had been in decreasing manner started to increase a little. So, it is possible to state that squeezing increased the temperature values a little on the die surface in a short time.

4.3. Variation in Chip Length

In order to investigate the relation between squeeze casting pressure and chip length, almost all of the specimens were machined by lathe. This was also a preparation for tensile testing. After a cleaning pass, 1 mm. machining pass was given to specimens. By the way since this operation was applied for four different turning speeds, the relation between the cutting speed and chip length at a constant squeeze casting pressure was also obtained. During all these operations chips are collected and sorted in different nylon bags. The lengths of each chip were measured by the help of a small plier. The curls of each chip were opened very carefully not to break off them. The lengths of longest four chips are written and average values of these are calculated. In Table 4.4., the cutting speed, squeezing pressure, and average lengths are written with the units rpm, MPa and mm respectively.

Table 4.4. Chip length values

Cutting Speed	Specimen No	Squeezing Pressure	Lengths of Longest 4 Chips				Average Length
180	1	0	385,0	320,0	175,0	140,0	255,0
	5	0	415,0	340,0	150,0	135,0	260,0
	10	0	375,0	315,0	225,0	151,0	266,5
	11	0	495,0	415,0	210,0	190,0	327,5
	7	100	295,0	210,0	125,0	110,0	185,0
	9	100	270,0	255,0	170,0	95,0	197,5
	13	100	245,0	225,0	185,0	154,0	202,3
	14	100	230,0	185,0	170,0	120,0	176,3
	15	150	165,0	145,0	115,0	90,0	128,8
	16	150	155,0	150,0	195,0	95,0	148,8
	17	150	170,0	125,0	105,0	90,0	122,5
	18	150	183,0	140,0	105,0	100,0	132,0
355	1	0	340,0	255,0	195,0	150,0	235,0
	5	0	305,0	190,0	175,0	130,0	200,0
	10	0	295,0	245,0	165,0	145,0	212,5
	11	0	305,0	225,0	185,0	150,0	216,3
	7	100	230,0	135,0	110,0	65,0	135,0
	9	100	195,0	155,0	120,0	90,0	140,0
	13	100	175,0	155,0	95,0	90,0	128,8
	14	100	195,0	180,0	115,0	100,0	147,5
	15	150	140,0	120,0	85,0	75,0	105,0
	16	150	130,0	105,0	80,0	60,0	93,8
	17	150	140,0	95,0	85,0	70,0	97,5
	18	150	125,0	90,0	70,0	65,0	87,5
710	1	0	240,0	165,0	145,0	100,0	162,5
	5	0	275,0	210,0	140,0	110,0	183,8
	10	0	265,0	195,0	180,0	95,0	183,8
	11	0	285,0	175,0	140,0	105,0	176,3
	7	100	160,0	100,0	90,0	75,0	106,3
	9	100	200,0	145,0	90,0	40,0	118,8
	13	100	185,0	125,0	100,0	90,0	125,0
	14	100	190,0	120,0	110,0	90,0	127,5
	15	150	120,0	100,0	85,0	60,0	91,3
	16	150	100,0	95,0	85,0	55,0	83,8
	17	150	95,0	70,0	60,0	35,0	65,0
	18	150	105,0	85,0	55,0	30,0	68,8
1000	1	0	150,0	135,0	110,0	95,0	122,5
	5	0	205,0	180,0	80,0	55,0	130,0
	10	0	165,0	105,0	100,0	80,0	112,5
	11	0	140,0	120,0	75,0	95,0	107,5
	7	100	120,0	95,0	65,0	45,0	81,3
	9	100	160,0	120,0	50,0	40,0	92,5
	13	100	140,0	105,0	80,0	35,0	90,0
	14	100	120,0	90,0	70,0	45,0	81,3
	15	150	55,0	40,0	25,0	15,0	33,8
	16	150	85,0	60,0	45,0	30,0	55,0
	17	150	60,0	50,0	35,0	20,0	41,3
	18	150	55,0	50,0	40,0	15,0	40,0

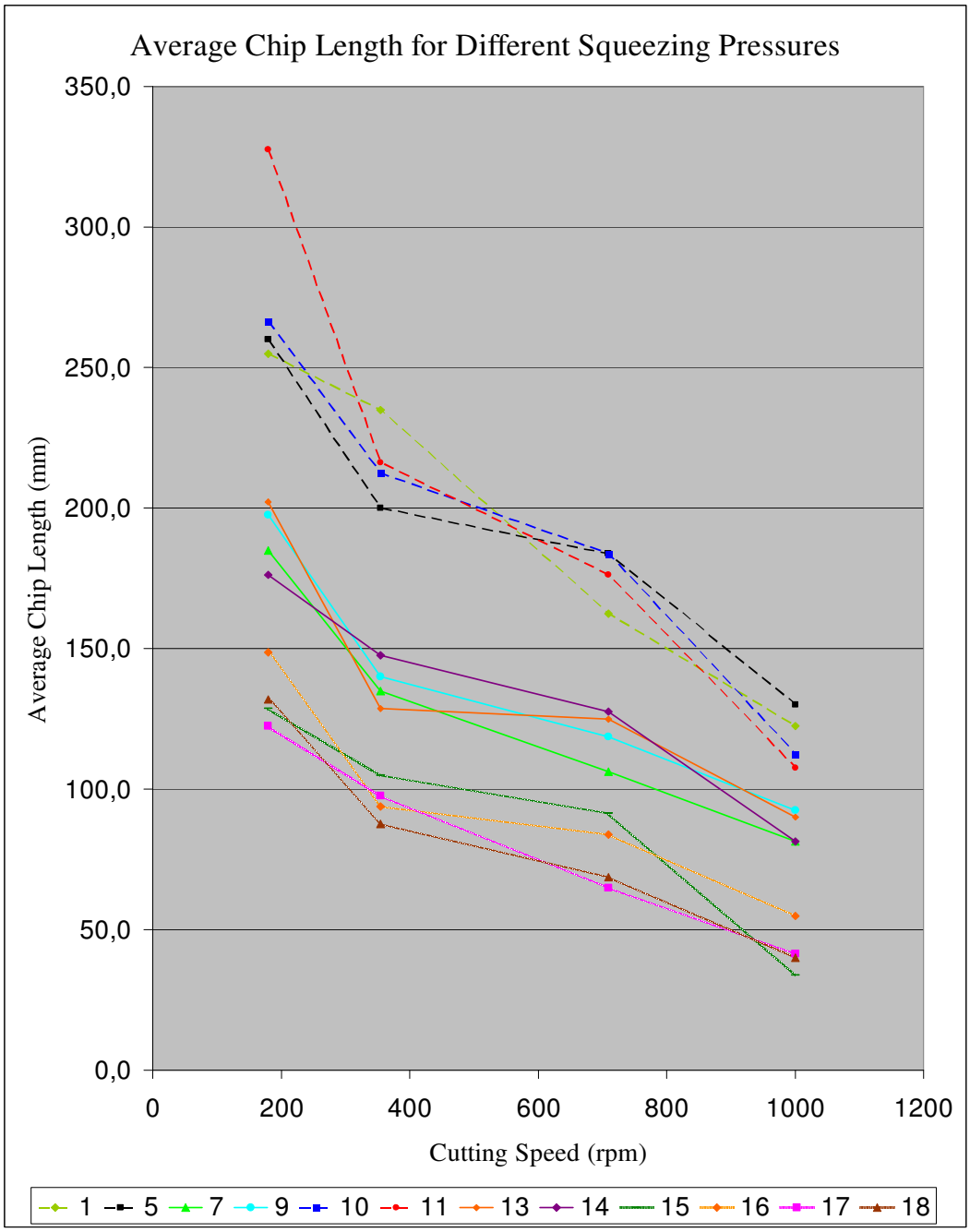

Figure 4.11. Average chip lengths for 0,1 , 100 and 150 MPa squeezing pressures

In the above graphic, calculated average chip lengths of the specimens are shown. Four different cutting speeds were subjected to specimens which had been already subjected three different squeezing pressures. Specimens 1,5,10 and 11 were subjected to 0,1 MPa squeezing pressure which was the atmospheric pressure; specimens 7,9,13 and 14 were subjected to 100 MPa squeezing pressure; and specimens 15,16,17 and 18 were subjected to 150 MPa squeezing pressure. As it is clearly seen in the Figure 4.10, the increase in cutting speed and increase in squeezing pressure result in decrease in chip length. The four dashed lines, at the top, belong to specimens cast under 0,1 MPa atmospheric squeezing pressure, the four continues lines, at the middle, belong to specimens cast under 100 MPa squeezing pressure and the last four framed lines, at the bottom, belong to specimens cast under 150 MPa squeezing pressure. So, by increasing the squeeze casting pressure, the chip lengths were decreased. Beside these, all the lines are in decreasing manner. If we consider only one line belongs to any specimen, it is obvious that increasing cutting speed decreases the chip length. Finally, we can say that if we increase cutting speed to an allowable degree or increase the squeezing pressure, we increase the machinability for ZA-27 alloys.

4.4. Variation in Surface Roughness

Surface roughness of all specimens was measured after machining them by lathe with the speed of 1240 rpm. The turning speed was kept same and constant for all specimens.

Figure 4.12. Machining by lathe of specimens for surface roughness measurement

Table 4.5. Surface roughness values

No	Squeezing Pressure	Surface Roughness Values (μ)		
		Ra	Rz	Rmax
1	0,1	2.97 – 3.07	15.3 – 16.0	20.4 – 21.2
2	0,1	3.17 – 3.25	16.4 – 17.4	19.2 – 21.8
3	0,1	2.45 – 2.57	14.1 – 14.8	19.0 – 20.0
4	0,1	2.66 – 2.75	13.1 – 13.8	18.1 – 18.7
5	0,1	2.62 – 2.68	12.1 – 13.0	17.0 – 17.8
6	0,1	2.17 – 2.25	13.7 – 14.2	16.0 – 17.0
7	100	2.20 – 2.29	12.0 – 12.8	13.7 – 14.2
8	100	1.97 – 2.08	10.1 – 11.0	12.3 – 12.8
9	100	2.12 – 2.22	12.4 – 12.9	14.8 – 15.5
10	0,1	3.34 – 3.45	15.1 – 16.0	20.8 – 21.4
11	0,1	2.85 – 2.97	15.3 – 16.4	19.7 – 22.2
12	0,1	2.75 – 2.83	13.7 – 14.3	18.4 – 19.2
13	100	2.10 – 2.19	11.0 – 11.7	13.3 – 14.5
14	100	1.85 – 1.92	10.7 – 11.3	12.2 – 12.9
15	150	1.83 – 1.94	10.3 – 11.6	11.9 – 12.4
16	150	1.72 – 1.83	9.6 – 10.4	11.5 – 12.3
17	150	1.76 – 1.84	9.6 – 10.4	11.1 – 11.9
18	150	1.67 – 1.73	8.3 – 9.1	10.3 – 10.9
19	150	1.70 – 1.79	9.4 – 10.3	11.4 – 12.2

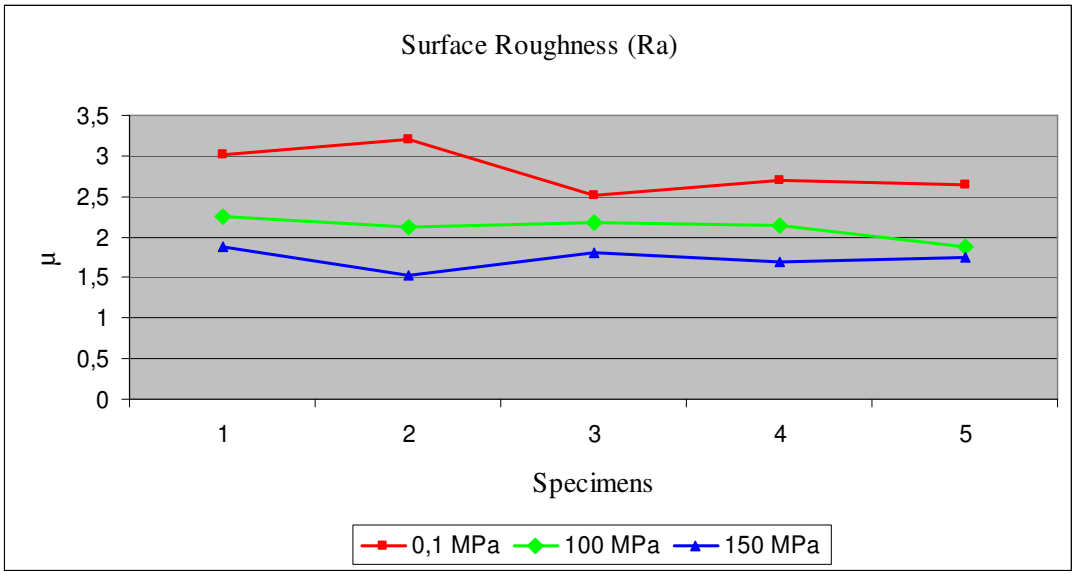

Figure 4.13. The average deviation (Ra) for different squeezing pressures

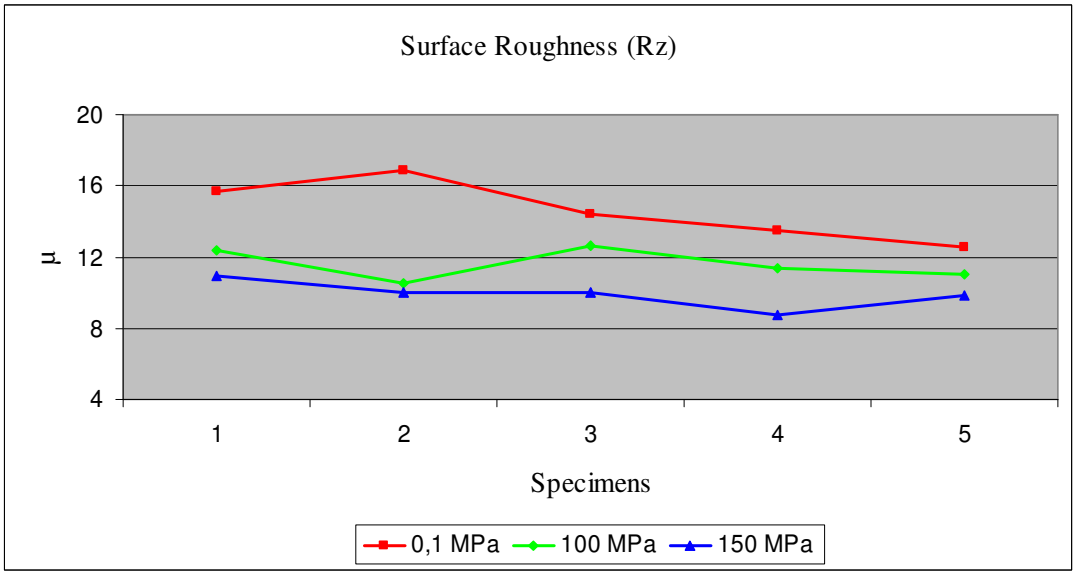

Figure 4.14. The average height of profile (Rz) for different squeezing pressures

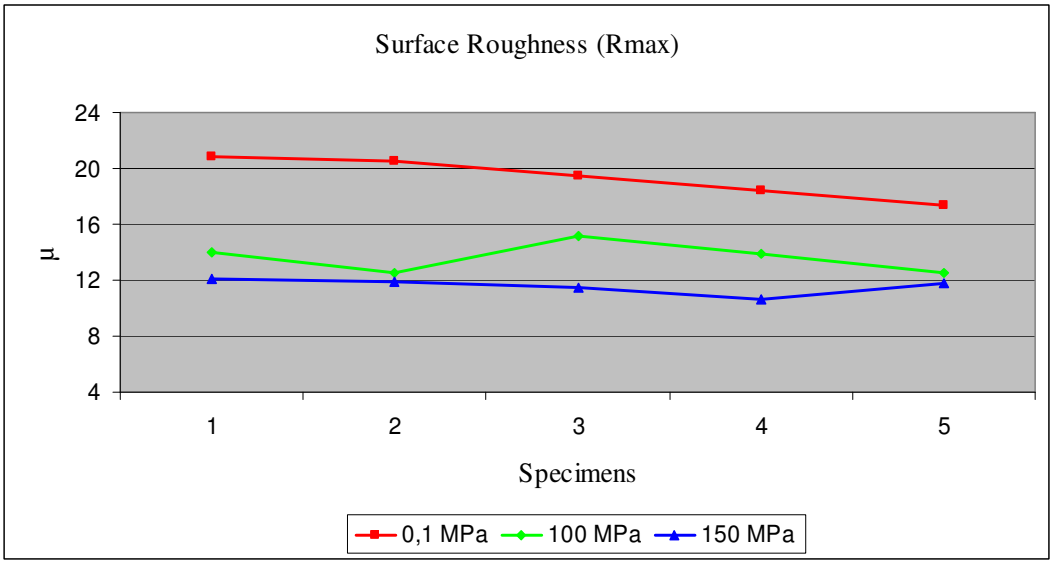

Figure 4.15. The largest peak to valley height (Rmax) for different squeezing pressures

As it is clearly seen in the figures 4.12, 4.13 and 4.15, the surface roughness values are decreased if the squeezing pressure is increased. These figures were drawn depending on the surface roughness analysis results obtained from KOSGEB-Istanbul for the specimens 1 to 5, 7 to 9 and 13 to 19.

4.5. Variation in Hardness

Brinell method was carried out with 62.5 kg. pressing force, 2.5 mm. ball diameter and 15 seconds pressing time. The ball material is Wolfram Carbide. The left sides of the specimens were machined to get a fine and smooth surface with circular section. This surface was subjected to hardness test and four measurements were taken from different points on this surface. This analysis was done in KOSGEB-Istanbul.

Table 4.6. Brinell hardness analysis results

Specimen No	Brinell Hardness Test Results				
	1st Measurement	2nd Measurement	3rd Measurement	4th Measurement	Average
1	81,3	81,3	79,5	79,5	80,4
2	83,8	83,8	81,9	81,9	82,85
3	84,9	84,9	83	83	83,95
4	84,9	84,9	83	83	83,95
5	83	81,3	81,3	79,5	81,275
6	84,9	84,9	83	83	83,95
7	86,8	86,8	84,9	84,9	85,85
8	84,9	84,9	83	83	83,95
9	83	83	81,3	81,3	82,15
10	82,3	82,1	81,6	81,3	81,825
11	82,1	79,8	78,9	78,9	79,925
12	81,6	81,5	79,7	79,8	80,65
13	87,2	87,8	85,9	86,1	86,75
14	84,9	84,9	83	83	83,95
15	89,6	90,2	90,5	90,6	90,225
16	92,6	92,7	90,5	90,7	91,625
17	93,2	94	92,3	92,1	92,9
18	90,1	90,3	91,3	90,5	90,55
19	95,2	95,4	94,6	94,1	94,825

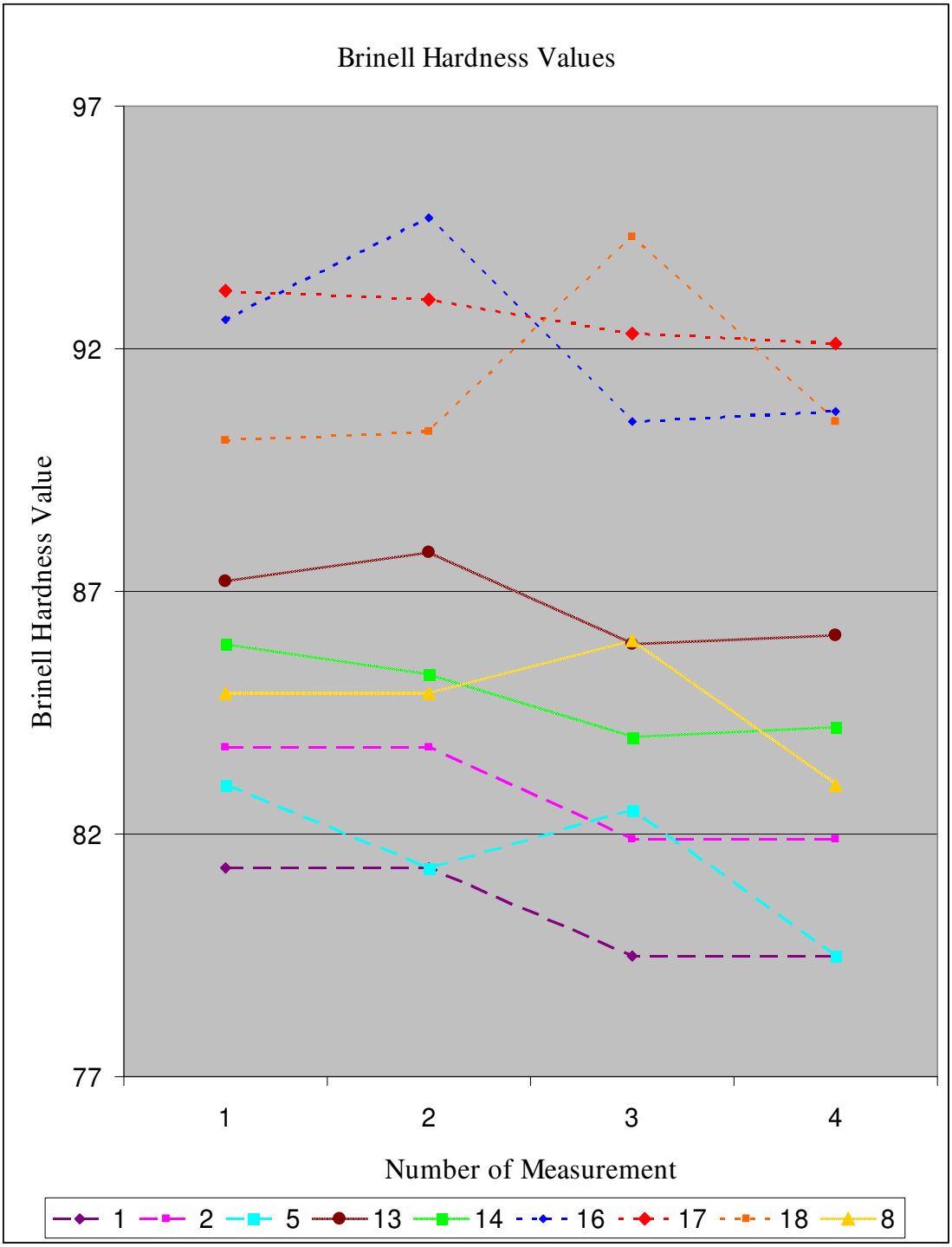

Figure 4.16. Brinell hardness values for random specimens

The Figure 4.16 involves Brinell hardness values of 9 different specimens. The short dashed lines belong to specimens 16,17 and 18 were squeezed under 150 MPa; the continuous dashed lines belong to specimens 13,14 and 8 were squeezed under 100 MPa; and long dashed lines belong to specimens 1,2 and 5 were squeezed under atmospheric pressure, 0,1 MPa. It is easily seen that the increase in squeezing pressure results in increase in hardness values

4.6. Variation in Tensile Testing

All of the specimens were subjected to Tensile Testing in KOSGEB-Istanbul. The test results are seen in Table 4.7. and 4.8.

Table 4.7. Tensile test results

Specimen No	Squeezing Pressure MPa	First Diameter. (mm)	Last Diameter (mm)	First Area (mm^2)	Last Area (mm^2)	Reduction in Area (%)	First Length, L_0 (mm)	Last Length, L_f (mm)
1	0,1	10	10,0	78,54	78,54	0,0%	50	50,0
2	0,1	10	10,0	78,54	78,54	0,0%	50	50,0
3	0,1	10	10,0	78,54	78,54	0,0%	50	50,0
4	0,1	10	9,9	78,54	76,98	2,0%	50	51,0
5	0,1	10	10,0	78,54	78,54	0,0%	50	50,0
6	0,1	10	9,9	78,54	76,98	2,0%	50	50,2
7	100	10	9,4	78,54	69,40	11,6%	50	53,0
8	100	10	9,2	78,54	66,48	15,4%	50	52,5
9	100	10	9,8	78,54	75,43	4,0%	50	51,8
10	0,1	10	10	78,54	78,54	0,0%	50	50,0
11	0,1	10	9,8	78,54	75,43	4,0%	50	51,5
12	0,1	10	10	78,54	78,54	0,0%	50	50
13	100	10	9,3	78,54	67,93	13,5%	50	52,8
14	100	10	9	78,54	63,62	19,0%	50	53
15	150	10	9,1	78,54	65,04	17,2%	50	53,1
16	150	10	9,3	78,54	67,93	13,5%	50	52,1
17	150	10	9,3	78,54	67,93	13,5%	50	52,3
18	150	10	9,2	78,54	66,48	15,4%	50	53,5
19	150	10	9	78,54	63,62	19,0%	50	53,3

Table 4.8. Tensile test results

Specimen No	Squeezing Pressure MPa	Elongation (%)	Yield Strength (N)	Yield Stress (N/mm^2)	Tensile Strength (N)	Tensile Stress (N/mm^2)
1	0,1	0,0%	0	0	9.840	125
2	0,1	0,0%	0	0	11.260	143
3	0,1	0,0%	0	0	10.940	139
4	0,1	2,0%	10.367	132	11.080	141
5	0,1	0,0%	0	0	12.960	165
6	0,1	0,4%	13.902	177	15.430	196
7	100	5,7%	20.656	263	22.290	284
8	100	4,8%	17.200	219	19.360	246
9	100	3,5%	19.556	249	22.060	281
10	0,1	0,0%	0	0	10.125	129
11	0,1	2,9%	19.949	254	23.450	299
12	0,1	0,0%	0	0	12.150	155
13	100	5,3%	18.771	239	21.231	270
14	100	5,7%	19.949	254	23.785	303
15	150	5,8%	20.970	267	24.379	310
16	150	4,0%	20.499	261	25.123	320
17	150	4,4%	20.735	264	24.985	318
18	150	6,5%	21.284	271	25.854	329
19	150	6,2%	20.106	256	22.576	287

The average values of elongation, reduction in area, tensile strength and yield strength values are calculated from the tables above depending on the squeezing pressure. Figure 4.17. was drawn by these average values.

Table 4.9. Average values of tensile test results

Squeezing Pressure MPa	Yield Stress (N/mm^2)	Tensile Stress (N/mm^2)	Reduction in Area (%)	Elongation (%)
0,1	62,56	165,72	0,9%	0,6%
100	244,80	276,83	12,7%	5,0%
150	263,80	313,01	15,7%	5,4%

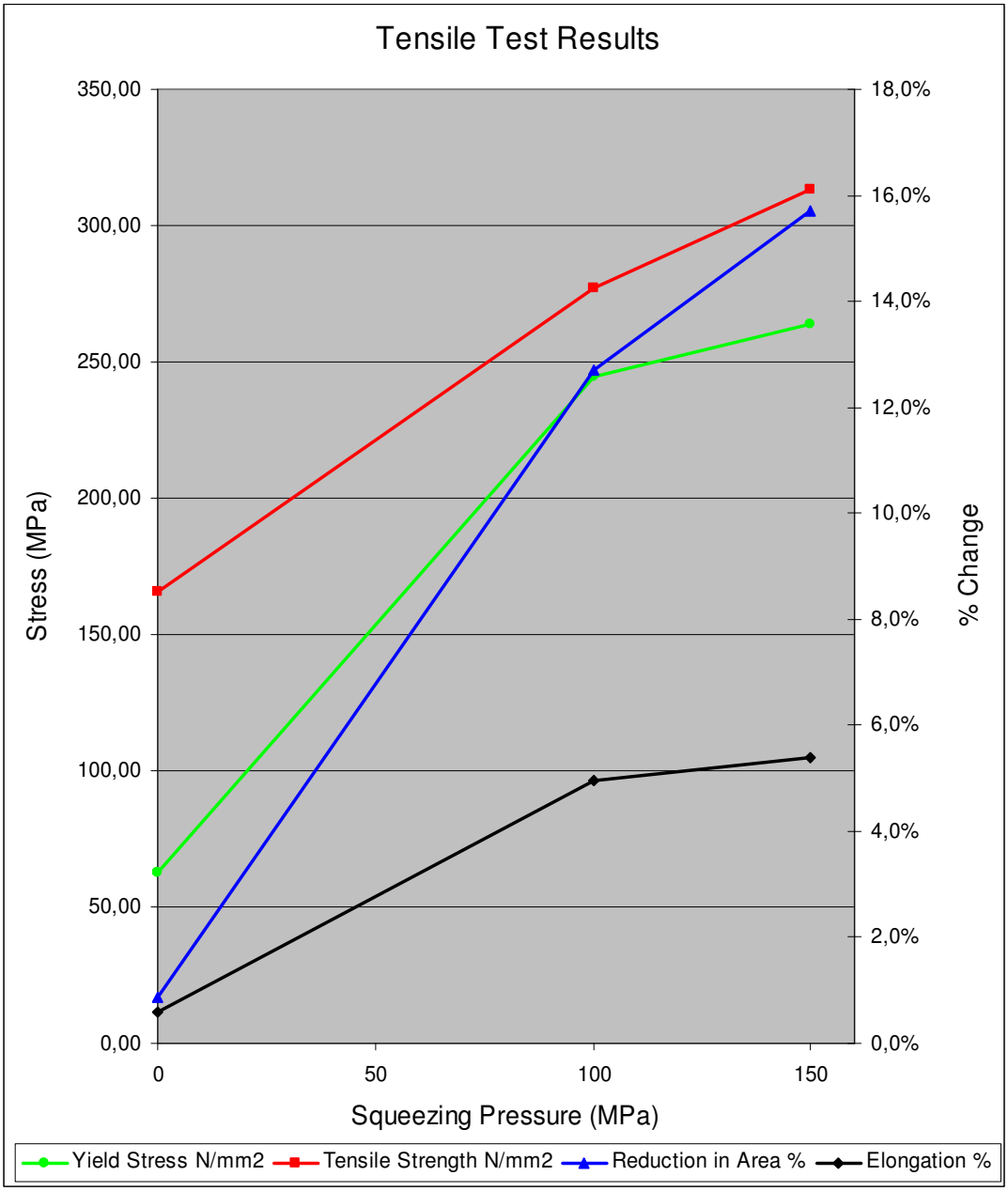

Figure 4.17. Average values of stresses and % changes with squeezing pressure

Figure 4.18. A broken specimen in tensile testing

It is clearly seen in Figure 4.17 that an increase in squeezing pressure results in increase in yield stress, tensile strength, elongation and reduction in sectional area. Some of the specimens were broken without yielding during tensile testing. This was occurred mostly for squeezing with atmospheric pressure. Since this pressure is low, there could be some cavities in the specimen and they could have broken without yielding from the sections which involved cavities. By increasing the squeezing pressure to 100 MPa or 150 MPa, all the specimens started to yield. By squeezing the specimens, the occurrence of cavities inside the specimen and unexpectedly broken of specimens were prevented. The increases, in all results obtained from tensile testing, from 0,1 to 100 MPa is much higher than 100 MPa to 150 MPa squeezing pressures.

M. Skalinos, G. Kiourtsidis and T. Xatzifotiou have researched the effect of applied pressure on mechanical properties of squeeze-cast aluminum AA6061 alloy. They applied squeezing pressure starting from 0 to 100 MPa by 20 MPa increments. The increase in elongation and tensile strength depending on an increase applied pressure was observed by them [8].

4.7. Variation in Microstructure

4.7.1. Scanning Electron Microscope

Figures from 4.19 to 4.22 show the fracture surfaces of ZA-27 squeezed under 0,1 MPa, that was gravity casting. These micrographs belong to specimen 11. The dendritic structure and the interdendritic porosity are evident of the fracture surfaces.

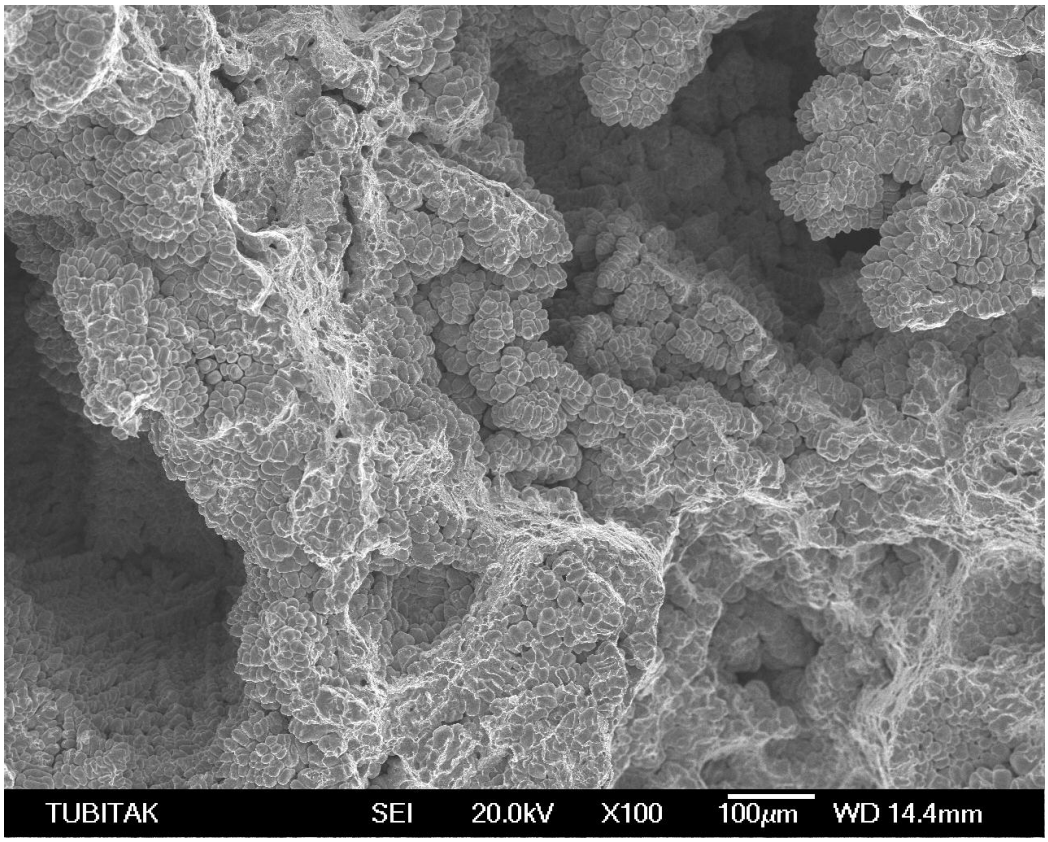

Figure 4.19. The SEM photograph of specimen 11 under X100 magnification

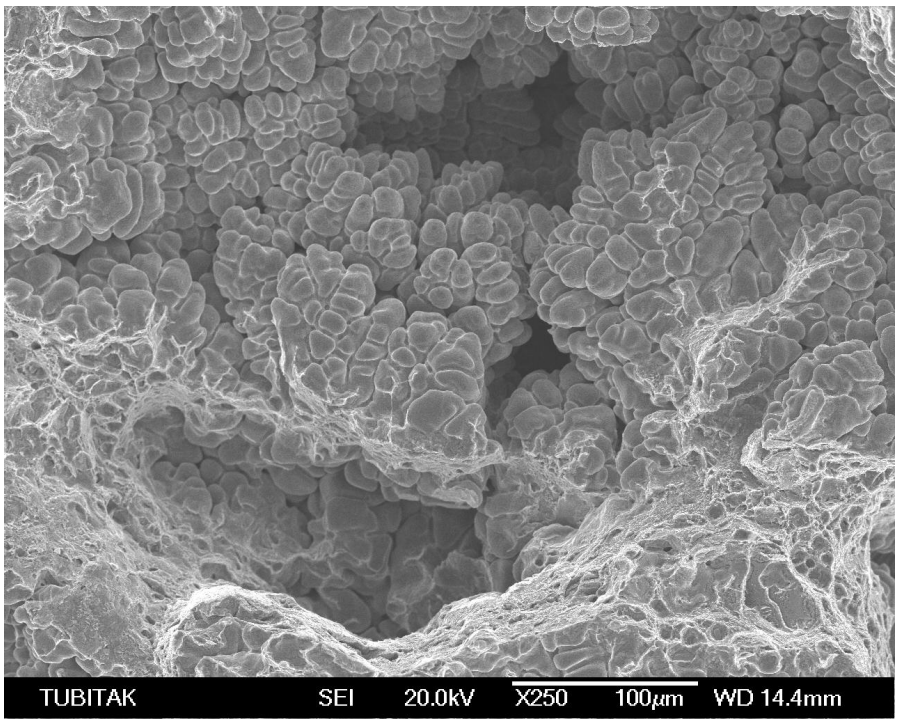

Figure 4.20. The SEM photograph of specimen 11 under X250 magnification

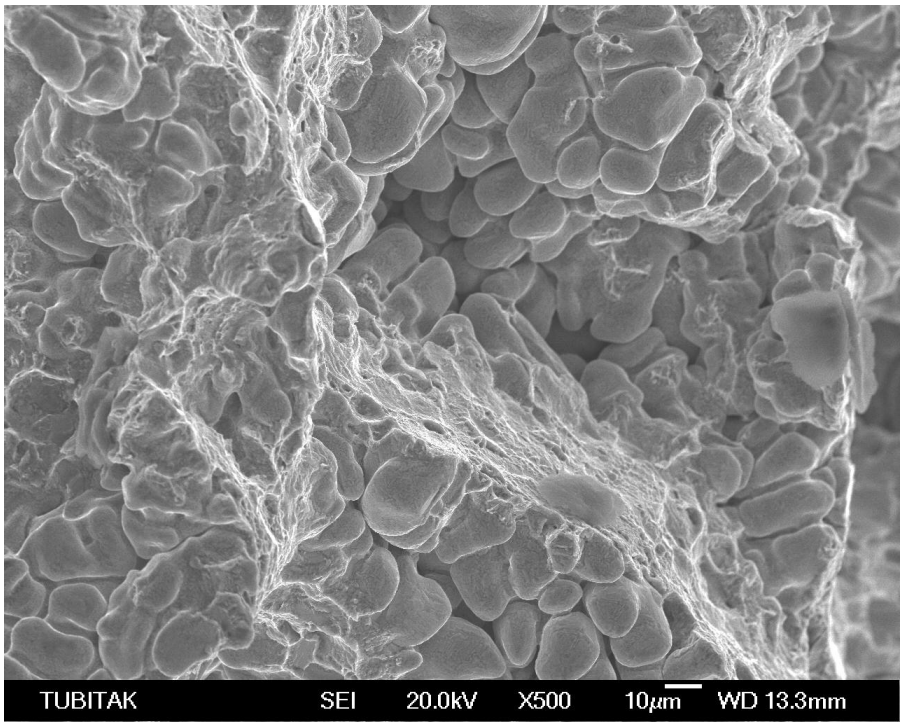

Figure 4.21. The SEM photograph of specimen 11 under X500 magnification

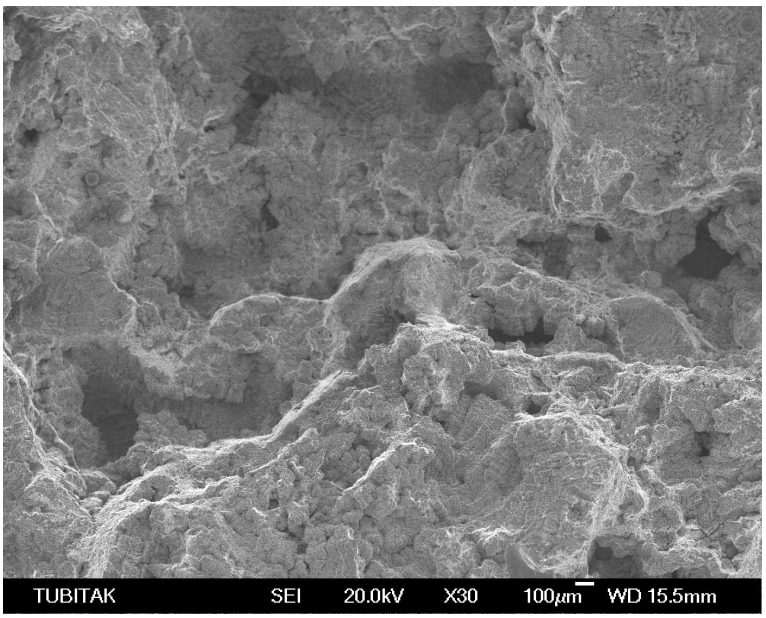

Figure 4.22. The SEM photograph of specimen 11 under X30 magnification

Figures from 4.23 to 4.25, belonging to specimen 14, show the fracture surfaces of ZA-27 squeezed under 100 MPa. Squeezing the solidifying alloy removes interdendritic porosity and increases cast quality. Hence, tensile properties and hardness also increase.

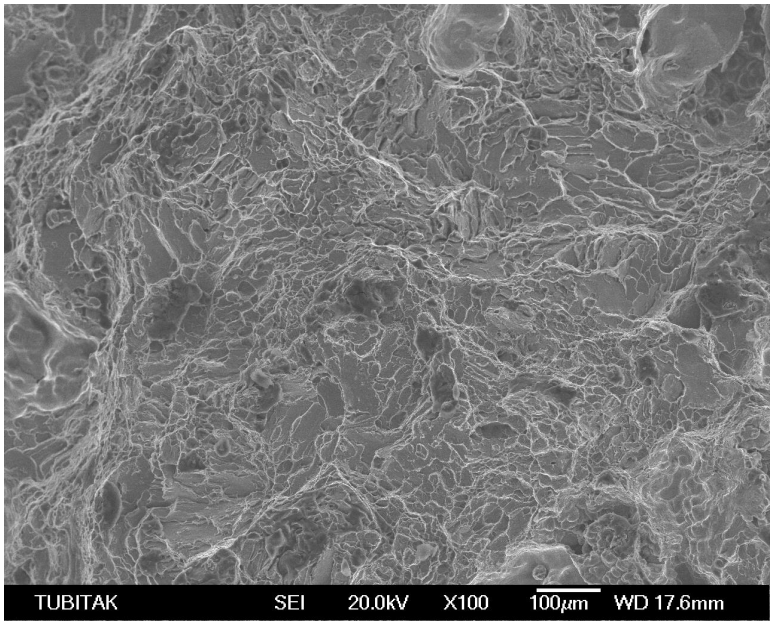

Figure 4.23. The SEM photograph of specimen 14 under X100 magnification

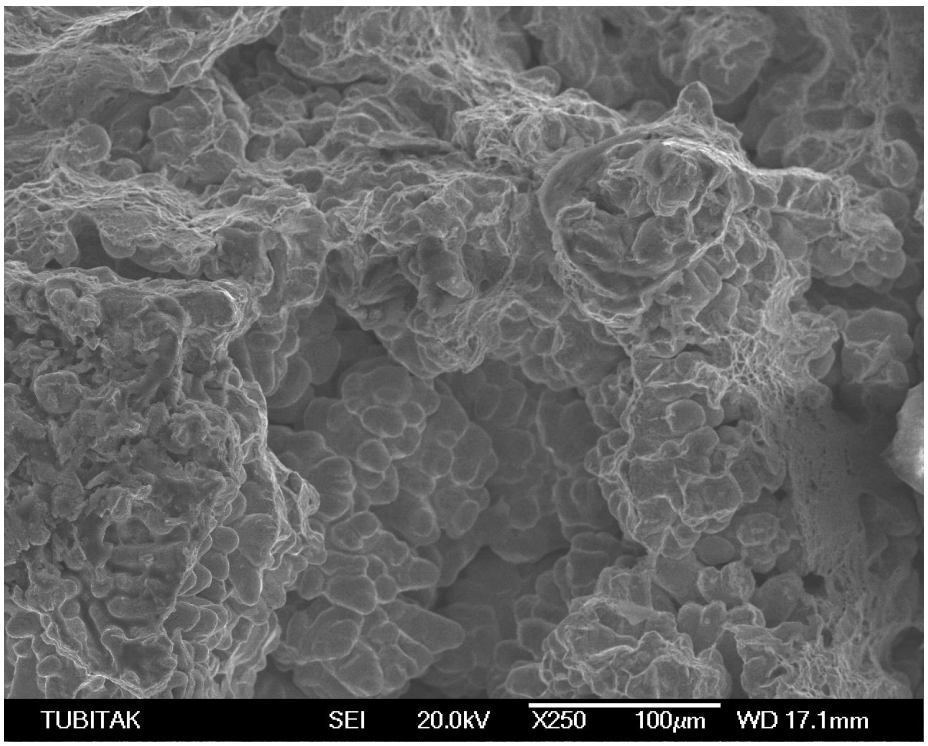

Figure 4.24. The SEM photograph of specimen 14 under X250 magnification

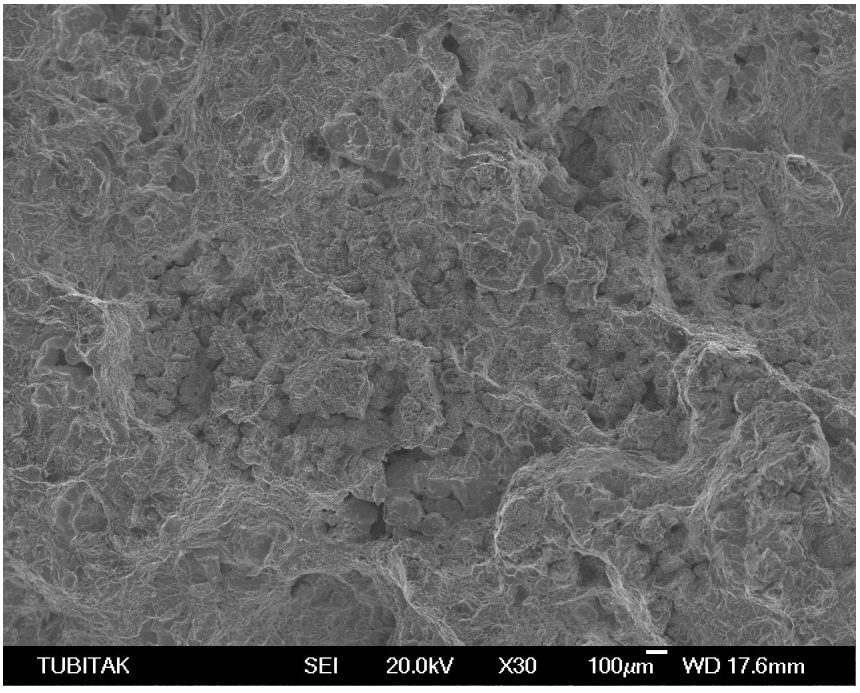

Figure 4.25. The SEM photograph of specimen 14 under X30 magnification

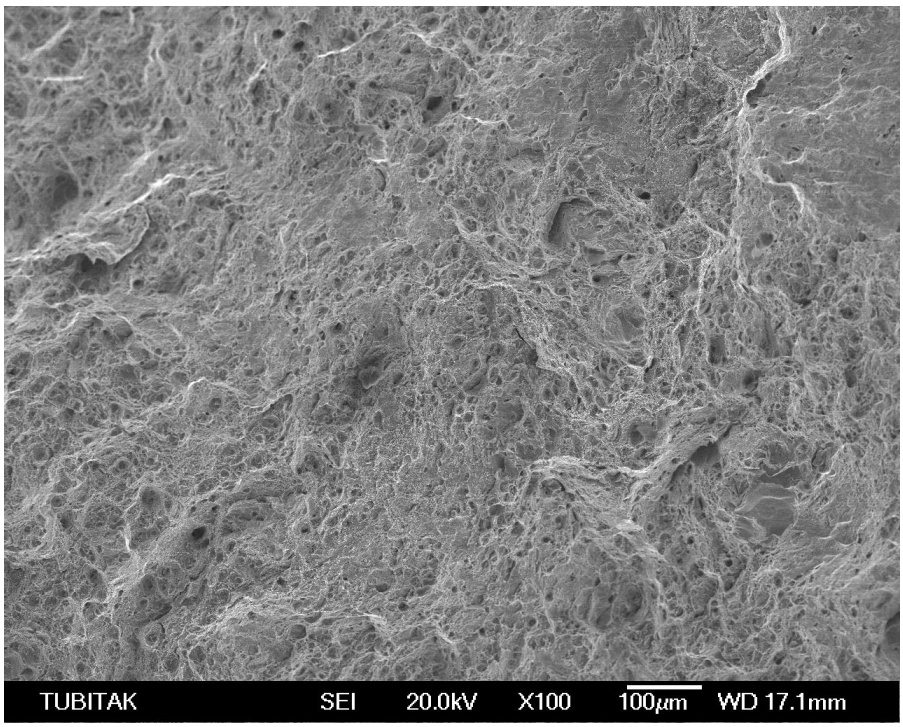

Figure 4.26. The SEM photograph of specimen 17 under X100 magnification

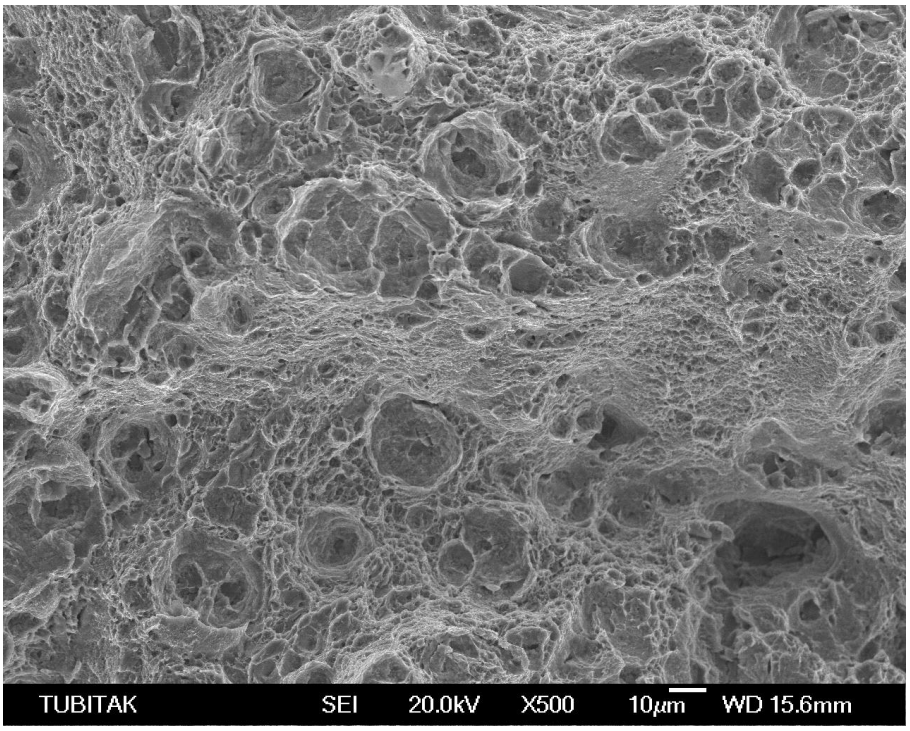

Figure 4.27. The SEM photograph of specimen 17 under X500 magnification

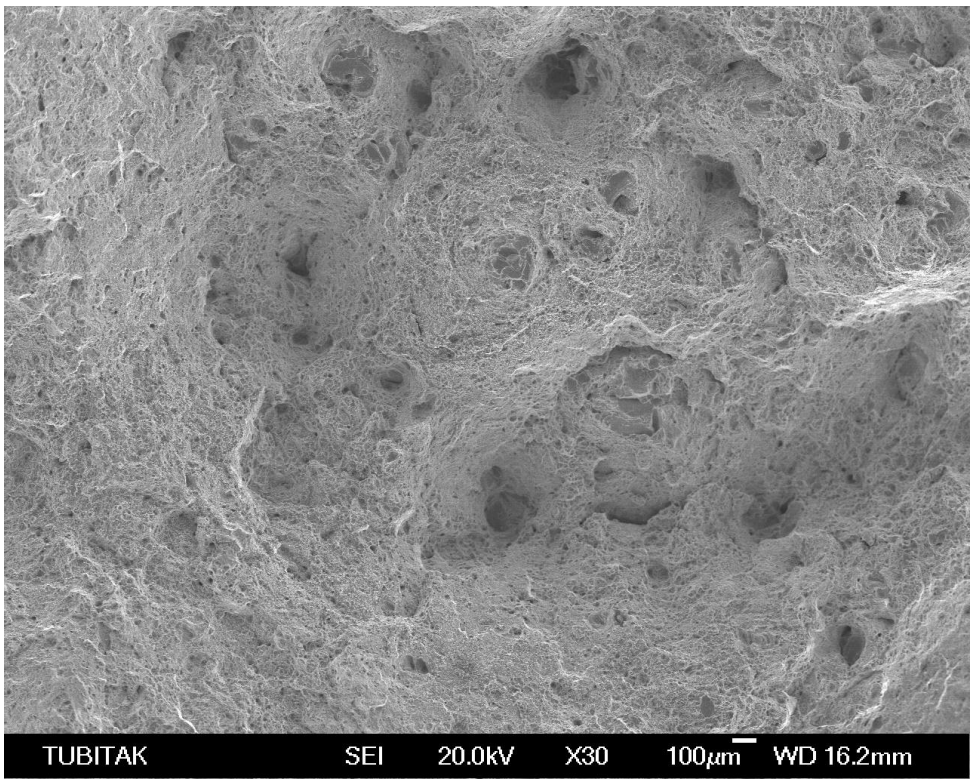

Figure 4.28. The SEM photograph of specimen 17 under X30 magnification

Figures from 4.26 to 4.28 show the fracture surfaces of ZA-27 squeezed under 150 MPa. These figures belong to specimen 17.

By comparing the all figures it is seen that the fracture profiles and porosity depths change depending on the squeezing pressure. For specimen 11, the fracture lines are seen as a net of short straight and curved lines like wool ball as in related figures above. Hence because of interdendritic porosity, the cracks extended along the dendritic arms and separated the dendrites from each other. This resulted in fracture. However, for specimen 14 and especially for specimen 17, these fracture profiles becomes a net of spongy structures as seen in the figures above. The type of fracture lines gives hints about fracture mechanism. If the lines look like a wool ball, it means that a brittle fracture took place; and if the lines look like a spongy structure, it means that a ductile fracture took place. So, it can be stated that the increase in squeezing pressure results in a ductile fracture. This was due to the elimination of interdendritic porosity. Since the porosity was removed, cracks only could extend themselves through the dendrites. Beside this, the number and depth of

holes on fracture surface also decreases from specimens 11 to 17. So, it is seen that, by increasing the squeezing pressure, the quantity and depth of porosities on fracture surfaces are started to decrease.

By SEM, four specimens, which were 11, 14, 15 and 17, were also subjected to sectional chemical analysis for investigating the both weight and atomic percentages of Zn and Al elements on fracture surface. The chemical analysis results are given in Table 4.10.

Table 4.10. Chemical analysis result of fracture surface by SEM

Specimen 11 (P=0,1 MPa)		
Element	Weight %	Atomic %
Al K	19.85	37.50
Zn K	80.15	62.50
Totals	100.00	

Specimen 14 (P=100 MPa)		
Element	Weight%	Atomic%
Al K	16.01	31.60
Zn K	83.99	68.40
Totals	100.00	

Specimen 15 (P=150 MPa)		
Element	Weight%	Atomic%
Al K	17.06	33.26
Zn K	82.94	66.74
Totals	100.00	

Specimen 17 (P=150 MPa)		
Element	Weight%	Atomic%
Al K	28.15	48.69
Zn K	71.85	51.31
Totals	100.00	

For all specimens in the Table 4.10., in the composition of fracture surface the weight percentages of Zn were much more than Al. The weight percentage of Zn is more than Al in ZA-27 by naturally. But the weight percentages of Zn are also higher than the weight percentage of Zn that exists in ZA-27 naturally. The Zn concentration is increased since it solidified after the aluminum reach dendrites. It is possible to state that during tensile testing fractures occurred more readily in those regions containing more Zn.

Figure 4.29. shows the area of point chemical analysis on the fracture surface of the specimen 17 which was squeeze cast under 150 MPa and the concentrations of Zn and Al are seen in Figure 4.30. as graphically.

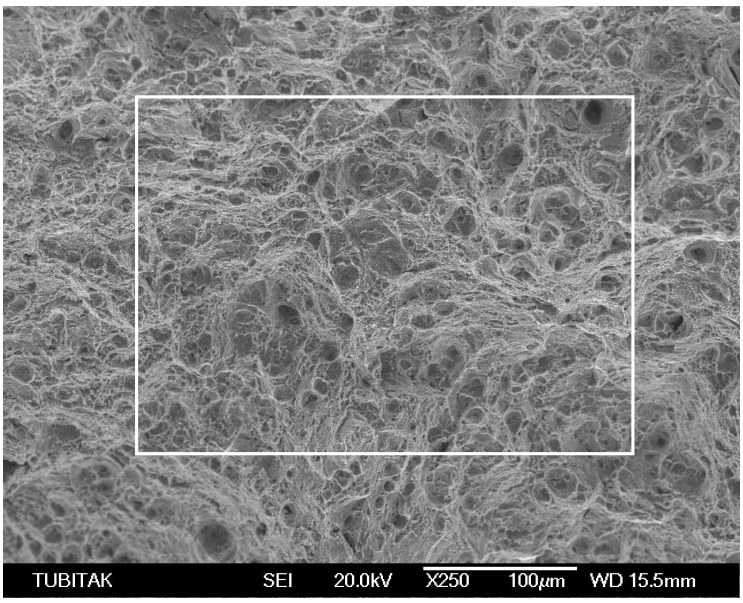

Figure 4.29. The area of point chemical analysis on the fracture surface for specimen 17

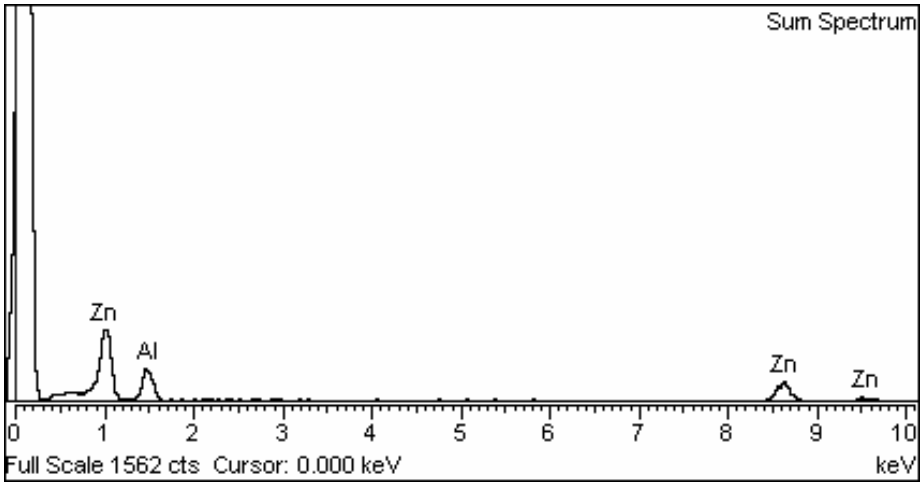

Figure 4.30. Zn and Al concentrations at the fracture surface for specimen 17

4.7.2. Metallographic Results

In this experiment specimens 11, 14 and 17 were used for metallographic observation. They were squeeze cast under the pressures 0,1 MPa, 100 MPa and 150 MPa.

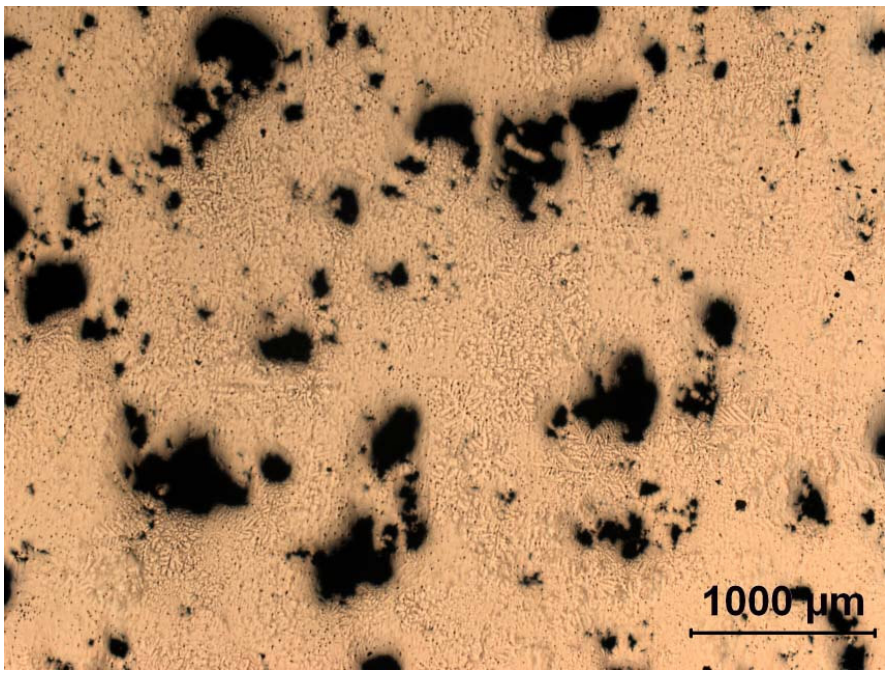

Figure 4.31. 25X magnification of specimen 11 before etching (P=0,1 MPa)

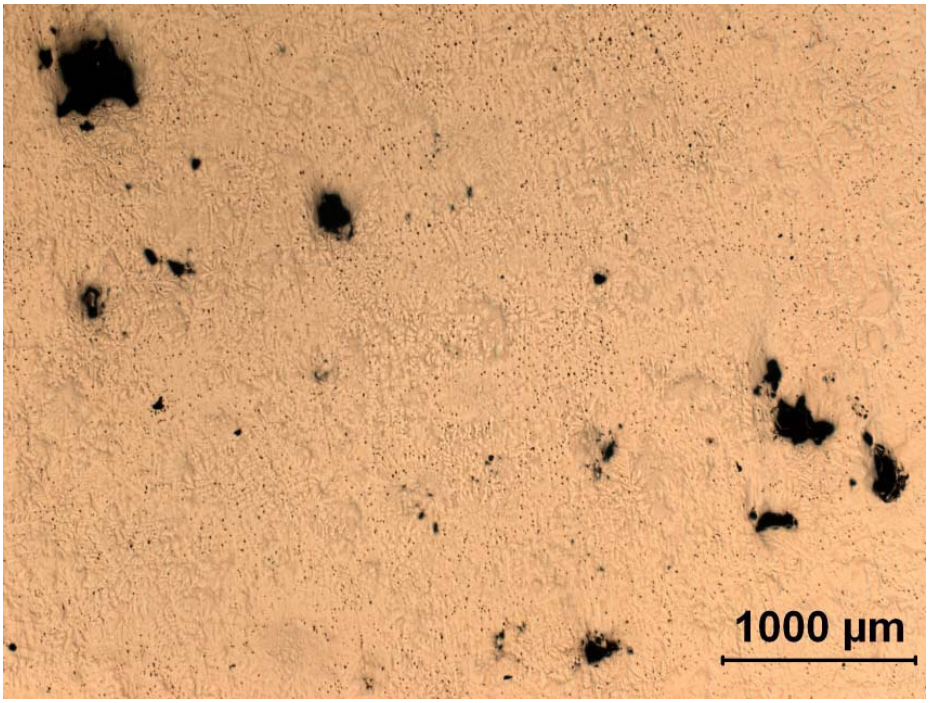

Figure 4.32. 25X magnification of specimen 14 before etching (P=100 MPa)

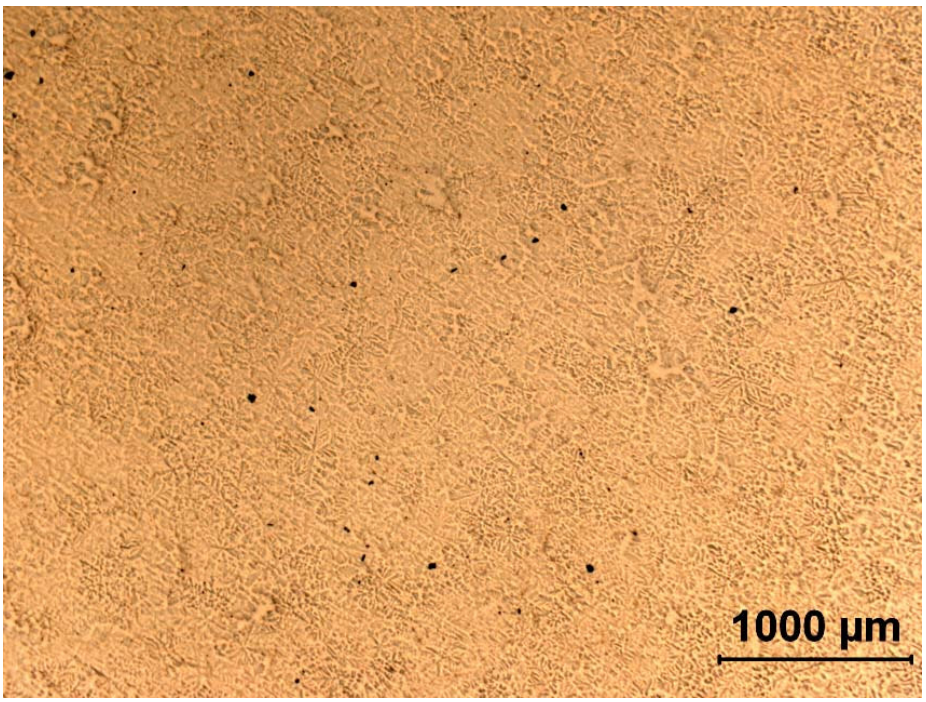

Figure 4.33. 25X magnification of specimen 17 before etching (P=150 MPa)

In the Figures from 4.31. to 4.33., which are taken with 25X magnification, there are black regions which signify the porosities. The amount and size of these black regions are the highest in Figure 4.31. and the lowest in Figure 4.33. Figures 4.31, 4.32 and 4.33. belong to specimens 11, 14 and 17 respectively. As it seen in the Figures from 4.31 to4.33, the increase in squeezing pressure results in a decrease in the amount and size of porosities. In these figures, the dendrites are not seen very clearly. By etching the dendrites becomes more visible.

In the Figures from 4.34. to 4.36., which were taken with 100X magnification, the dendrites are seen very clearly. The black regions have the same manner with the Figures from 4.31. to 4.33. regarding the amount and size.

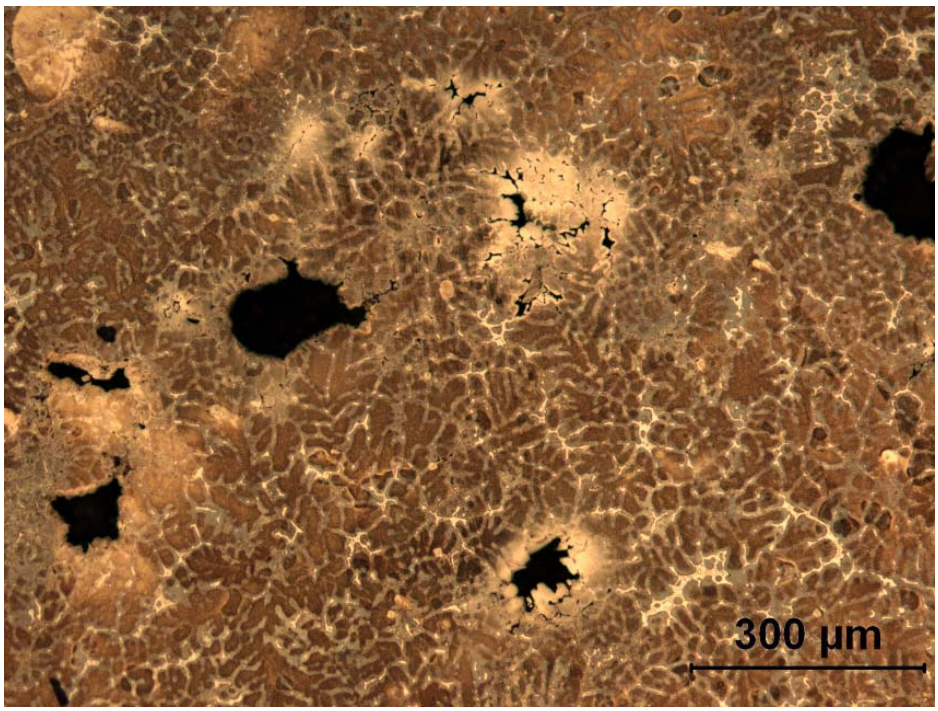

Figure 4.34. 100X magnification of specimen 11 after etching (P=0,1 MPa)

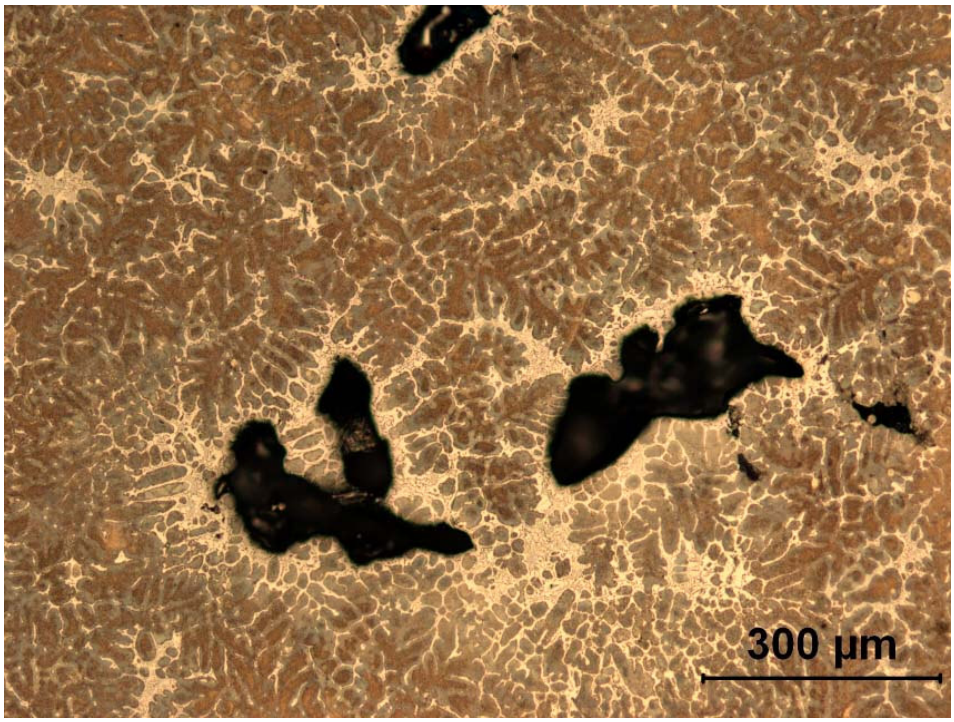

Figure 4.35. 100X magnification of specimen 14 after etching (P=100 MPa)

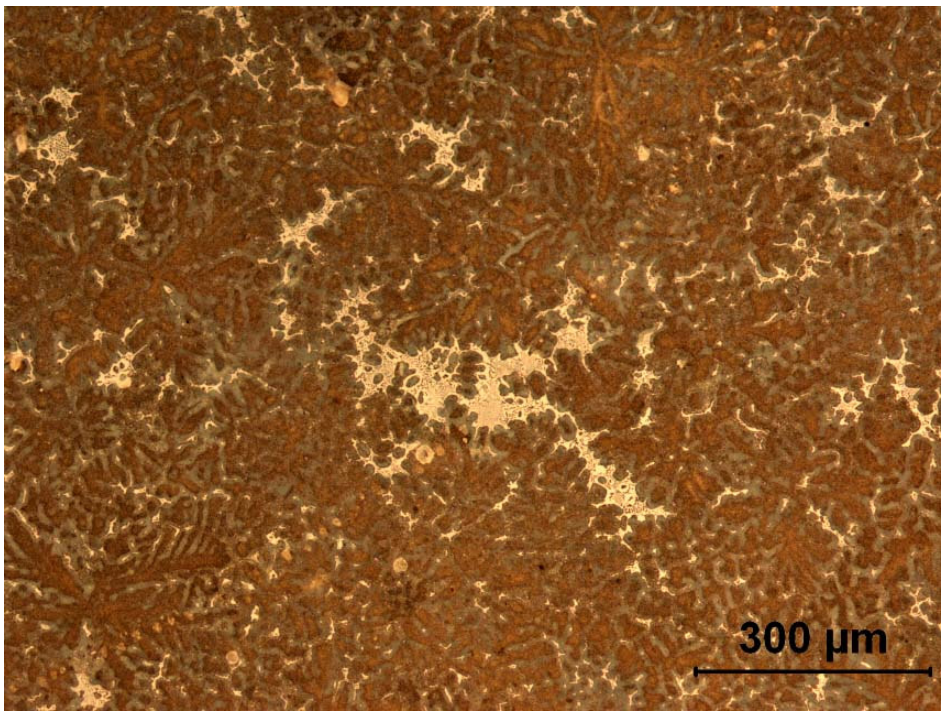

Figure 4.36. 100X magnification of specimen 17 after etching (P=150 MPa)

5. CONCLUSIONS AND RECOMMENDATIONS

In this survey, thermal solidification behavior and mechanical properties of a squeeze cast ZA-27 alloy in three different pressure ranges, including gravity casting, have been examined and presented. The following conclusions were established:

An inverse method has been applied to find the heat transfer coefficient between the molten metal and die, and it was found that increasing the squeezing pressures result in an increase in heat transfer coefficient. The heat transfer coefficients generally rise to a peak and the decrease with time during solidification.

The usage of infrared camera allowed us to examine the temperature values on the die outer surface. This was a process that did not need any touch to the die. The photos of die outer surface were taken during whole casting process which was also recorded as a movie. The cooling curves for the die outer surface were obtained. In the cooling curves, the rapid increase and slow decrease in temperature values are found.

The chip length, also machinability of ZA-27 alloy are dependent to not only squeezing pressure but also cutting speed. If we increase the cutting speed to an allowable degree or increase the squeezing pressure, then the chip lengths becomes shorter that means the machinability of ZA-27 alloy has been improved.

The level of squeeze casting effects the surface roughness directly.

From mechanical properties view points, it can be stated that increasing the squeezing pressure improves the mechanical properties. This statement was proved by tensile testing analysis and hardness tests in this research and found that tensile strength, yield strength, elongation, reduction in area and also hardness values were increased by increasing the squeezing pressure.

Regarding the microstructure properties, the squeezing causes a decrease in amount and sizes of interdendritic porosity in the microstructure. Since the tensile strength is

increased with squeezing pressure, the brittle fracture transforms to ductile fracture. Better dendrite structures are obtained with increasing squeezing pressure.

As a result, this work shows that increasing the squeezing pressure improves the quality and properties of ZA-27 alloy in thermal, mechanical and microstructural aspects.

As a future work, the value of critical squeezing pressure limiting the increase of pressure may be found. Regarding the thermal analysis, numerical simulation of solidification may be carried out applying boundary conditions in order to have more accurate results. The number of thermocouples may be increased to find more temperature values for using in inverse method more precisely.

APPENDIX A: THERMAL PHOTOGRAPHS AFTER POURING OF ZA-27 MELT FOR CASTING UNDER 0,1 MPa in COLD DIE

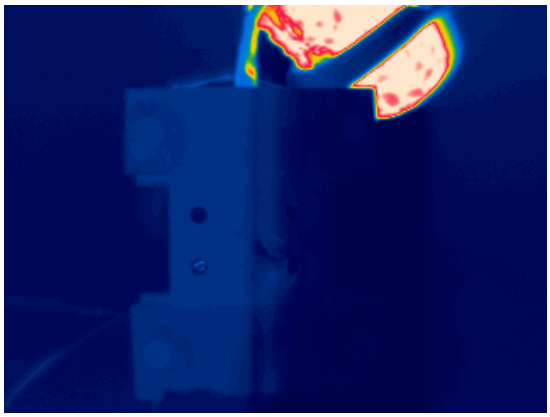

Figure A.1. During pouring ZA-27 melt

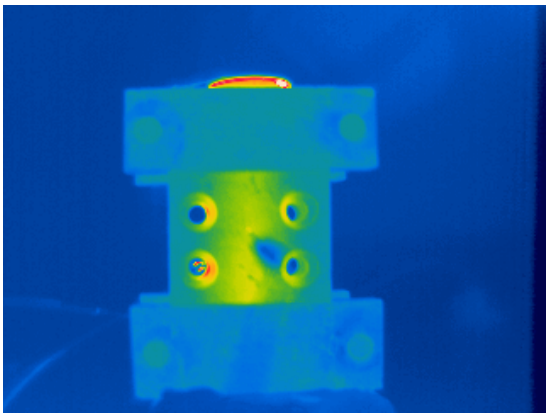

Figure A.2. After 6 seconds

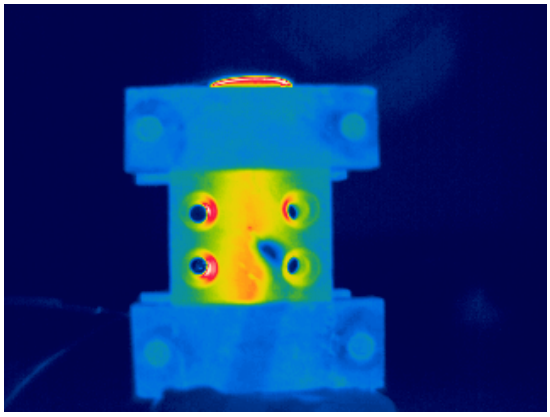

Figure A.3. After 7 seconds

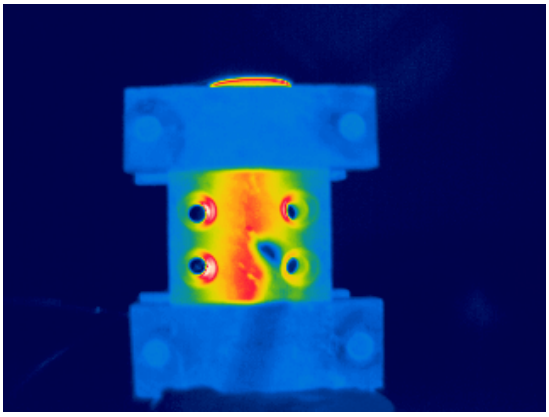

Figure A.4. After 9 seconds

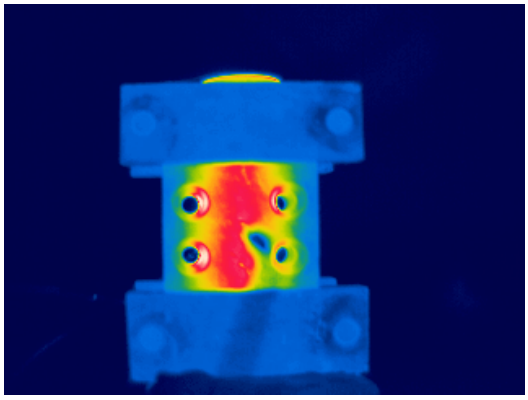

Figure A.5. After 12 seconds

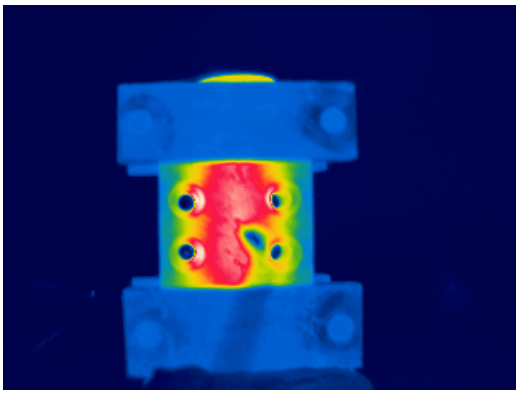

Figure A.6. After 15 seconds

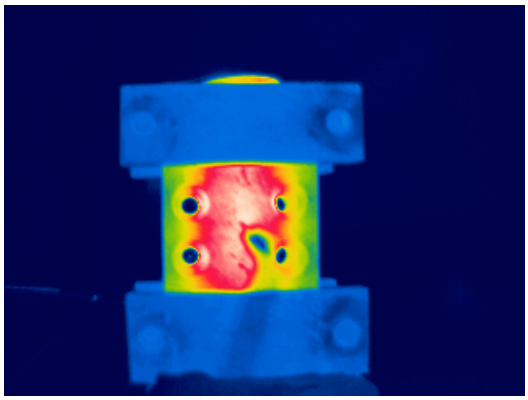

Figure A.7. After 19 seconds

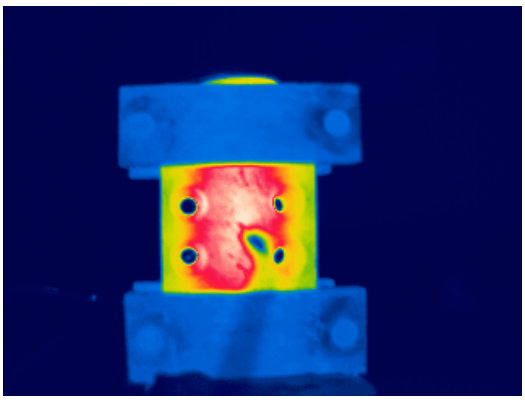

Figure A.8. After 23 seconds

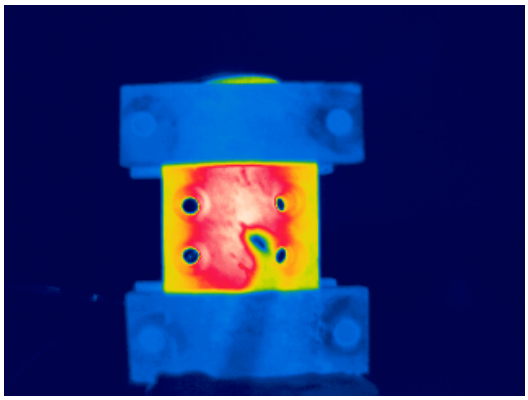

Figure A.9. After 28 seconds

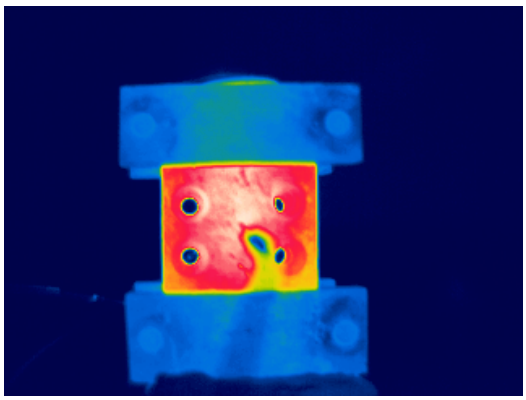

Figure A.10. After 41 seconds

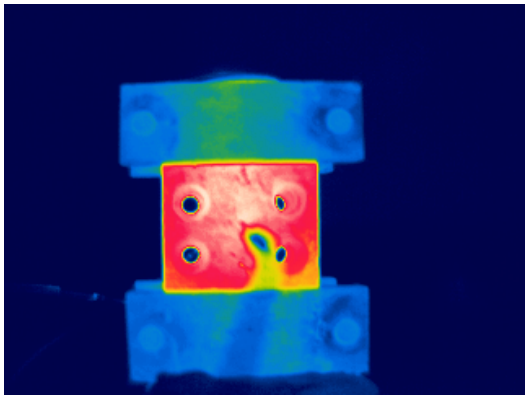

Figure A.11. After 51 seconds

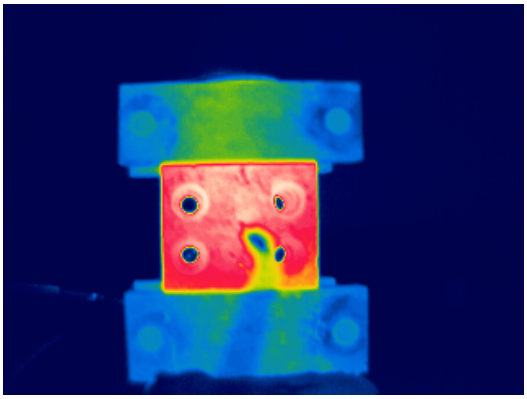

Figure A.12. After 66 seconds

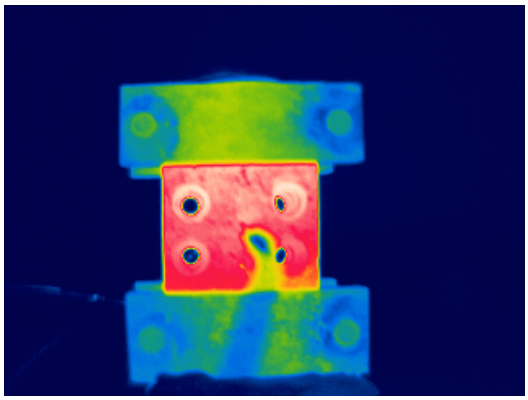

Figure A.13. After 96 seconds

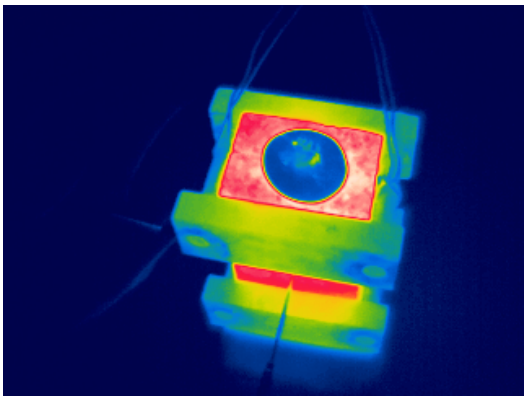

Figure A.14. After 106 seconds

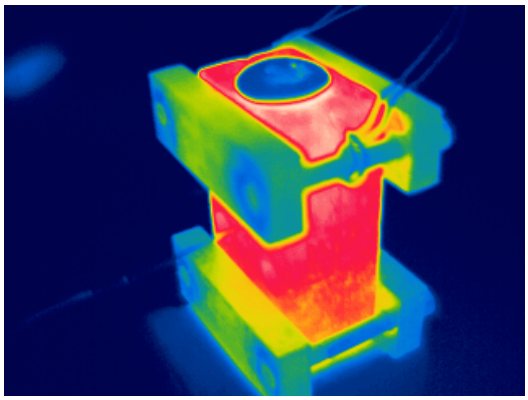

Figure A.15. After 112 seconds

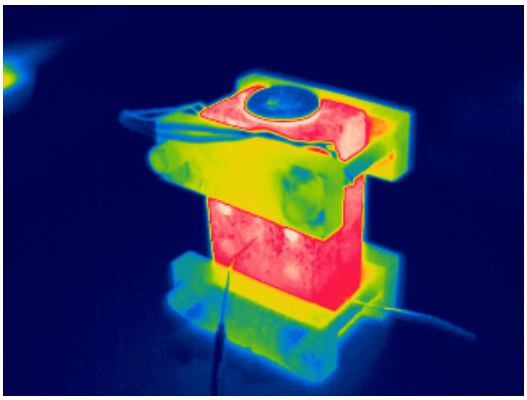

Figure A.16. After 138 seconds

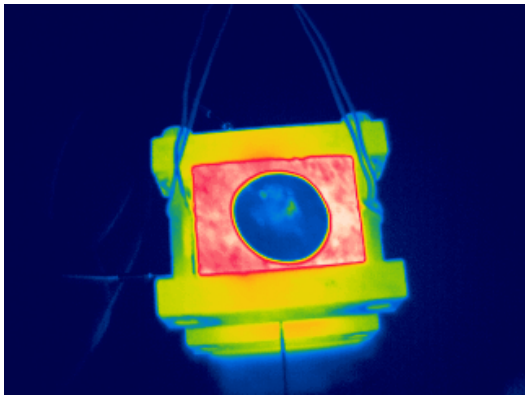

Figure A.17. After 154 seconds

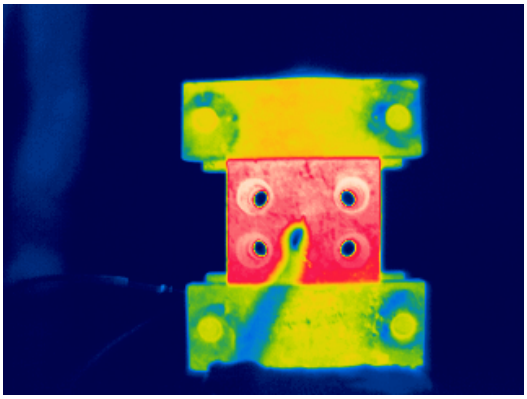

Figure A.18. After 196 seconds

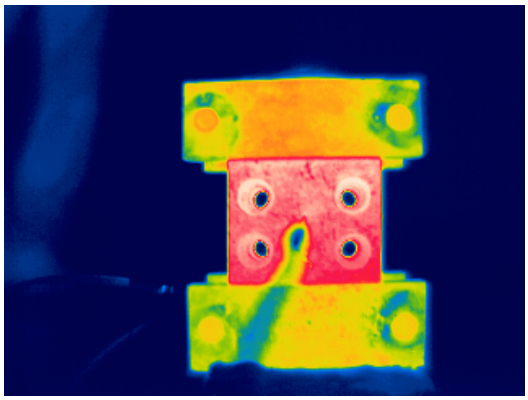

Figure A.19. After 256 seconds

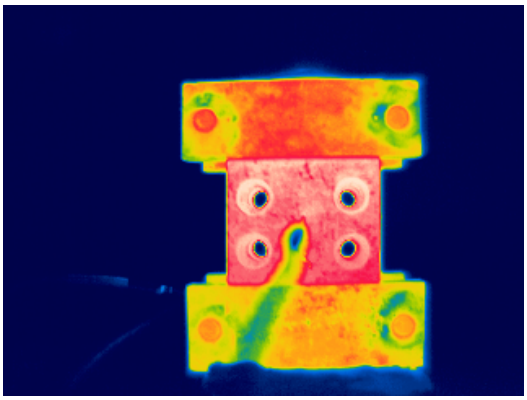

Figure A.20. After 336 seconds

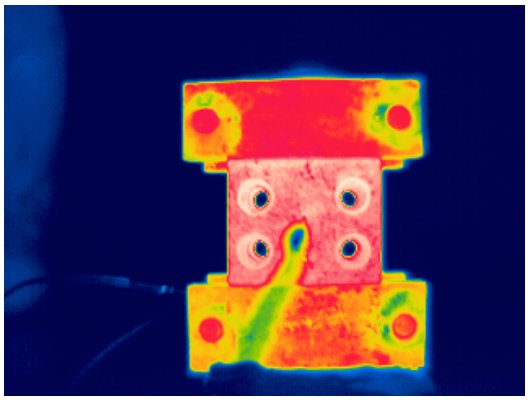

Figure A.21. After 456 seconds

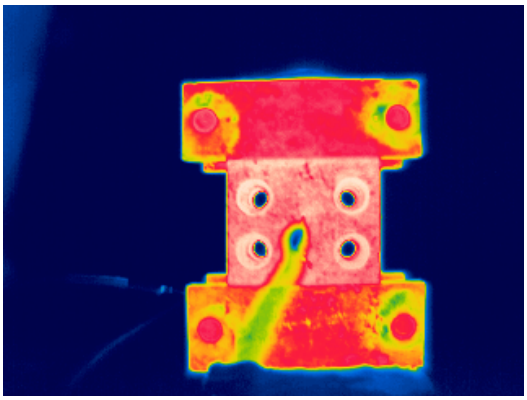

Figure A.22. After 614 seconds

APPENDIX B : SEM MICROGRAPHS OF THE FRACTURE SURFACES OF THE TENSION TEST SAMPLES

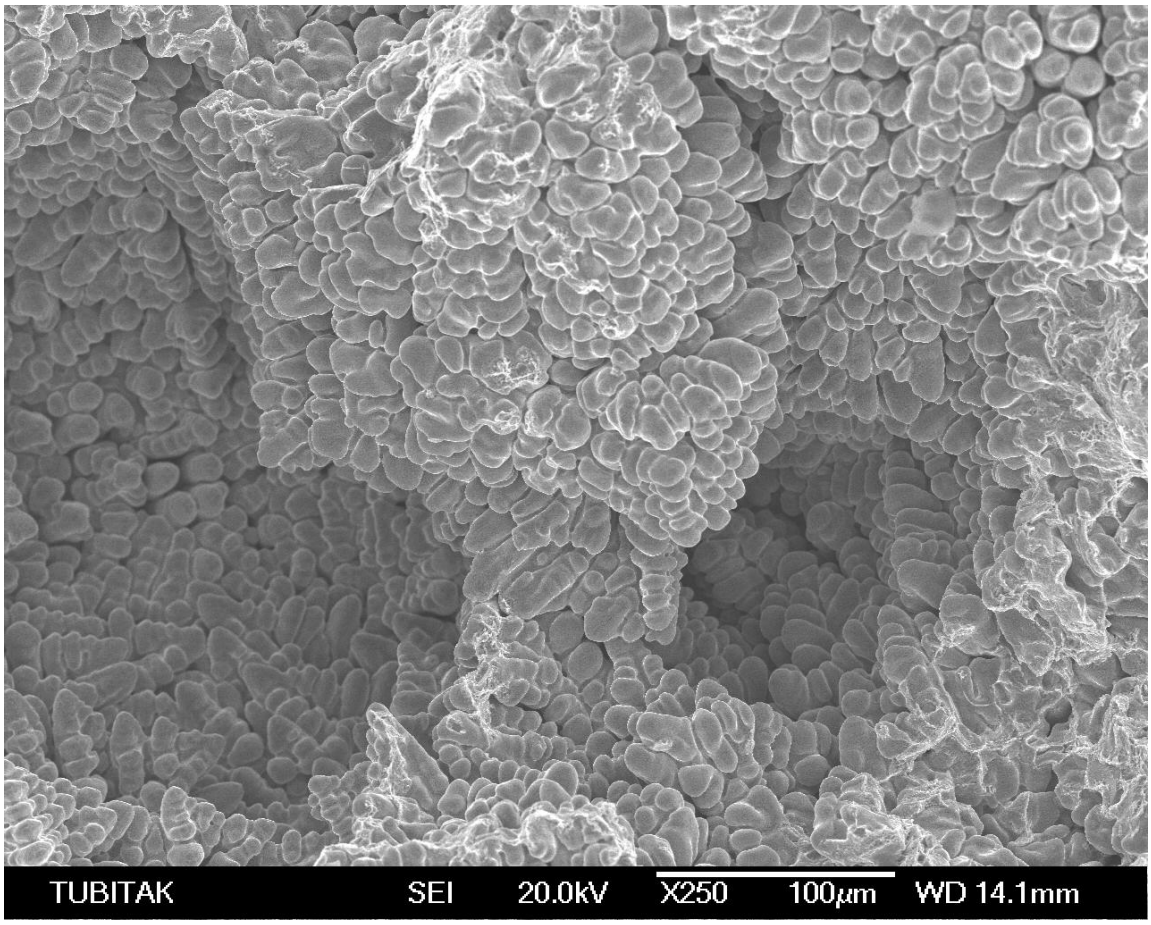

Figure B.1. The SEM micrograph of the fracture surface of specimen 10 with 0,1 MPa

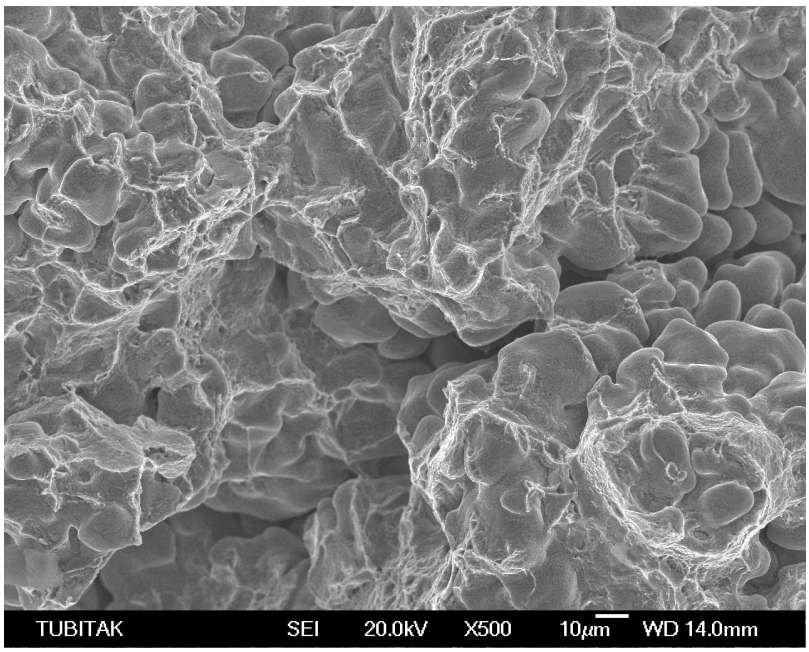

Figure B.2. The SEM micrograph of the fracture surface of specimen 10 with 0,1 MPa

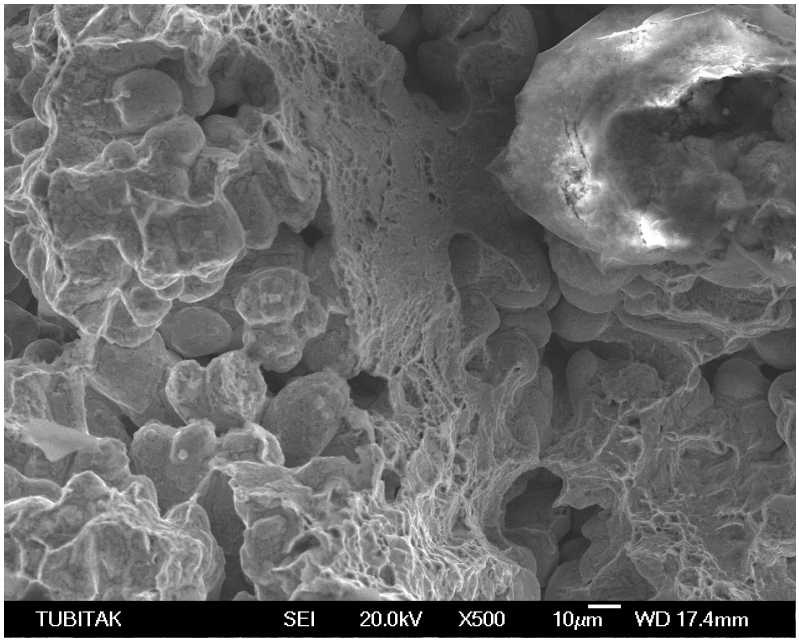

Figure B.3. The SEM micrograph of the fracture surface of specimen 9 with 100 MPa

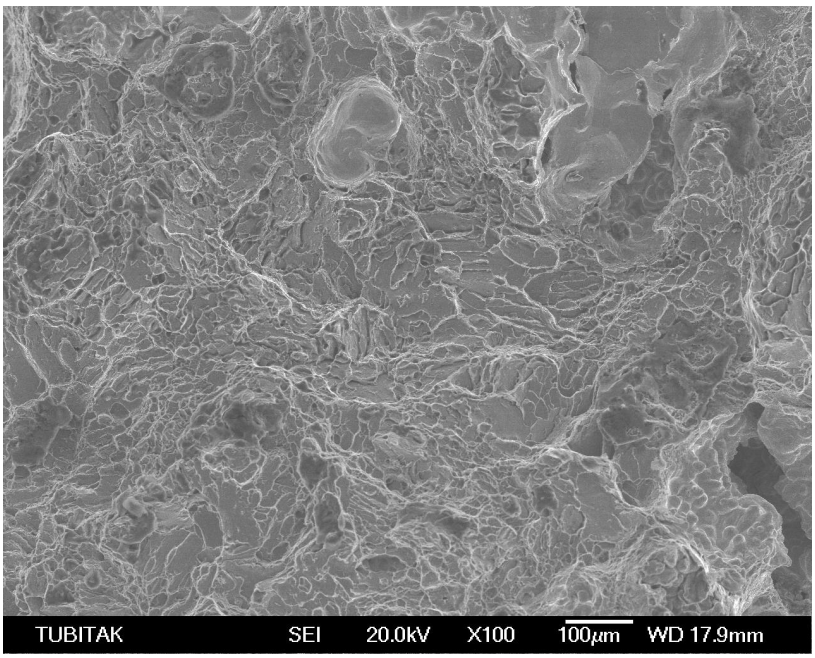

Figure B.4. The SEM micrograph of the fracture surface of specimen 9 with 100 MPa

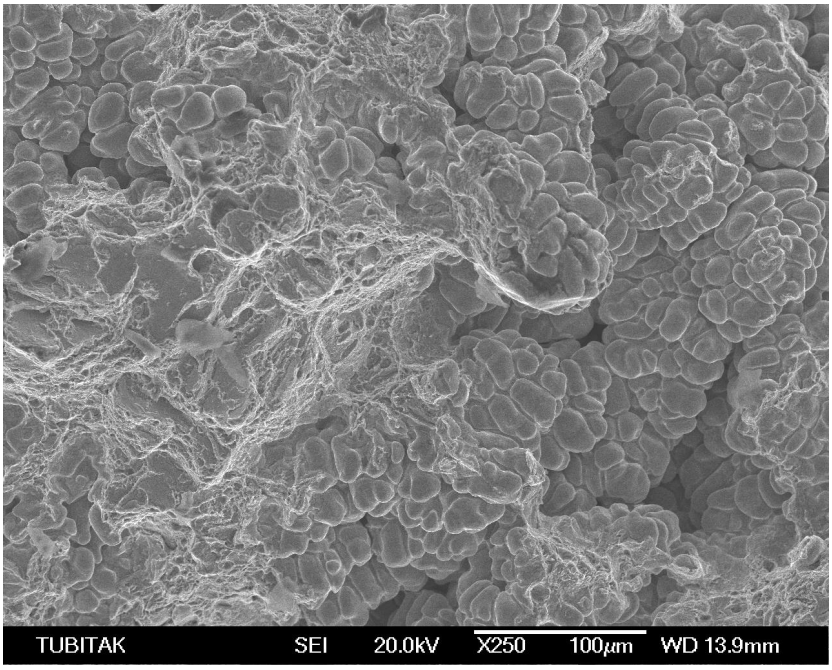

Figure B.5. The SEM micrograph of the fracture surface of specimen 16 with 150 MPa

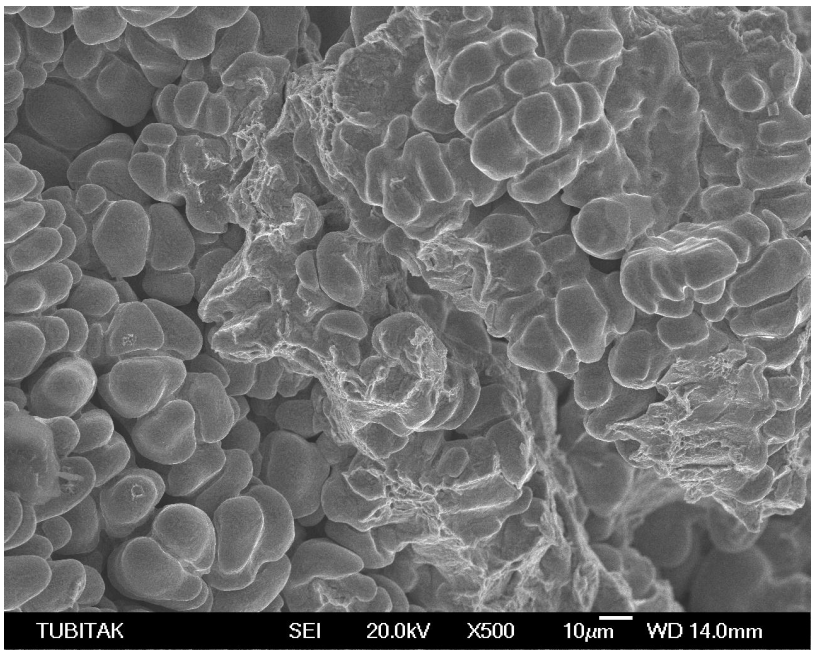

Figure B.6. The SEM micrograph of the fracture surface of specimen 15 with 150 MPa

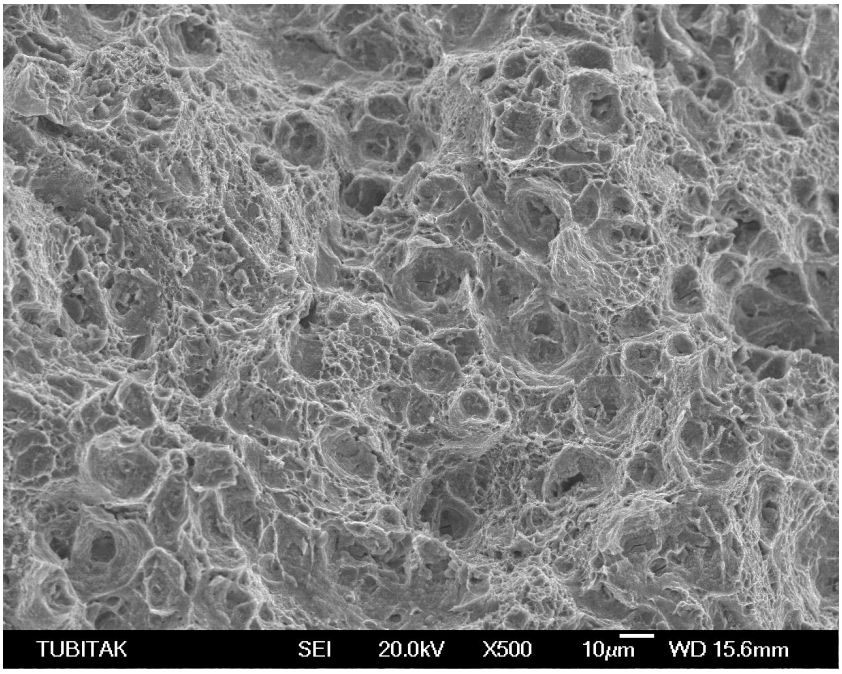

Figure B.7. The SEM micrograph of the fracture surface of specimen 18 with 150 MPa

REFERENCES

1. Ghomashchi, M. R. and A. Vikhrov, "Squeeze casting: an overview", *Journal of Materials Processing Technology*, Vol 1-9, pp.101, 2000.
2. Allison, C. R., "The Effect of Pressure on the Solidification of Aluminium and Aluminum-Silicon Alloys", *PhD Thesis, University of Cincinnati*, Ohio, USA, 1969.
3. Savas, M. A., H. Erturan and S. Altıntaş, "Effects of squeeze casting on the properties of Zn-Bi monotectic alloy", *Metallurgical and Materials Transactions*, Volume 28A, pp. 1509-1515, July 1997.
4. Yang, L. J., "The effect of casting temperature on the properties of squeeze cast aluminum alloys", *Journal of Materials Processing Technology*, Vol 140, pp.391-396, 2003
5. Youn, S. W., C. G. Kang and P. K. Seo, "Thermal Fluid/Solidification Analysis of Automobile Part by Horizontal Squeeze Casting Process and Experimental Evaluation", Journal of Materials Processing Technology 146 (2004) 294-302
6. Erturan, H., "Squeeze Casting of Zn-Bi Monotectic Alloy", MS Thesis, Mechanical Engineering Department, Boğaziçi University, 1994
7. Akyüz, M., "Mechanical Properties and Machinabilty of Aluminium-Magnesium Casting Alloys" *MS Thesis,* Boğaziçi University, 1994
8. Skolianos, S. M., G. Kiourtsidis and T. Xatzifotiou, "Effects of Applied Pressure on the Microstructure and Mechanical Properties of Squueze-Cast AA6061 Alloy", *Journal of Materials Science and Engineering* A231 (1997) 17-24
9. Chadwick, G. A. and T. M. Yue, "Principles and Applications of Squueze Castings", Met. Mater. 5 (1) (1989) 6-12
10. Crouch, I. G., "Aluminium Squeeze Casting Technology", a European Researches Viewpoint, Australian Conference on Materials for Industrial Development, Christchurch, New Zealand, 24-26, 1987
11. Rajagopal, S., "Squeeze Casting: A Review and Update", J. Appl. Metalworking ASM 13–14, 1981
12. Lee, C., K. H. Baik, B. T. Lee and K. S. Han, "Study of Sueeze Csting Cnditions and Mcrostructure in Pure Aluminium", Res. Inst. Ind. Sci. Technol. (Pohang City) Technical Res. Rep. 4 (3) (1990) 191-198

13. Okada, S., N. Fujii, A. Goto, S. Moritomo and T. Yasuda, “Development of a Fully Automatic Squeeze Casting Machine”, AFS transactions, Vol16., pp.136-146, 1982
14. Savaş, M. A. and S. Altıntaş, ‘Effects of Squueze Casting on Wide Freezing Range Binary Alloys’ Materials Science and Engineering, Vol A173, pp.227-231, 1993
15. Ultracast, “ZA Advantages”, http://pages.infinit.net/ıdsw/ucframes/productbot. html, 2006
16. Dynacast, “Zn Alloys”, http://www.dynacast.com/pdfcontent/en.znalloy.pdf, 2002
17. Eastern Alloys, Inc. , “Material Properties”, http://eazall.com/ materialproperties.aspx, 2004
18. Xue, X., R. Luck, B. Dawsey and J. T. Berry, “Modelling of Temperature Measurement Process with a Themocouple: A Comprehensive Parametric Study and Some Experimental Results”, AFS Transactions, Paper 04-0444 (01).pdf, 1-18, 2004
19. Weathers, J., A. Johnson, R. Luck, K. Walters and J. T. Berry, ,“Effects of Thermocople Placement on Highly Transient Temperature Measurement in Mold Media for Aluminum Castings”, AFS Transactions, Paper 05-194 (02).pdf, 1-11, 2005
20. Attia, M. H. and L. Kops, “Distortion in Thermal Field Around Inserted Thermocouples in Experimental Interfacial Studies”, Journal of Engineering for Industry, 1988, vol. 110, pp. 7-14
21. Woodbury, K. A., Y. Chen, J. K. Parker and T. S. Piwonka, “Measurement of Heat-Transfer Coefficients Between Al Castings and Resin-Bonded Molds”, AFS transactions, Vol 116, pp.705-711, 1996
22. Hwang, J. C., H. T. Chuang, S. H. Jong and W. S. Hwang, “Measurement of Heat Transfer Coefficient at Metal/Mold Interface During Casting”, AFS Transactions, Vol. 102, pp. 877-883, 1994
23. Smith, W. F., “Principles of Materials Science and Engeneering”, Second Edition, McGraw-Hill, Inc., 1990, pp. 270-272
24. Prabhu, K. N., S. A. Kumar and N. Venkataraman, “Effect of Coating/Mold Wall/Casting Thickness on Heat Transfer and Solidification of Al-Cu-Si Alloy (LM-21) in Cast Iron Molds”, AFS Transactions, 1994, vol. 109, pp. 827-832
25. Chattopadhyay, H., “Simulation of Transport Processes in Squeeze Casting”, Journal of Materials Processing Technology 186 (2007) 174-178